AER/AGS Special Report 110

Alberta Energy Regulator

Calgary-Lethbridge Corridor Geophysical Survey: Interpretation of AeroTEM Airborne Data

AGS
ALBERTA GEOLOGICAL SURVEY

AER/AGS Special Report 110

Calgary-Lethbridge Corridor Geophysical Survey: Interpretation of AeroTEM Airborne Data

L. Davis and R.W. Groom

Petros Eikon Incorporated

September 2018

ISBN 978-1-4601-2216-7

Davis, L. and Groom, R.W. (2018): Calgary-Lethbridge Corridor geophysical survey: interpretation of AeroTEM airborne data; Alberta Energy Regulator, AER/AGS Special Report 110, 119 p.

Author addresses:
L. Davis and R.W. Groom
Petros Eikon Incorporated
10A Bram Court, Unit 9-10
Brampton, Ontario, L6W 3R6
Canada

Published September 2018 by:
Alberta Energy Regulator
Alberta Geological Survey
4th Floor, Twin Atria Building
4999 – 98th Avenue
Edmonton, AB T6B 2X3 Canada

Tel: 780.638.4491
Fax: 780.422.1459
E-mail: AGS-Info@aer.ca
Website: www.ags.aer.ca

Foreword

In 2007, the Alberta Geological Survey, in partnership with Alberta Environment and Sustainable Resource Development, initiated the Provincial Groundwater Inventory Program, a multi-year program established to support the key outcomes defined by *Water for Life* and focused on improving knowledge and long-term management of groundwater resources in Alberta.

In February and March of 2011, Aeroquest Airborne was contracted to perform a geophysical survey of the Calgary-Lethbridge corridor area in southern Alberta using two helicopter borne AeroTEM III airborne time domain electromagnetic (AEM) systems. The purpose of the survey was to evaluate the use of airborne electromagnetic and magnetic geophysical survey techniques for groundwater mapping in the Calgary-Lethbridge corridor study area. Alberta Environment and Sustainable Resource Development funded the survey. The geological and hydrogeological results of the study in the Calgary-Lethbridge Corridor are available here: https://ags.aer.ca/publications/REP_91.html.

This report by Petros Eikon Incorporated provides a preliminary interpretation of the AEM data from the Aeroquest Airborne survey.

Interpretation of the 2011 AeroTEM Airborne Data

in Southern Alberta

for Alberta's Provincial Groundwater Inventory Program

May 2011

Petros Eikon Incorporated
10A Bram Court, Unit 9-10
Brampton, ON, L6W3R6

Laura Davis, BSc
Ross W Groom BMATH, MSc, PhD

Preface

The report was prepared by Laura Davis and Ross Groom both of Petros Eikon Incorporated except for the parts of the Introduction and Section 2. Section 2 was prepared by Aeroquest Airborne. This section relates to the conductivity depth section computed with the differential resistivity algorithm. The remaining sections within this report were prepared by Petros Eikon Incorporated.

The contents of this interpretation report are not intended to be viewed as a final interpretation. The time limits on the delivery of this work dictate a relatively narrow scope considering the vast amount of geophysical information available in the AeroTEM data sets and the large amount of other geophysical, and geological information that should be considered and integrated with the AeroTEM survey results.

Contents

1.0 Introduction

In February and March 2011, Aeroquest Airborne Surveys collected 27,000 km of airborne time domain-electromagnetic (AEM) data in southern Alberta. The data were collected for Alberta Environment (AENV) as part of Alberta's Provincial Groundwater Inventory Program (PGIP). The purpose of the survey was to map aquifers with EM techniques.

The survey area, southeast of Calgary and north of Lethbridge, is shown in **Figure 1**. The survey area was about 200 km north-south by 150 km east-west. Line spacing was 750 m and traverse lines were oriented at an azimuth of approximately 158^0 in the 10TM coordinate system. Tie lines, perpendicular to the traverse lines, were flown at a tenth the spacing (7500 m).

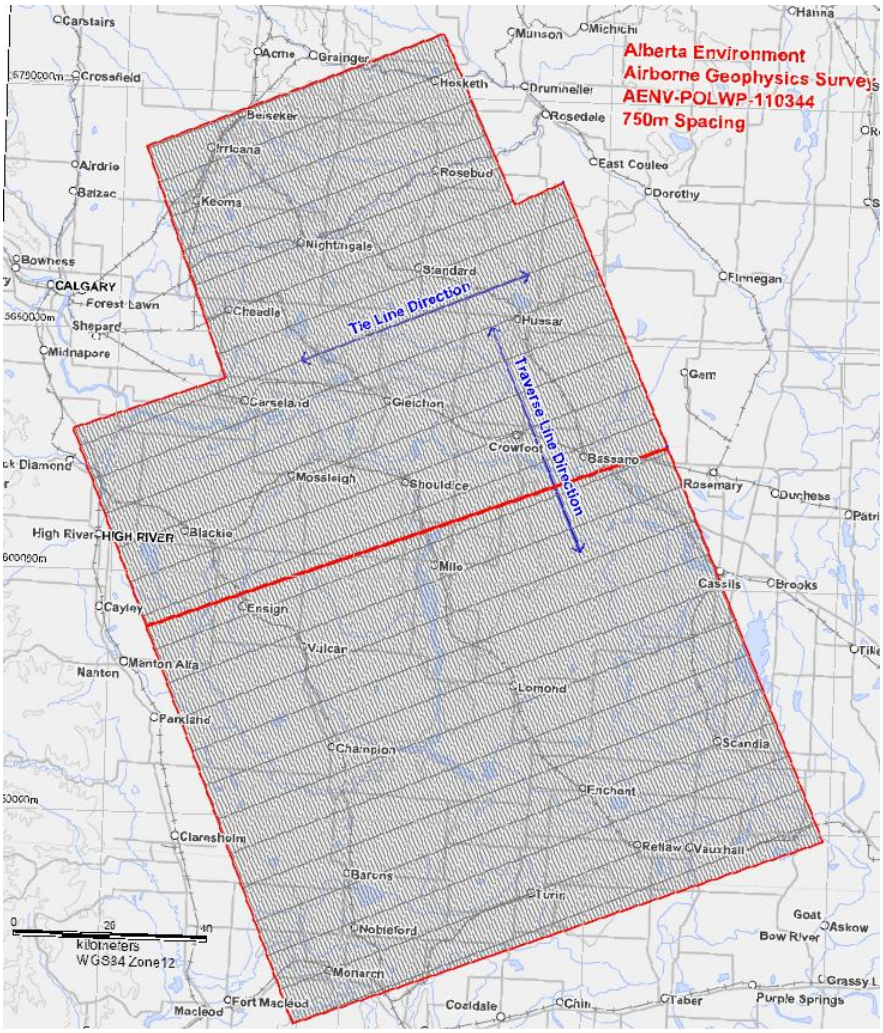

Figure 1: Airborne TEM survey location in southern Alberta

The data were collected with Aeroquest's AeroTEM III system. This is a helicopter-borne TEM system, utilizing a triangular waveform. A base frequency of 90 Hz was used, and thirty off-time channels of data were delivered. Further details on the system may be found in Aeroquest's logistics report. Two different AeroTEM III systems were used to collect the survey data, Mike and November.

The data were processed by Aeroquest, and inversions were performed by Petros Eikon. The traverse and tie line Hz data were inverted using 1D stacked inversions, and depth slices and sections were produced from these inversions and delivered to AENV. A preliminary interpretation of the data is provided in this report. For the purposes of this report, the survey data was divided into four (4) areas labeled Area 1 (NW), Area 2 (NE), Area 3 (SE) and Area 4 (SW).

The contents of this interpretation report are not intended to be viewed as a final interpretation. The time limits on the delivery of this work dictate a relatively narrow scope considering the vast amount of geophysical information available in the AeroTEM data sets and the large amount of other geophysical, and geological information that should be considered and integrated with the AeroTEM survey results. The current work provides an initial look at what information the data are likely to hold and be able to deliver. A more focused, fully-integrated, and customized interpretation is highly recommended to recover the full benefits of the data sets.

The off-time Z-component data set was analyzed and interpreted using two algorithms to produce models of the ground conductivity distribution across the survey area and to depth. This dual method approach is designed to provide an effective first-pass look at understanding the general geologic trends in the survey area, and to provide an understanding of the strengths and limitations of the AeroTEM data sets.

The first algorithm is a conductivity depth imaging (CDI) method called differential resistivity. This method is an approximate inversion method which produces an excellent image of the lateral conductivity variation, and a relatively smooth result in the depth model. This work was performed by Aeroquest Airborne. The second method is a true 1D inversion which uses a geologic model of a small number of layers. This few-layer inversion method generally produces a model which yields accurate depth models with strong depth variation. This method can produce a relatively poor image of the lateral variation, particularly in the near-surface.

2.0 Conductivity Depth Imaging – Differential Resistivity

A conductivity depth image of the entire data set was computed using the differential resistivity algorithm (Huang, 2008). This algorithm produces a rapid first-pass look at the conductivity distribution across the survey area and to depth. The results are concatenated to produce a 3D approximation of the ground conductivity. The results are presented as depth slices and can also be displayed as sections along each survey line. This CDI product provides a good look at the lateral conductivity variation and the spatial detail in the data sets. The CDI produces a relatively smooth depth section, but is good at mapping high-contrast conductive layers to depth.

2.1 The Method

The differential CDI method is described in Rudd et al, 2008. The method employs the pseudo-layer apparent resistivity model in a time-domain implementation. The off-time z-component AeroTEM data were used to compute apparent resistivity and depth pairs for each portion of the decay, from early time to late time. The method builds a depth section at each point along the flight line by transforming the rate of EM data decay from surface (early time) to depth (late time). These results are then interpolated onto a regular grid in the depth (z) dimension to allow for the generation of sections and depth slices.

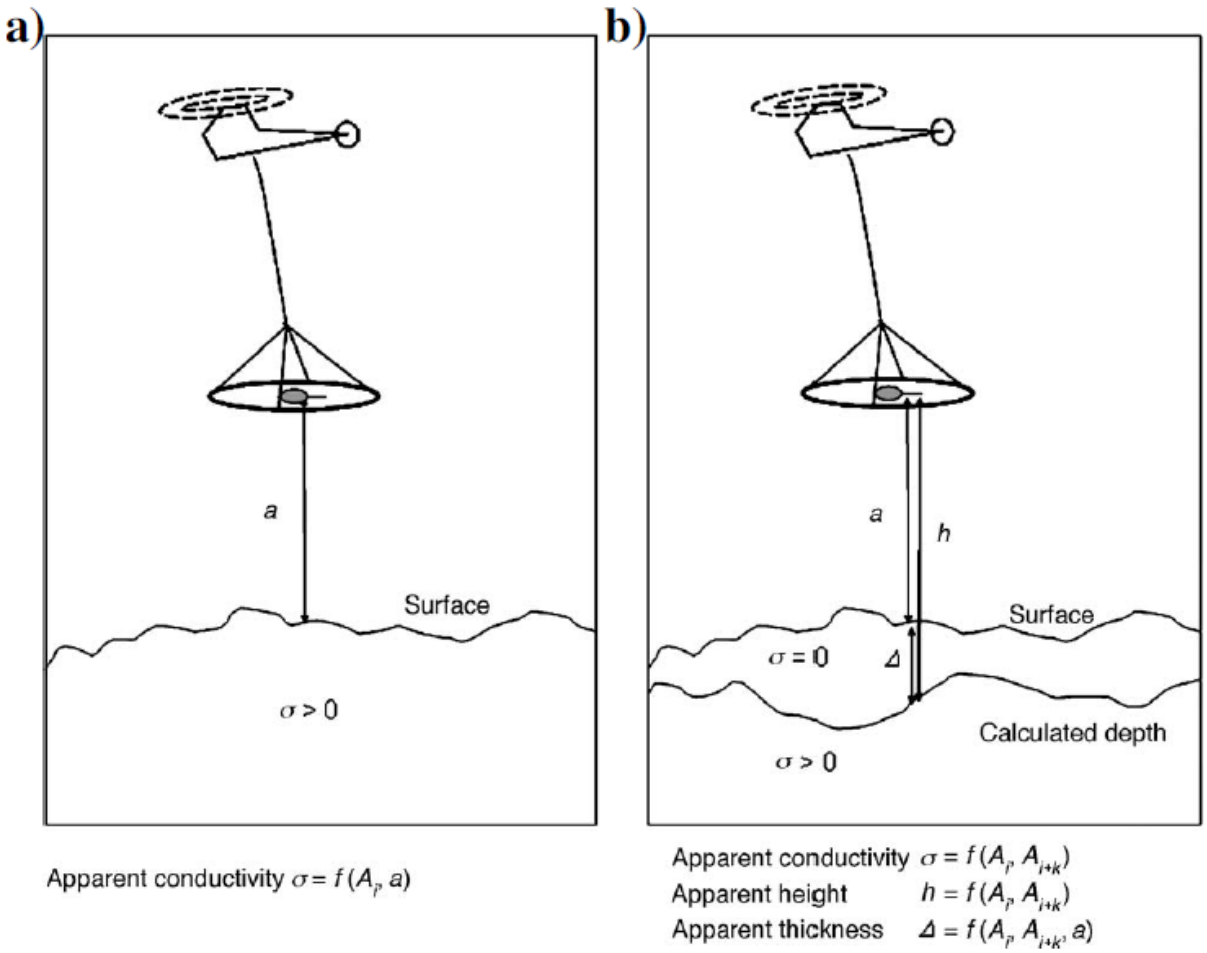

Figure 2.1: a) The half-space method of computing apparent resistivity versus b) the pseudo-layer method for computing apparent resistivity

For this survey, channels 1 through 30 were used for the computation. A differential resistivity was computed for every point, and then all the points along each line are concatenated to produce a continuous, complete section for each line. The results along a given line are not filtered or smoothed in order to retain the maximum amount of information along the lines. All of the sections are then merged together and interpolated between lines to produce a pseudo 3D model of the ground conductivity.

The algorithm involves the use of line-to-line constraint in the generation of the final CDI plan images and sections to limit the effect of minor variations in the response between lines. This constraint is designed to improve the visual continuity of the final CDI plan images while retaining all of the structural character in the results.

The advantages of this method include:

- The algorithm can be run rapidly
- Any inaccuracies in the measurement of the air layer (the ground clearance of the system) are minimized in the conductivity sections
- The results can be concatenated

The disadvantages of the method include:

- Since it is not a true inversion, the resistivity and depth values do not necessarily represent a numerically exact model of the geology at each point
- The algorithm assumes a layered earth, so any lateral inhomogeneity will affect the accuracy of the computed resistivity and depth values.
- The smoothness of the result in the depth (z) dimension limits the ability to define the depth and thickness of discrete, anomalous conductive or resistive layers

2.2 CDI Results

The CDI results are presented in digital and map form. The digital files are stored in a Geosoft GDB format and contain the original resistivity and depth pairs at each station, and the interpolated depth grid. The interpolated and concatenated results are presented as grids at predetermined depths of 20 m, 30 m, 60 m, and 120 m. The CDI images provide an excellent representation of the conductivity distribution across the survey area (see Figure 2.2). Correlation of the major features within this image to known surficial geologic and cultural features confirms that the method is effectively mapping the near-surface geology. Well-defined, complex features in the southwest portion of the survey area show the ability of the method to map the geology in considerable detail.

In some areas the CDI results show a correlation with cultural features. In the northwest portion of the survey, noise sources related to the southern portion of the city of Calgary are clearly affecting the results, so any interpretation in this area must be done with extreme caution. In addition, in areas where a cultural feature has required the EM system to be flown at a higher ground clearance, the CDI generally reflects this as a more resistive response. This effect is the result of the CDI algorithm and does not reflect the geology, so interpretation of the CDI across these features and in their immediate vicinity should be done with care. The inversion method described in the following sections handles these areas with more accuracy, so any interpretation should utilize the inversion results.

There is a general increase in the conductivity of the mapped geology from west to east. Many of the known watercourses across the survey area are imaged well in the CDI results. Most of these are imaged as relative conductivity highs. This may be caused by accumulation of conductive materials, or because the watercourse has eroded through a resistive overlying layer, exposing a more conductive layer beneath.

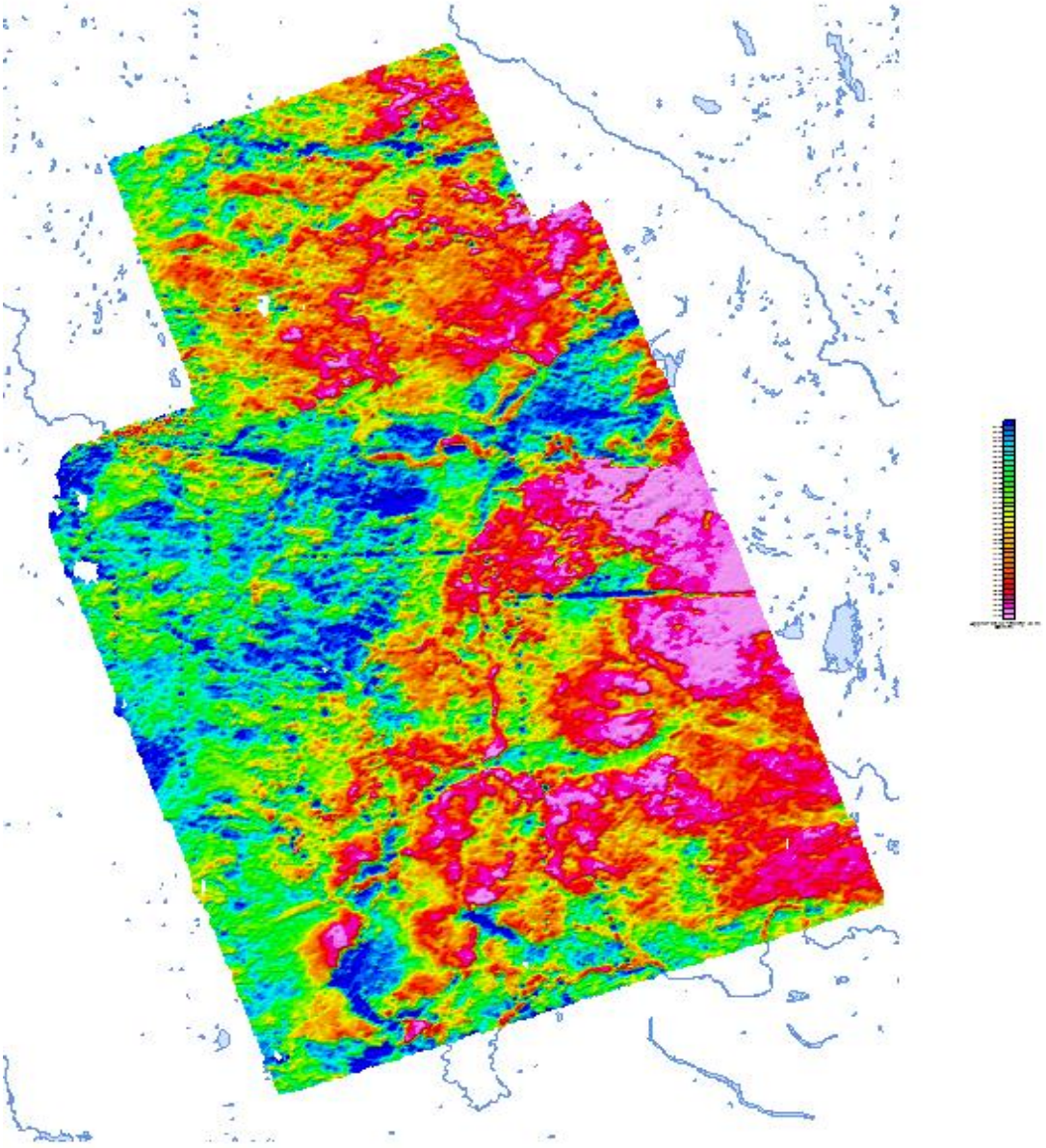

Figure 2.2: Resistivity at 20m depth calculated from the CDI algorithm

3.0 Initial Analyses of Data

Prior to performing the inversions, data along several survey lines across the survey area were analyzed to examine data quality and determine appropriate settings for the inversions. 1D forward modeling was

conducted using EMIGMA v8.5 (Petros Eikon, 2011) and was used to evaluate the data. In additional to forward modeling, decays were compared on repeat lines and grids of the data were created to examine the consistency of the data. This section serves as an introduction to the data quality issues in the survey. These are further discussed in Section 6.0 with reference to the inversion results.

3.1 Initial Examination of Decays

3.1.1 Late-Time Noise and Repeatability

Figure 2 displays the decays at seven points in the decimated data between 5566000 and 556100 on Line 20200 (November). The plot indicates noise in the last two channels, with limited repeatability between stations. The amplitude of the response at these channels is below 20 nT/s.

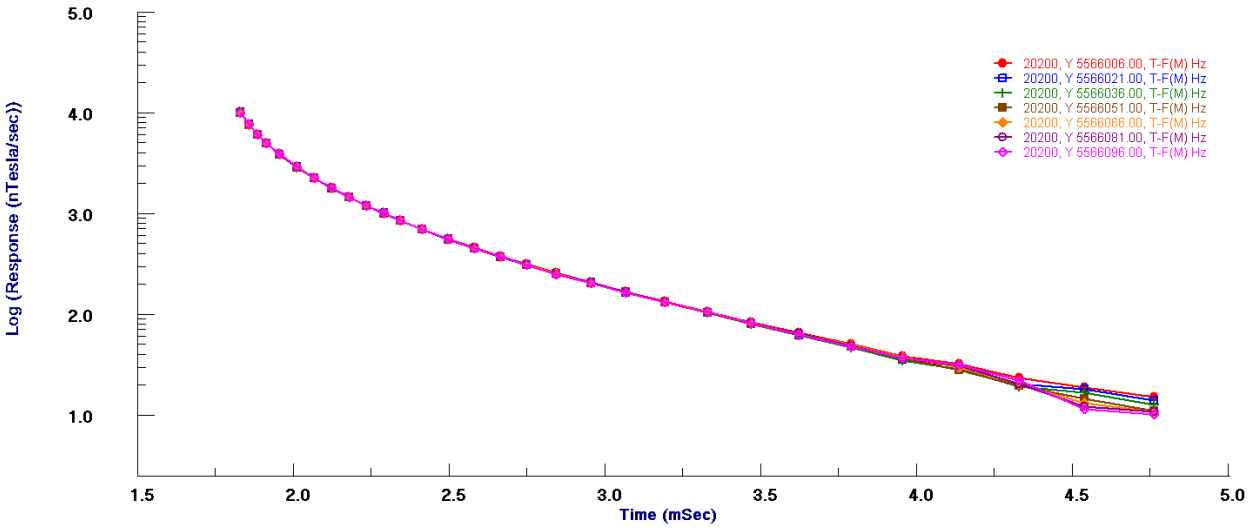

Figure 2: Decays for decimated data between 5566000 and 5566100 on Line 20200. Channels 1-30.

A second example of several adjacent decays is shown in **Figure 3** for 10940 (Mike). There is significant noise in the decays beyond Channel 26, and Channels 23-25 are noisy as well. Note that the noise appears coherent across several points. The reason for this is not known. The amplitude of the noise is approximately ±4 nT/s.

In general, the data is not reliable beyond Channel 26. In some sections of the data, the decays vary significantly between points in these channels, while in others, the noise appears somewhat coherent, but the decays are not physically possible. It is possible that this is caused by the system, but it could also be due to manmade features on the ground. Due to the late-time noise, these channels should not be used in the inversion. Some decays are noisy beginning several channels earlier than Channel 26, with the Mike data typically being noisier than the November data.

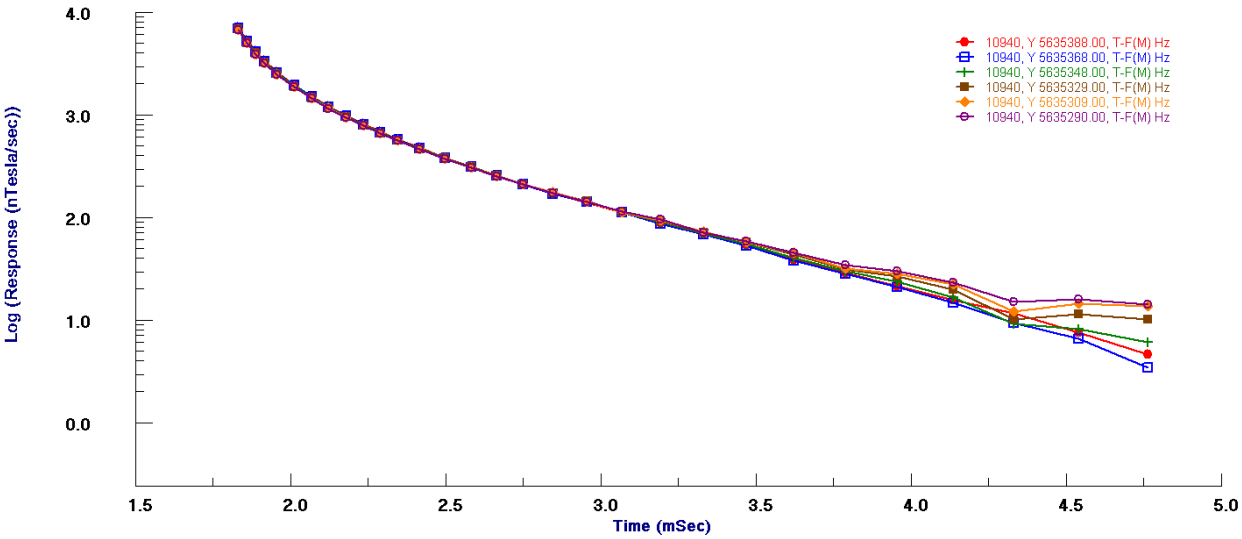

Figure 3: Decays for decimated data between 5635290 and 55635390 on Line 10940. Channels 1-30.

3.1.2 Other Decay Features

Figure 4 displays several decays near a power line. The data become noisy around Channel 4 as a result of the power line. Due to the significant effect that the power lines have on the data, these sections of the data should not be used in the inversion. Some areas of the data near cities and towns are also particularly noisy, especially the north ends of Lines 11200-11430 in the northwest and decays are similar to those near power lines.

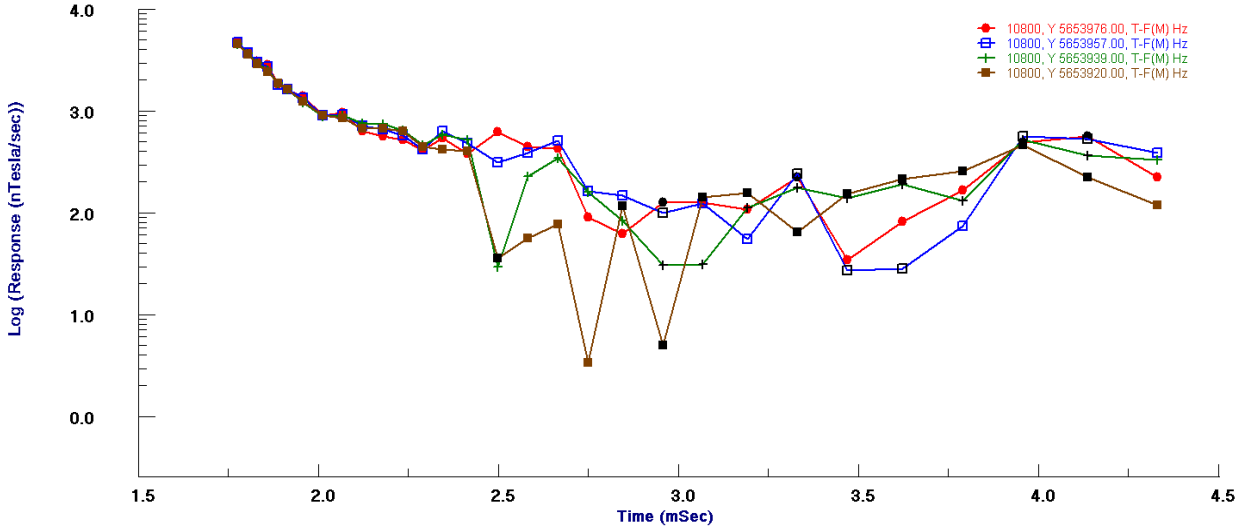

Figure 4: Decays near a power line on Line 10800.

Several lines contain mid-time channels that appear to be inconsistent with the rest of the decay. An example of this is shown in **Figure** 5, where Channel 10 is not consistent with the other mid-time channels over a significant section of the line.

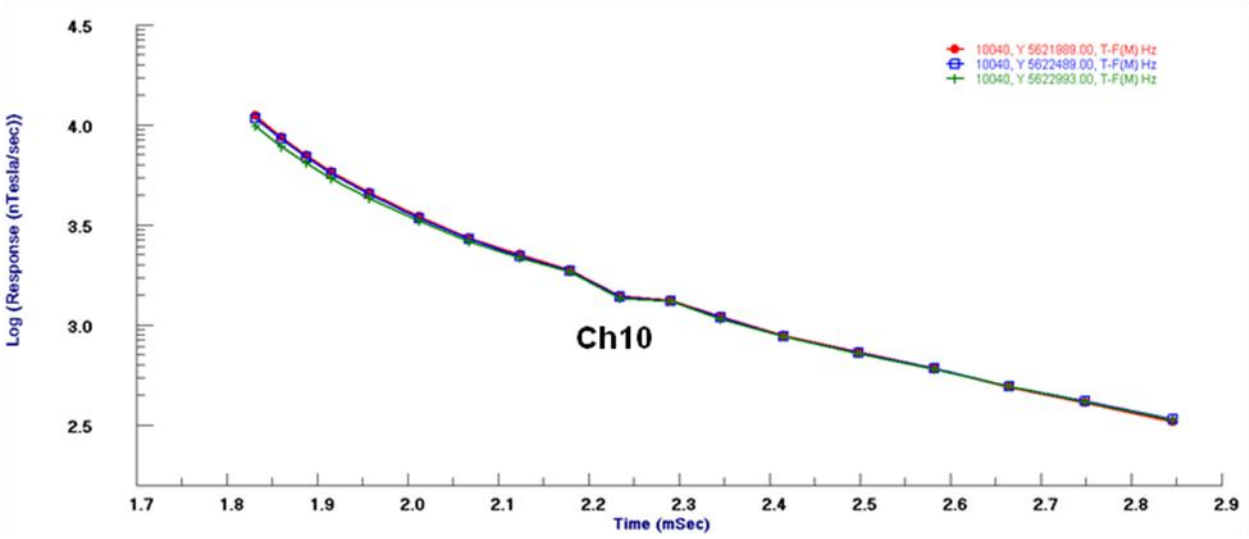

Figure 5: Three decays, 500 m apart, on Line 10040, illustrating the unusual response at Channel 10, which persists across most of the line.

In some areas, there is a rapid decay at late times often with a change in sign at very late times. An example is shown in **Figure** 6. This rapid decay is cannot be fit by modeling and is not geologic in nature. Also of note in this decay is the noise in the mid-time data.

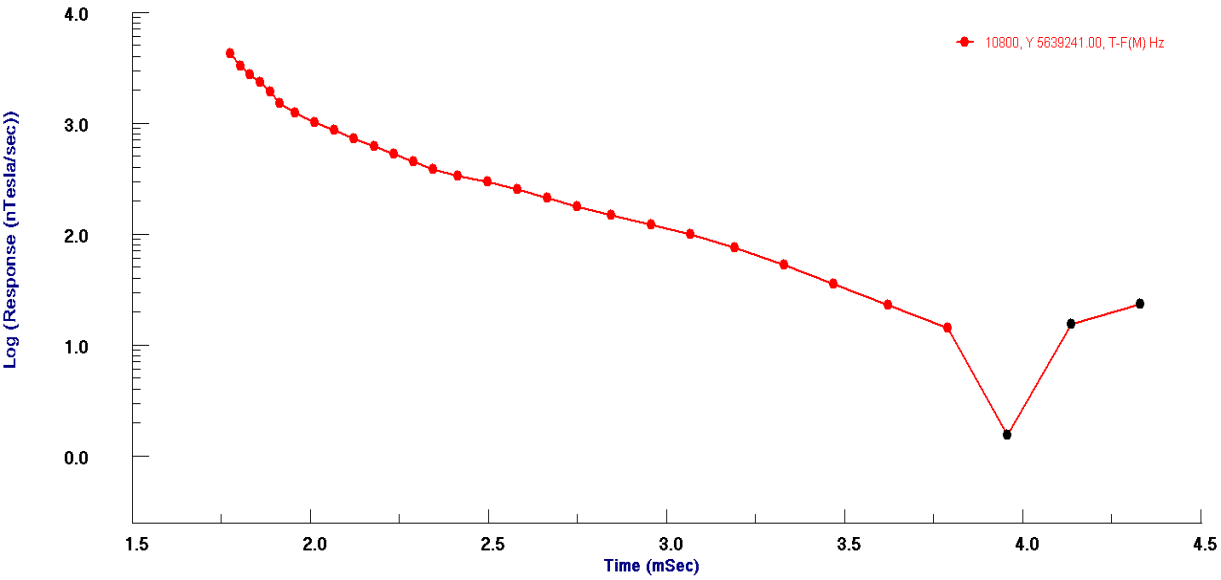

Figure 6: Measured data at 5639241 on Line 10800. This is an example of a decay in which the decay rate has become quite rapid by about Channel 24, and the last several channels are negative.

3.2 1D Modeling and Depth Resolution

Forward modeling is necessary for evaluation of the data and was used to:

1) Find the general resistivity structure in the area.
2) Determine which channels have reliable data by comparison with simulated data.
3) Examine the depth resolution.
4) Examine repeatability and consistency of the data.
5) Use the results of 1-3 to determine appropriate settings for the inversions. (Discussed further in Section 5.0)

Results for two stations are presented below and the general resistivity model and resolution are discussed.

A two-layer model was found that fits the main characteristics of the response near 5566006 on Line 20200. The model is 12 Ohm m down to 85 m depth, and a 100 Ohm m half-space below that. The model is a good fit to the data although at late times the data is somewhat is noisy (**Figure** 7).

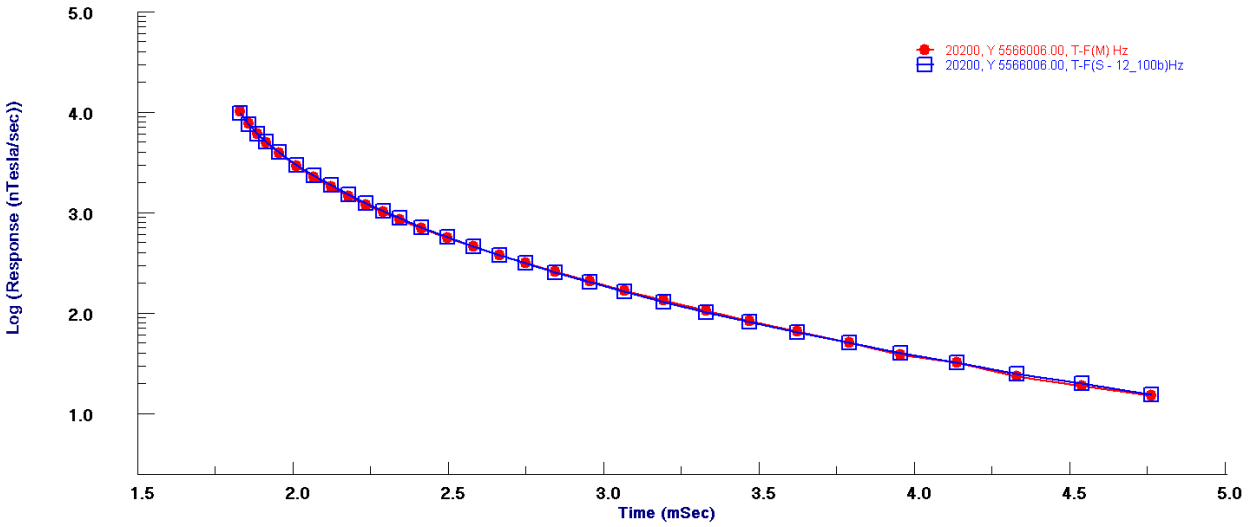

Figure 7: Measured data vs. 1D model at 5566006 on Line 20200. Channels 1-35. Model: 12 Ohm m for 85 m over 100 Ohm m.

Figure 8 compares the measured data, the model, and a 12 Ohm m half-space. While there is a slight difference in response at mid-times between the model and the half-space, the decay curves do not separate until Channel 23, i.e., this is when the currents enter the resistor. A modified version of the model, in which the depth of the resistor was increased to 110 m, was also simulated, and the results are shown in **Figure** 8. In comparing the response of this model and the half-space, it is observed that the currents enter the resistor about Channel 26. Note that due to noise in the data, it is not possible to resolve the resistivity deeper than about Channel 25 or 26. Thus, depth resolution at this station is approximately 110 m. Furthermore, the response has limited sensitivity to the basement resistivity: there is little difference between the response of a model with 200 Ohm m and 100 Ohm m as the basement resistivity, and there is negligible difference between 100 Ohm and 50 Ohm until about Channel 26.

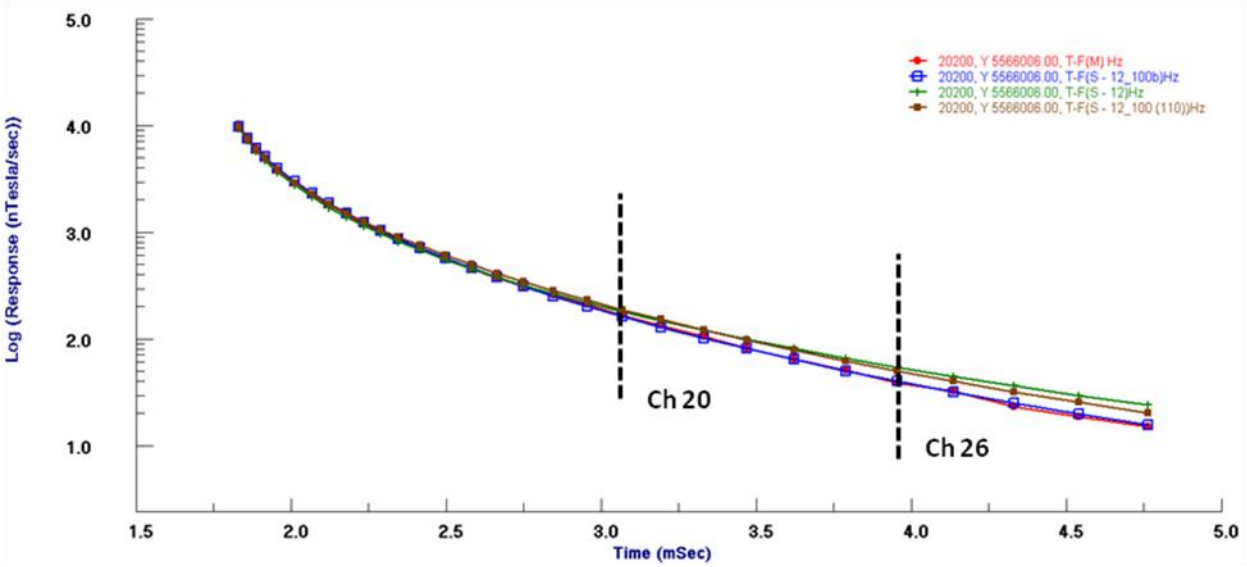

Figure 8: Measured data (red) vs. 1D model (blue) at 5566006 on Line 20200. Model: 12 Ohm m for 85 m over 100 Ohm m. Also shown is a 12 Ohm m half-space (green). The decay of the model separates from that of the half-space at about Channel 20. A modified version of the model in which the thickness of the 12 Ohm m layer has been increased to 110 m is shown in brown. The decay of this model is fairly similar to that of the half-space until about Channel 26.

Figure 9 shows the modeling results for Line 10940 at 565388. The model is composed of three layers: 20 Ohm m between 0 and 35 m, 15 Ohm m between 35 and 100 m, and a 100 Ohm m half-space below that. This model fits the data well between Channels 1 and 25. Beyond Channel 26, the decay of the model is slower than that of the data. Even increasing the resistivity of the bottom layer to 10,000 Ohm m does not lower the response of the model to that of the data at late time. Thus, it is concluded that the rapid decay at this station cannot be fit by a 1D model, similar to the decay in Figure 6. As seen in Figure 3, the decay beyond Channel 26, particularly beyond Channel 28, is noisy, and as such, it is not unexpected that it cannot be fit. In fact, in an inversion, it would not be desirable to fit this part of the decay, as it is not geologic.

Based on forward modeling results, the system is unable to resolve the resistivity structure beyond 150 m, often not beyond 120 m or so. The depth resolution is partially limited by the noise in the late time data, but is mainly limited by the low resistivity of the subsurface (typically about 15 Ohm m). Based on forward modeling results, by Channel 18, the currents have penetrated approximately 100 m in 15 Ohm m. In 30 Ohm m material, they have penetrated about 150 m by this channel.

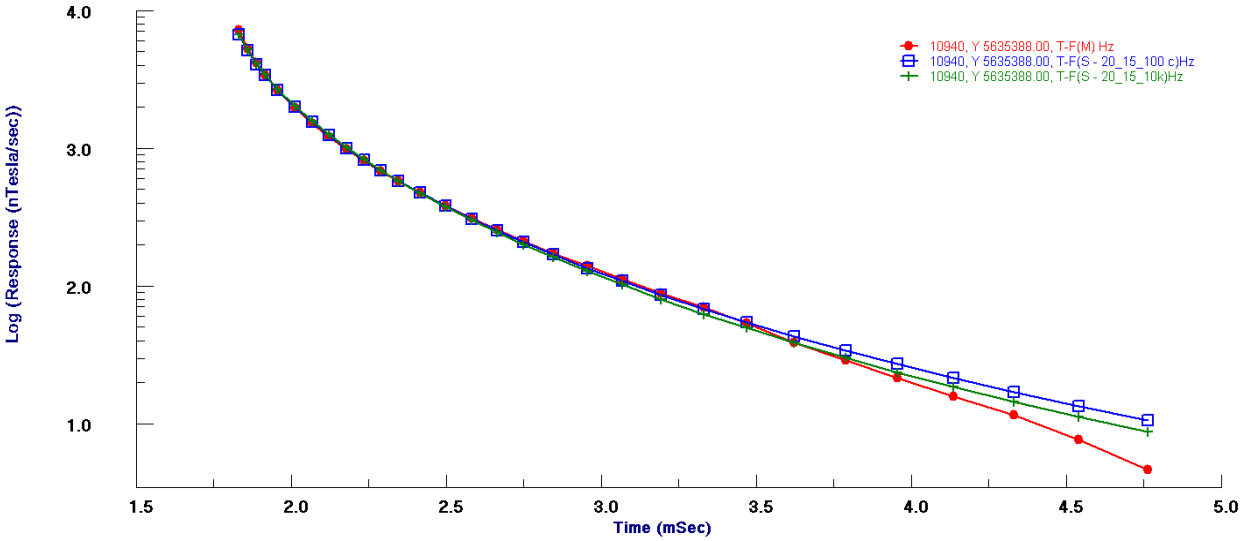

Figure 9: Measured data (red) vs. 1D model (blue) at 565388 on Line 10940. The three layer model is 20 Ohm m from 0-35 m, 15 Ohm m from 35-100 m, and 100 Ohm m below. Green is the model with a 10,000 Ohm m basement.

3.3 Refly Comparisons

Large sections of both Lines 20600 (on the edge of Areas 3 and 4) and 20760 (Area 4) were flown with both Mike and November. This enabled the direct comparison of decays at the same location for the two different systems.

3.3.1 Line 20760

There is a significant difference in the mid-late time decay (beyond about channel 14) for the two systems on this line. **Figure** 10 displays three decays for November and three decays for Mike within a 25 m stretch on the line. In this particular section of the line, the difference in altitude for the two systems is less than 1 m, so the difference in altitude would have negligible effect on the response. The decays for Mike are fairly consistent over the 25 m interval, as are the decays for November, although both are noisy beyond about channel 23. (Mike is somewhat noisier.) However, there are major differences in the decays beyond channel 14 between the two systems: November has a much slower decay than Mike.

Similar results are observed across the line. **Figure** 11 displays the profile response at Channel 20. The November data consistently have greater amplitude along the line. These results suggest a discrepancy between the mid-late time data for the two systems.

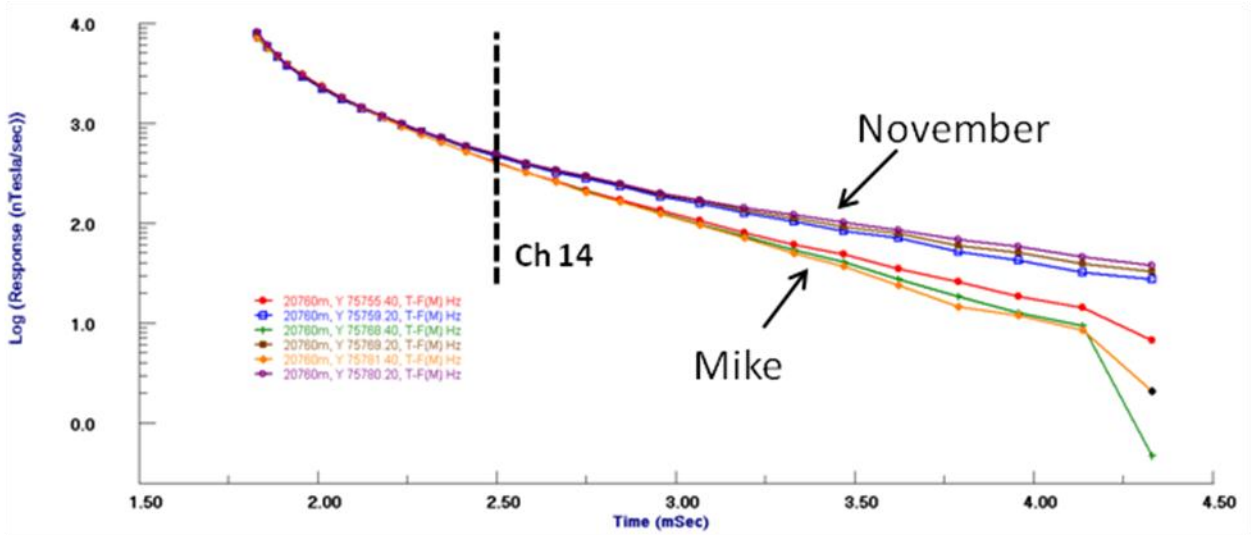

Figure 10: Decays over a 25 m interval on Line 20760 for both Mike (red, green, orange) and November (blue, brown, purple). Channels 1-28 are shown.

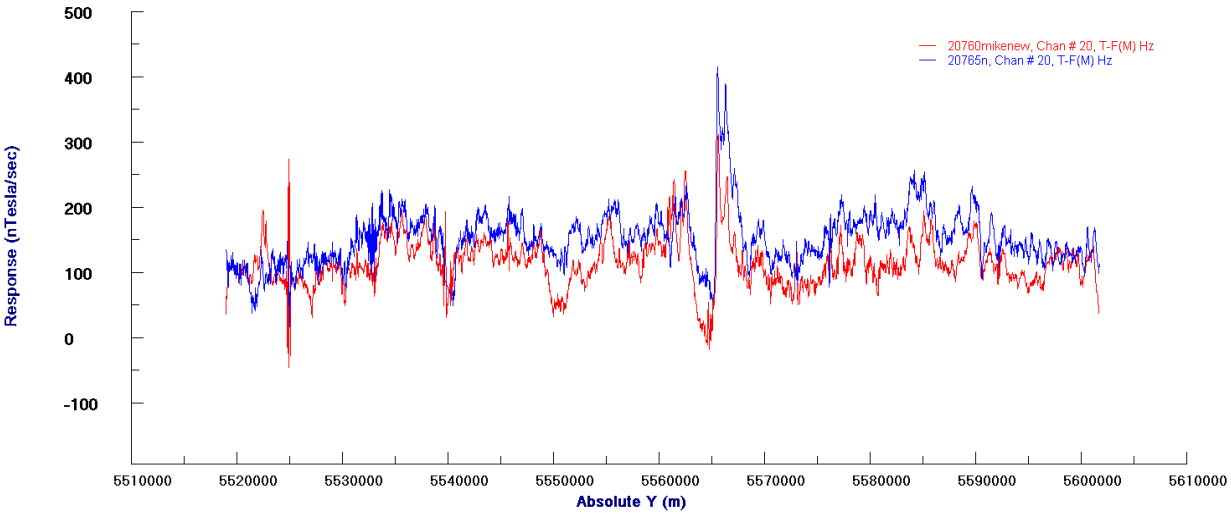

Figure 11: Channel 20 on Line 20760 for Mike (red) and November (blue).

3.3.2 Line 20600

Figure 12 displays three decays for November and three decays for Mike within a 40 m section of the Line 20600. Here, the decays are more similar than on Line 20760. There are slight differences in the response at mid-times (with Mike having a slightly lower response) and at late times beyond Channel 23 (with Mike having a greater response). The difference in the late-time response is in contrast to the results on Line 20760, where Mike had a much lower response than November.

Similar comparisons were made at other points along the Line 20600 and the results were variable. In general, the November and Mike data agreed better than on Line 20760, but differences in the decays varied depending on location.

These observations on Lines 20600 and 20760 show inconsistencies between the data from the two systems. However, the different results on the two lines suggest that there may be inconsistencies within the data collected with a given system.

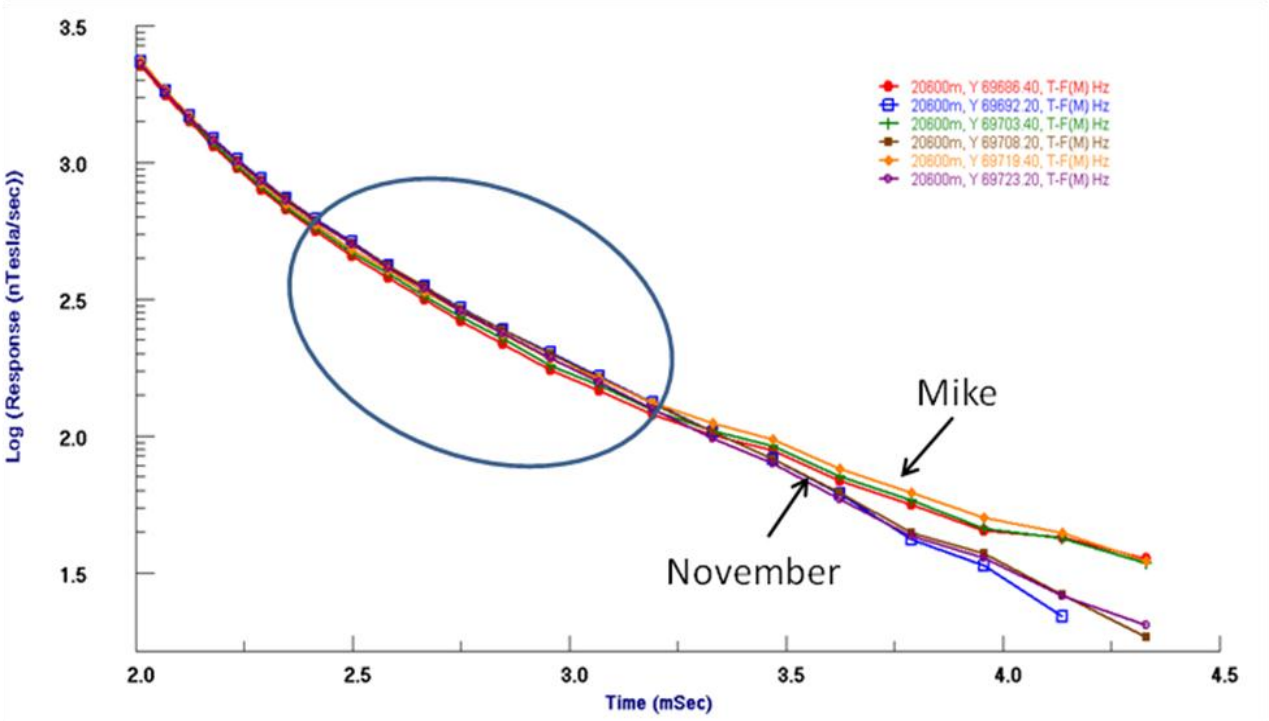

Figure 12: Decays over a 40 m interval on Line 20600 for both Mike (red, green, orange) and November (blue, brown, purple). Channels 7-28 are shown.

3.4 Decay Maps

As illustrated in Section 3.3, there is not a consistent difference in the decay between Mike and November. In fact, the mid-late time decays do not appear consistent within the data for a given system. In **Figure 13**, a decay map of off-time channels 14-18 (without tie lines) is shown for the southwest (Area 4). There are significant line-to-line effects (i.e., streaking).

This effect is more pronounced for the data collected with Mike: compare this figure with **Figure 14**, which displays the same decay for the northeast (Area 2). While there are unusual decays on a couple lines, the results are general more consistent than for Area 4.

This line-to-line variation cannot be caused by different altitudes of the system (which have minimal effect by this point in the decay) or by geology.

A ground calibration site would have assisted in understanding the issues with the decay. While at present it is clear that there are inconsistencies in the data, it is not clear which of the decays are correct.

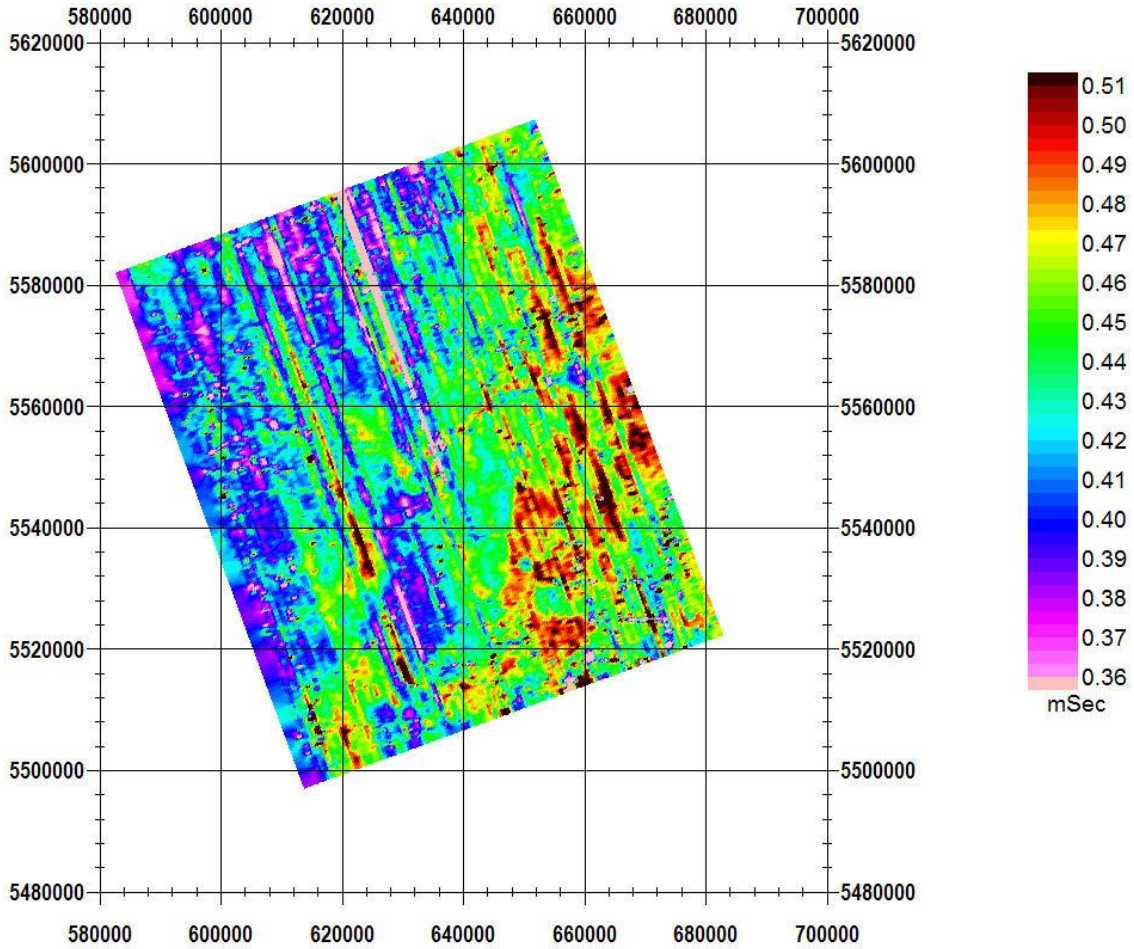

Figure 13: Decay rate (tau) between channels 14 and 18 for Area 4.

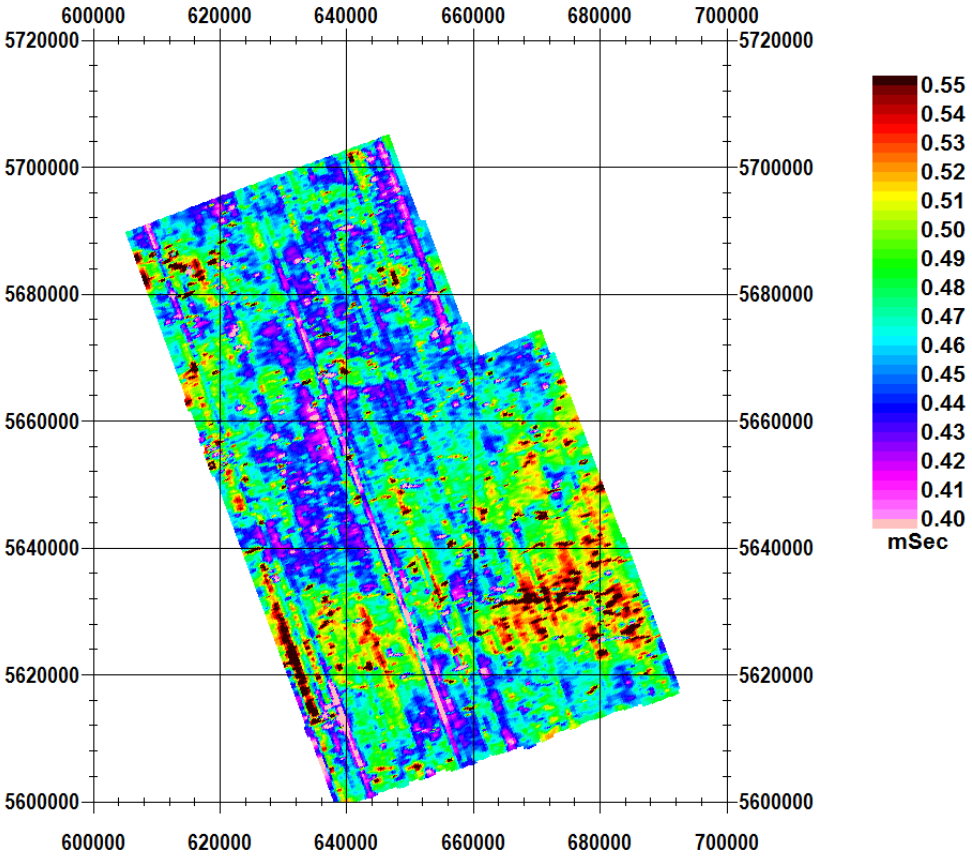

Figure 14: Decay rate (tau) between channels 14 and 18 for Area 2.

3.5 Tie lines

Tie lines, perpendicular to the survey lines, were flown at a spacing of 7.5 km throughout the survey area. The intersections of the tie lines and traverse lines were compared. Care must be taken in comparing the early-time amplitude as these are affected by the altitude of the system, which may be different on the traverse and tie lines. However, by mid-late time, the currents are deeper in the subsurface and the variation in altitude of the system has little effect.

It was found that at some of the intersections, the tie-line and traverse-line data were reasonably similar, while at other intersections, there were significant differences in the amplitude of the data. We estimate that at approximately one-third of the intersections, the data were similar. Another one-third had small differences in the data, and the remaining third had significant differences.

Figure 15 displays the tie and traverse line intersections over sections of tie Lines 19110, 19120, and 19130. The tie and traverse lines show the same general trends in amplitude, but some considerable differences are noted. For example, at (1), the data has lower amplitude on the tie line than on the traverse data over several lines. Other examples of intersections where the tie and traverse-line data disagree are marked by 2-5.

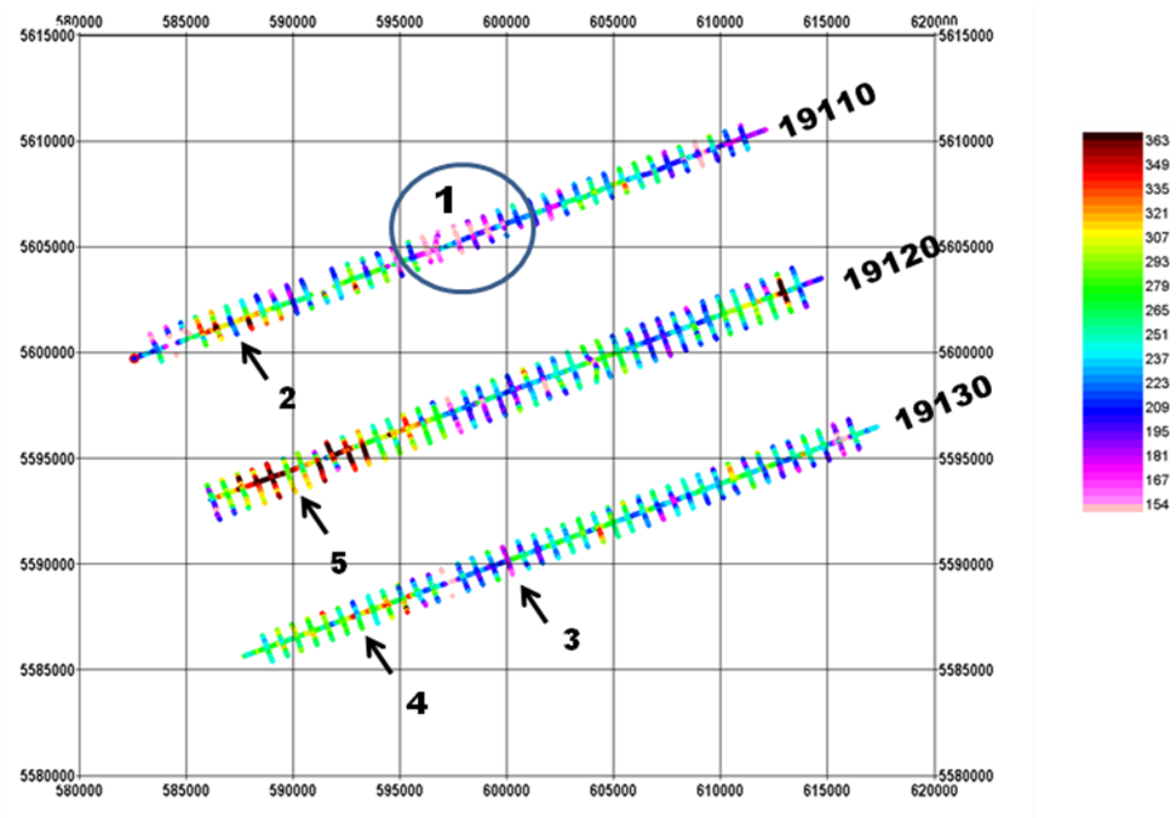

Figure 15: Traverse and tie line intersections over a section of tie lines 19110, 19120, 19130. Data for Channel 16 shown. 1-5 highlight some of the areas where significant differences at the intersections.

3.6 Summary of Data Quality Issues

1) Noise in late time: Data beyond Channel 26 is not usable in the inversion. Even if the data do not appear noisy, the fall-off is frequently too rapid to be fit with a model. Negative values are often observed.

2) Repeatability of mid-late time decay. As observed on Line 10760, different decays are frequently observed in the repeats. Furthermore, in examining grids of the decay, significant line-to-line effects are observed.

3) Noise in mid time: Variable noise in mid-time data. Some may be related to man-made structures. In some cases, a single channel will appear to be inconsistent with the rest of the decay over an entire line.

4) Significant cultural noise in the data. Many towns are within the bounds of the survey. The data to the northwest is quite noisy on several lines; this is likely due to the proximity to Calgary. Power lines and highways also affect the data in some areas.

4.0 Data Processing for Inversion

The traverse-line data were delivered to Petros Eikon in four blocks as processing was completed. The division of the survey area into blocks is shown in **Figure** 16. Each of these four blocks was prepared and inverted separately. Tie lines were inverted independently of the traverse lines.

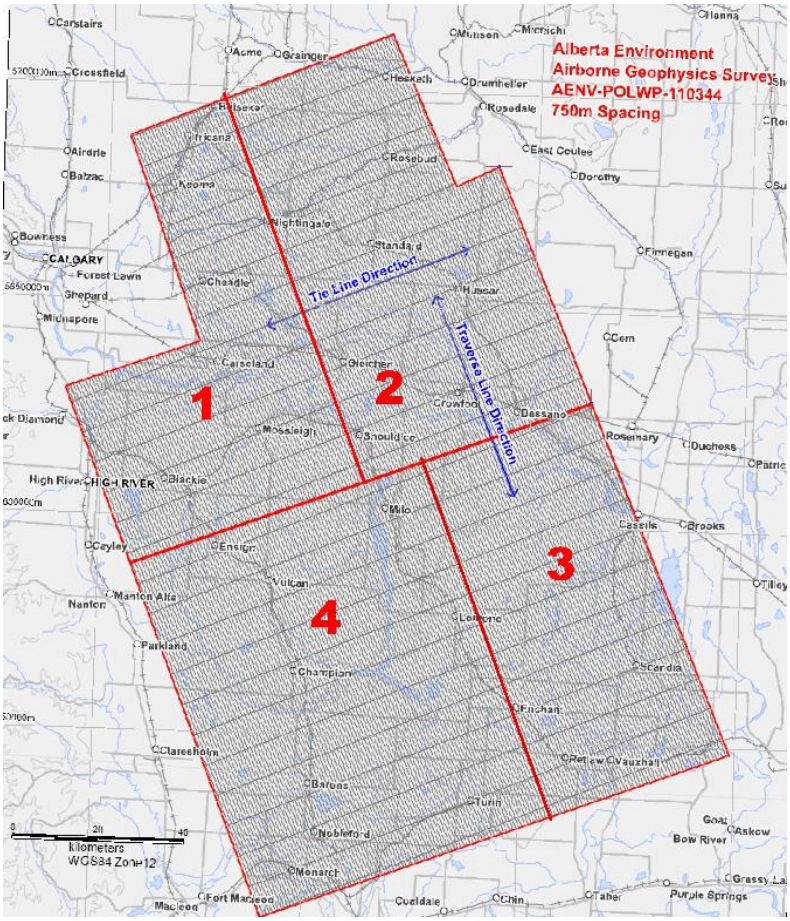

Figure 16: Division of survey area in four blocks.

Prior to inversion, a block of data was prepared by:

1) Merging survey lines that were flown in multiple flights. For example, Line 10050 was flown in two pieces: 10050 and 10051. These were merged and the overlap area cleaned to produce a single line.

2) Removal of data affected by power lines and other manmade features (e.g. cities). The data over these features is quite noisy and cannot be fit by the inversion. The power lines were removed with the aid of a) the power line monitor channel provided with the data and b) maps of major power lines. Typically a swath of data about 1 km wide was removed around a major power line.

3) Decimation and filtering of the data. The sampling along the line was 2.5-3 m. A statistical decimation was applied to increase the sampling to about 15 m. As the system is 35 m above the surface on average, inversion of the data at the original sampling is not meaningful. Following the decimation, a Gaussian filter was applied to the data to reduce noise in the late-time data. A filter with a width of eleven data points and a standard deviation of seven points was used.

4) Removal of stations flow at very high altitude, as well as stations without positional information.

5.0 Inversion of Data

5.1 Inversion technique

The data was inverted with EMIGMA v8.5. A Marquardt inversion was used. This is an underparametrized 1D inversion that allows for inversion of both the thickness and resistivity of each layer. An appropriate starting model is determined through forward modeling, and upper and lower bounds for both resistivity and thickness can be specified separately for each layer. A Marquardt inversion was used rather than a smooth, overparametrized inversion to allow identification of discrete layers.

Rather than finding a single 1D model at each station, a multi-station approach was used: a single inversion model was found for three consecutive stations along the line. Once a model was found for these stations, the following group of three stations was inverted. Following decimation of the data, station spacing was approximately 15 m, and so three stations cover roughly 45 m along the line. Given the instrument height was about 35 m, a window of 45 m was considered appropriate. The advantage of the multi-station approach is that it reduces the effect of geologic noise (i.e., small-scale structure that is not of interest), and instrument noise.

While it is possible to use a greater number of stations in the multi-station inversion, this would entail finding a single 1D model over a greater distance. Some tests were completed with five- and seven-point windows for the multi-station inversion. However, the results did not improve on the results for the three-point window. Furthermore, where the geology changes rapidly, a single model does not fit all stations across a distance of 100 m (seven-point window). Thus, it was decided that a three-point window was most appropriate.

5.2 Determination of inversion settings

Similar, but slightly different, settings were used to invert the four blocks of data. Inversion settings were determined based on:

1) Forward modeling results: both the range of 1D models in a given block and assessment of data quality through comparison with simulated 1D models.

2) Test inversions on a couple lines in a given block.

5.2.1 Time Windows

Thirty off-time channels were delivered by Aeroquest. The late time data were similarly not used in the inversion because the data were noisy. Inversion of noisy, late-time data can result in the inversion trying to fit aspects of the decay which are not geologic, but caused by the system.

Data beyond channel 26 was noisy throughout most of the survey. Data between channels 20 and 26 was of variable quality: in some areas, decays were relatively clean to channel 26 while in other sections of the data, decays were noisy by channel 26 or earlier.

The data were inverted either to channel 25 or 26 depending on the area. The data was inverted down to these channels rather than only to channel 20 to maximize depth resolution where the data were clean.

5.2.2 Starting Model

For each block, 1D models were found at several points on a couple different lines. Following the forward modeling, a representative model from the 1D models across the block was chosen as the starting model. Through test inversions, it was found that a four-layer model usually resulted in the most consistent results along a given line, and that four layers (three layers over a half-space) were needed to fit the data well in some areas.

5.2.3 Constraints

Appropriate constraints on the thickness and resistivity of each layer were based on the variation in 1D models across the block, and these were later refined following test inversion runs.

In initial tests, all thicknesses and resistivities (seven parameters total) were inverted. However, it was determined that the results were improved if the resistivity of the deepest layer (100 Ohm m resistivity for all four blocks) was not inverted. The reason for this is that the data are not very sensitive to the resistivity of this layer, as illustrated in Section 4.0. Fixing its resistivity resulted in cleaner inversion results that fit the data just as well as inversions in which the resistivity of this layer was not fixed.

While constraints varied slightly between blocks, the resistivities of the upper three layers were typically bounded between 3-6 Ohm m and 70 Ohm m. The top layer was constrained to be quite thin. The next two layers were constrained to be up to 100 m or more (depending on the block). Thus, in areas where the data cannot resolve the resistor, the top three layers are permitted to be thick enough such that the response is not sensitive to the fixed 100 Ohm m layer.

5.2.4 Misfit and Iterations

A misfit of 6.5% was used for the inversions. It was found that the inversion often had difficulty fitting the data better than 6.5%, and so using a lower misfit would have significantly increased computation time. Using a 6.5% misfit was necessary to deliver the inversion products on time. Had there been more time to complete the inversions, a misfit of 3-4% would have been used in areas where the data was relatively clean. This would have yielded inversion results that better fit the data in some places. However, a lower misfit would not have been appropriate in areas with noisy data at mid-times (particularly within the Mike data). In these areas, if the inversion was able to reduce the misfit below

6.5%, the results may not have been meaningful, as the inversion may have been trying to fit the noise in the data.

If the misfit was not reached, the maximum number of iterations was set as ten because it was found that the misfit did not usually improve beyond ten iterations.

5.3 Delivery of Inversion Results

Following inversion of traverse data and tie line data, the traverse and tie line inversions were merged for each of the four blocks. Depth slices, both with and without the tie lines, were created at 5 m intervals between 0 and 175 m below surface. These were provided both in .gdb and .qct (QCTool) formats as well as Geosoft grid files (.grd).

Inversion sections along each traverse and tie line are also available in .gdb (two or three files per block) and qct (one file per line) formats.

5.4 New Shallow, Smooth Inversions

The inversions were rerun a second time to produce cleaner images. Channels 2-18 were inverted so that the inconsistencies in the late-time decays would have less effect on the result on the inversions. Channel 1 was not inverted as well, as this channel was often inconsistent with the rest of the decay.

A three-layer starting model was used for all areas: 25 Ohm m (to 43 m), 10 Oh m (to 93 m) and 100 Ohm m below. The use of three layers rather than four layers removed a significant portion of the streaking in the inversion results. Further discussion as to the reason for these setting is provided in Section 6.0

The data were decimated further to produce in station spacing of roughly 50 m. A multi-station technique was not used i.e., a model was found for the data at a single station. The misfit was dropped to 4% due to the removal of the late channels, which were noisier, from the inversion

References to the inversion results in this report refer to the original inversions unless otherwise specified.

6.0 Results

Based on examination of the data and the inversion results, the survey was evaluated in terms of its ability to meet AENV's objectives. Several issues with the inversions are discussed by area below. The majority of the survey area is within Vulcan and Wheatland counties, and references to the Regional Groundwater Assessments for these counties are made. Lithological and geophysical logs within Wheatland (both in Area 1 and Area 2) were provided by AGS, and these are referenced as well.

6.1 Area 1 (NW)

6.1.1. Geophysical Logs vs. Inversions

6.1.1.1 Log 111837

Figure 17 displays the location of drill log 111837 within Wheatland county and the nearest survey line. The drill hole is very close to the survey line: the nearest location on the survey line is 40 m west of the drill hole. The resistivity log for this hole is shown in **Figure** 18.

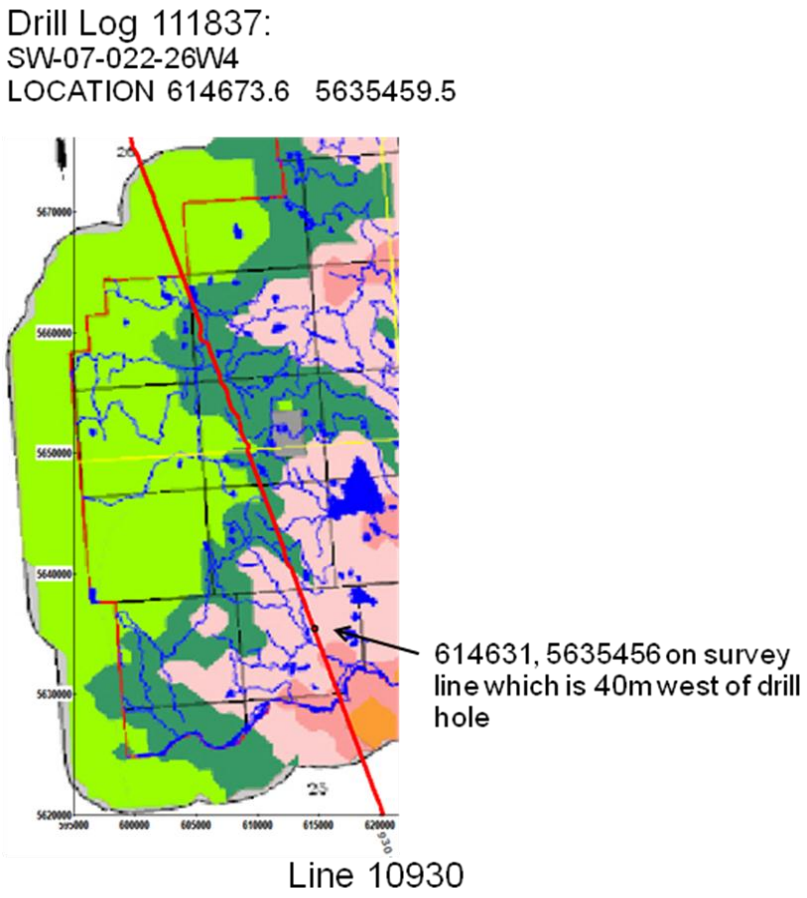

Figure 17: Western portion of Wheatland County (from HCL, 2003), showing the location of Line 10930 and drill hole 111837 (SW-07-022-26W4, at 614673.6, 5635459.5 in 10TM).

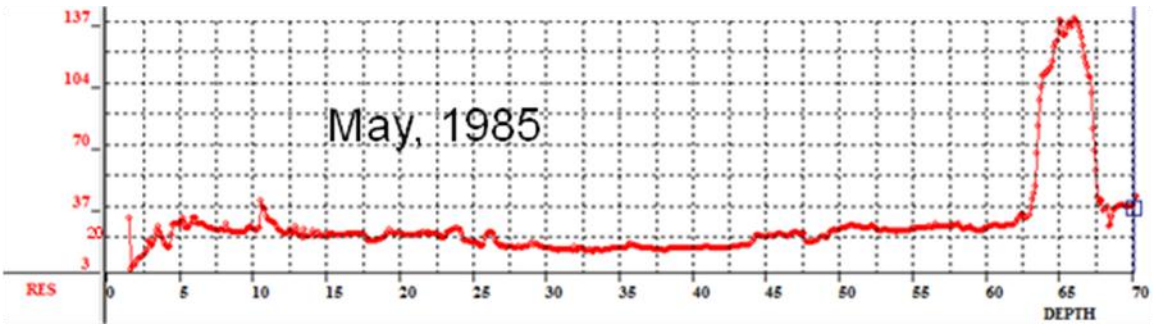

Figure 18: Resistivity log for 111837 (location shown on previous page). Resistivity data collected to 70 m depth in May 1985.

Data at Station 5635456 is shown in red (**Figure** 19) with the response of a model which closely approximates the resistivity log shown in blue. It is seen that while the shallow resistivities reflect the data, it would appear from the data that the ground is significantly more conducting at intermediate depths than represented by the log, as the log model has a smaller amplitude than the data beyond the early channels.

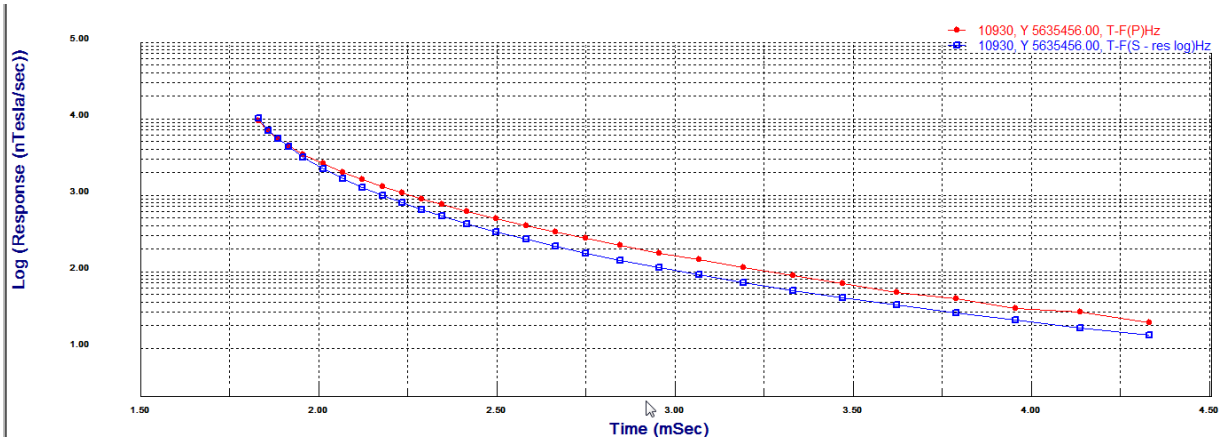

Figure 19: Data at 563456 in red and response of a model which closely approximates the resistivity log (Figure 18) in blue

The model that fits the data well is slightly less resistive than the resistivity log across the entire depth but the data require a conductive zone just below where the log ended. The resistor shown in the log at about 65m depth may or not be there as far as the data are concerned. The system is not sensitive to such a thin resistor at this depth. Additionally, the model requires a somewhat more resistive basement than 40 Ohm m, but the data cannot resolve this parameter well. This is partially because we were unable to use data channels later than 4.33msec and partially because of the low resistivities found in the top 70m of the geology, which limits the depth resolution (discussed earlier). **Figure** 20 displays the fit to the inversion model at this station.

The inversion section along a 1500-m length of Line 10930 is shown in **Figure 21**. As the basement resistivity is not resolvable, all resistivities about 80 Ohm m are shown in black.

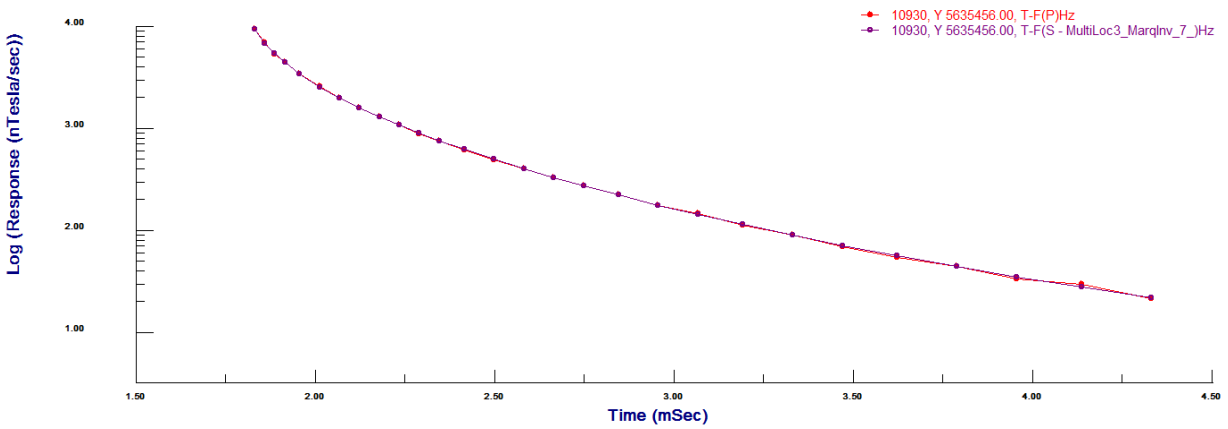

Figure 20: Data at 563456 in red and response of an inversion model which fits the data.

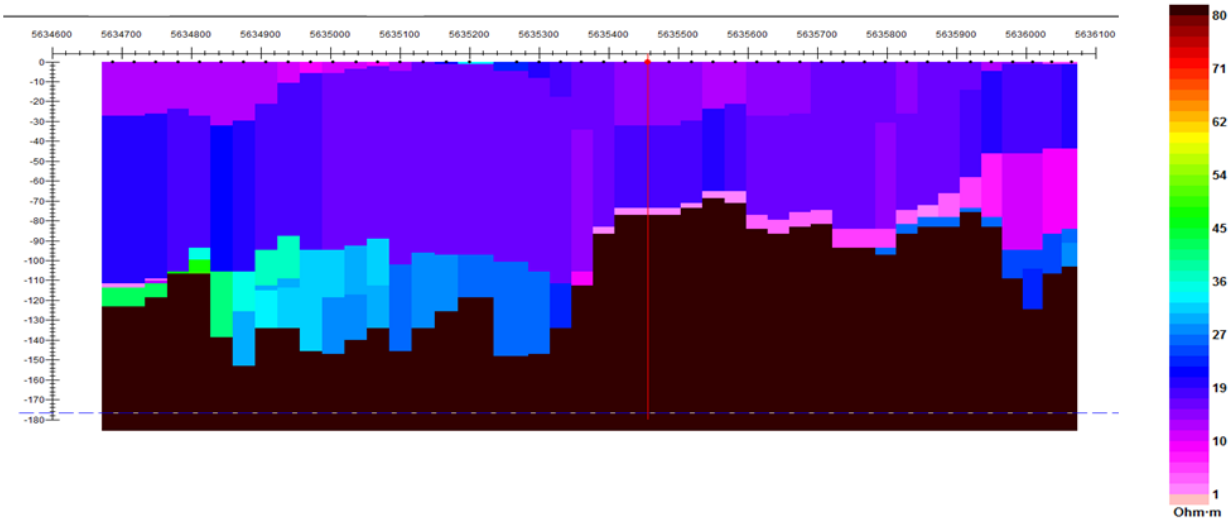

Figure 21: The inversion section is shown along the survey line (10930) for about 1500m. The location of the station proximate to the drill hole is shown by a red line.

6.1.1.2 Logs 111857 and 111858

These logs are from the same drill hole but read one month apart. The resistivities between logs bear no resemblance to each other. However, the March 1985 resistivity data (111857) is entirely implausible when compared to resistivities observed in other logs and from the AEM data. Log 111858 indicates a thin (2m) cover of about 15 Ohm m and then an almost constant resistivity of approximately 31 Ohm m to the bottom of the hole at 68.5m. There is a thin increase of about 20 Ohm m just before the bottom of the hole.

Figure 22 displays the data at the closest AEM station to the drill hole (a few hundred meters west). This is compared with the response of a model based on the well log, as well as the response of the inversion model. In this case, the inversion model indicates a few meters of 60 Ohm m material followed by a deep section of material at about 15 Ohm m to a depth of about 130m, and below that is the

unresolveable resistor. In general, we believe the resistivity log and the AEM do not disagree with each other as logging instrument will not produce exactly the same resistivities as the EM due to the difference in the physics associated with each instrument.

The remainder of the drill logs in Area1 for Wheatland County does not contain resistivity logs.

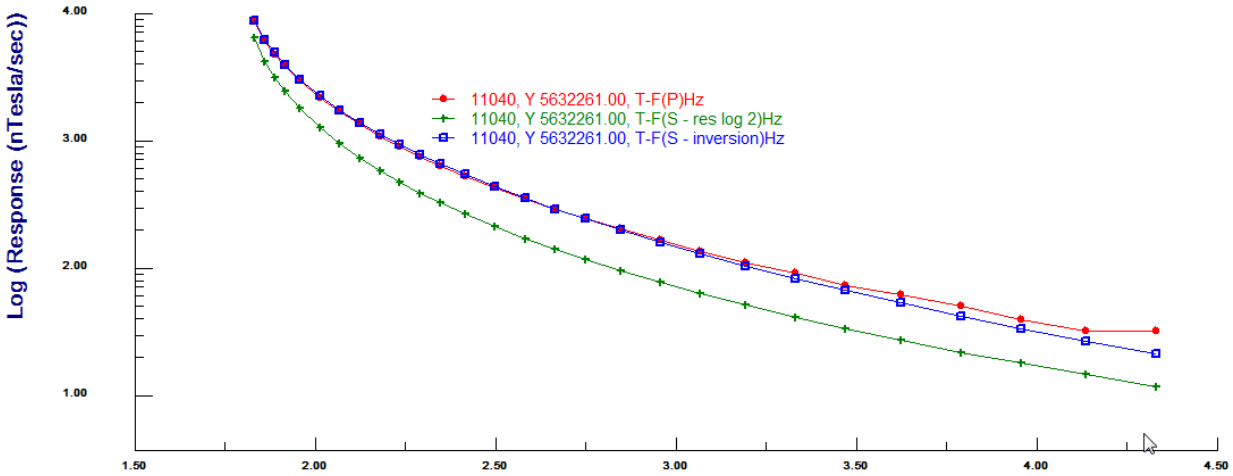

Figure 22: Data (red) at the closest AEM station from 111857/111858 (a few hundred meters west). The response due to a model as represented by the well log is shown in green while blue is the response of the inversion model. In this case, the inversion model indicates a few meters of 60 Ohm m material followed by a deep section of material at about 15 Ohm m to a depth of about 130m. Below that is the unresolveable resistor.

6.1.2 Depth Slices and Shallow Discriminatory Resolution

An example of a shallow depth slice (15m) for Area 1 is shown in **Figure** 23. There is streaking in the inversions, which is highly correlated with the flight paths. To examine this issue, we will look closely at two neighboring lines, namely 10930, which passed near the first drill log for this area, and line 10920 to the west. The area in the vicinity of the well is shown in the inset in **Figure** 23.

Figure 24 displays the depth slices over this sub-section of Area 1 at 15 m, 50 m, and 60 m. From the drill log resistivity (5.1.1.1), the resistivity is quite constant to a depth of 60m. Line 10930 agrees with this result although resistivities are somewhat lower than in the drill logs. Line 10920, however, indicates a resistor at intermediate depths. The reasons for these results are examined in further detail.

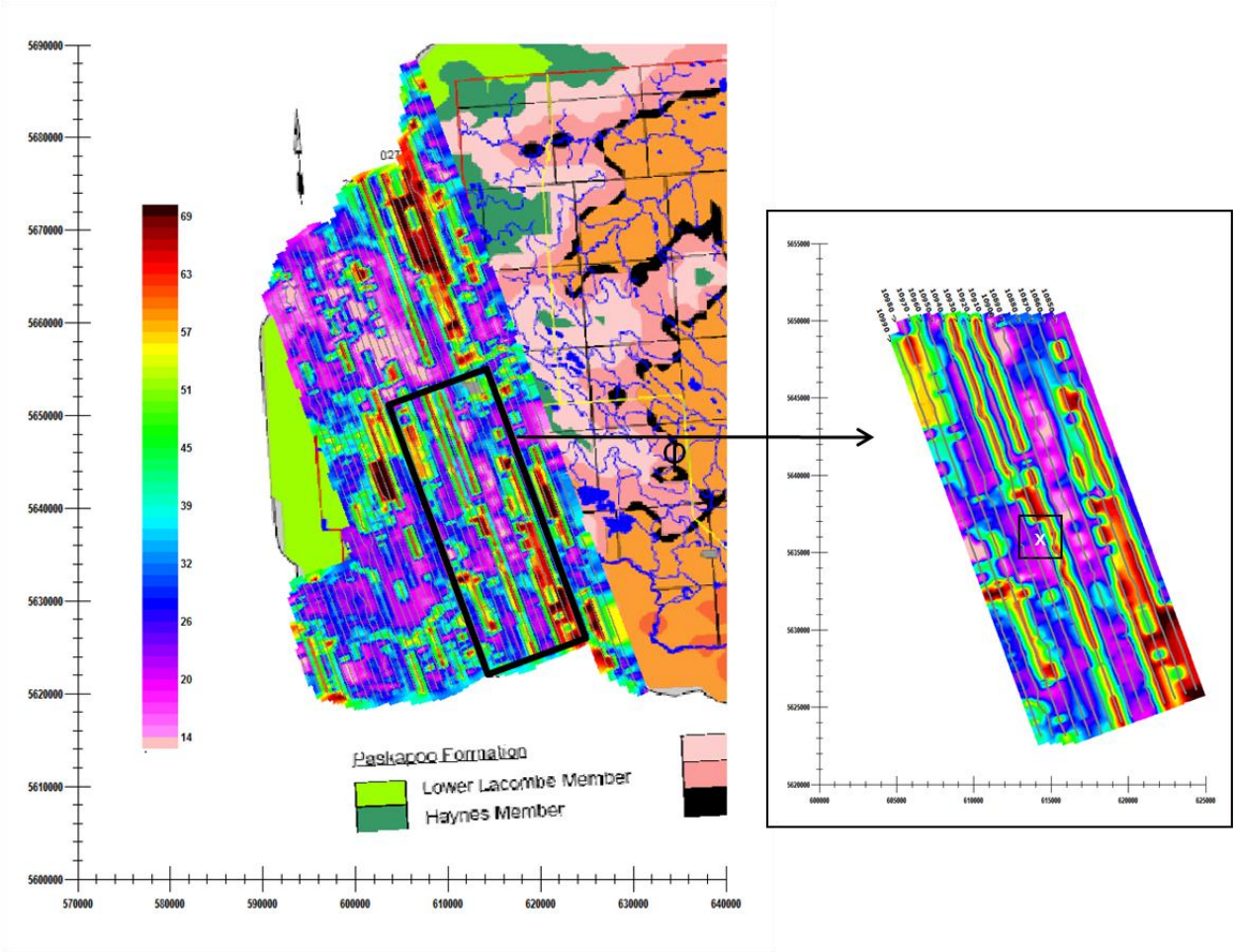

Figure 23: Depth slice for Area 1 over Wheatland County at 15 m. Inset is a close-up near 111837.

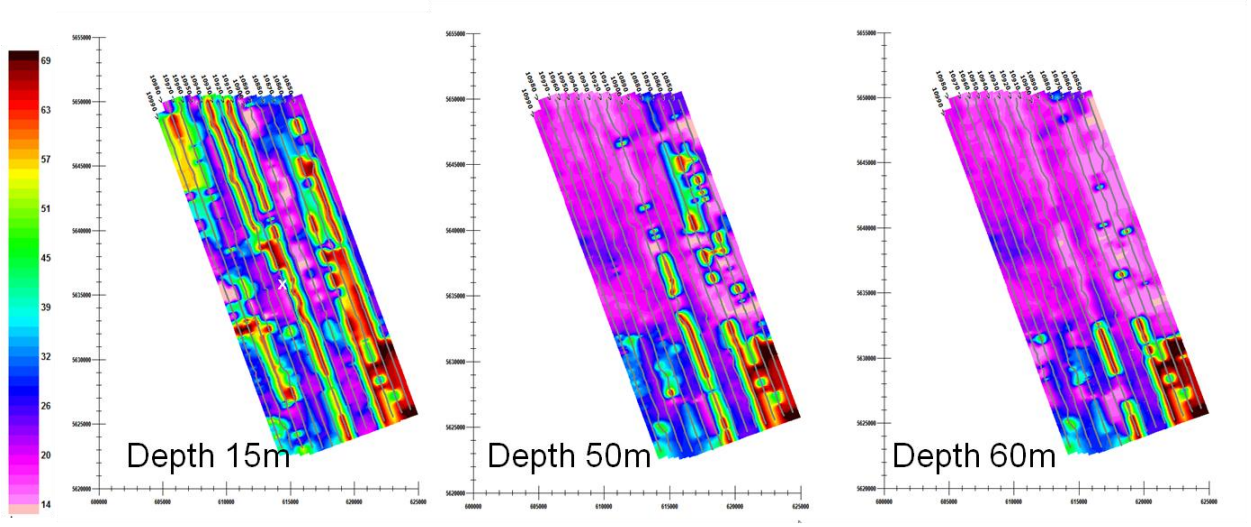

Figure 24: Depth slices over a subsection of Area 1 at three depths.

Figure 25 displays the inversion results over the southern sections of Line 10920 and 10930. A smaller section of each line (about 1 km) is shown in **Figure** 26.

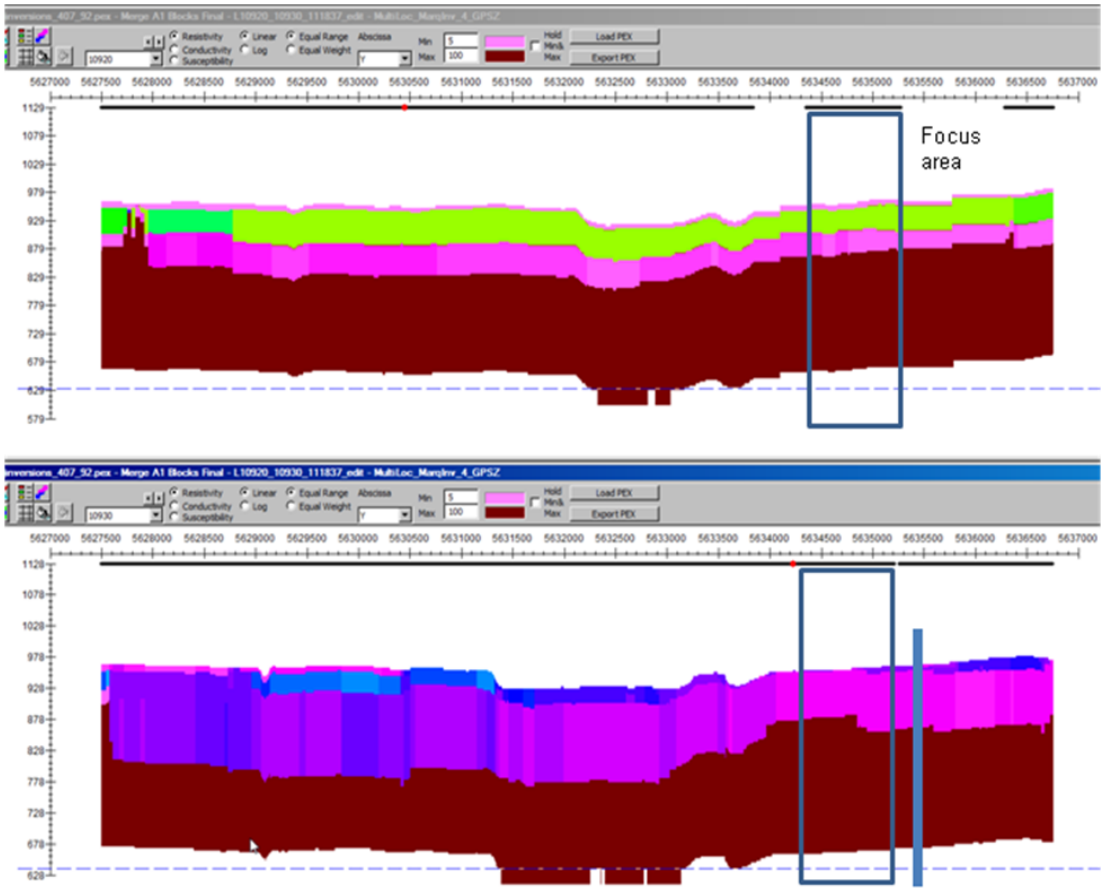

Figure 25: Southern sections of Line 10920 on top and 10930 on the bottom. Plotted in the same resistivity range. Location of well shown in grey-blue. There is little difference in topography on the two lines. Line 10920 is missing a section near the south due to noise effects. We will focus on the area between 5634350 and 5635240N.

In **Figure 27**, the data at a group of stations over 100 m over the central part of the focus area are shown for both lines. The data on Line10930 are remarkably similar in early and mid-times over 100m. The variation in late time must therefore be noise. This illustrates the difficulty in discrimination at depth as discussed previously. The data on L10920 begins to vary significantly in late-early time. This indicates either higher noise levels or a dramatically more complex shallow structure under this line. But of most importance significance in the variation in the inversion model is due to the amplitude of the first time channel. The first time channel in the above figure is significantly larger for L10920 (14125) over L10930 (11220). However, the second channel is very similar on the two lines (8510 vs. 8310). This would necessitate a more conducting top layer under L10920 followed immediately by a more resistive layer in order to bring the data to L10920 levels. Thus, the results hinge upon how to utilize Channel 1 as well as how much to force the middle time channels which have different levels of noise.

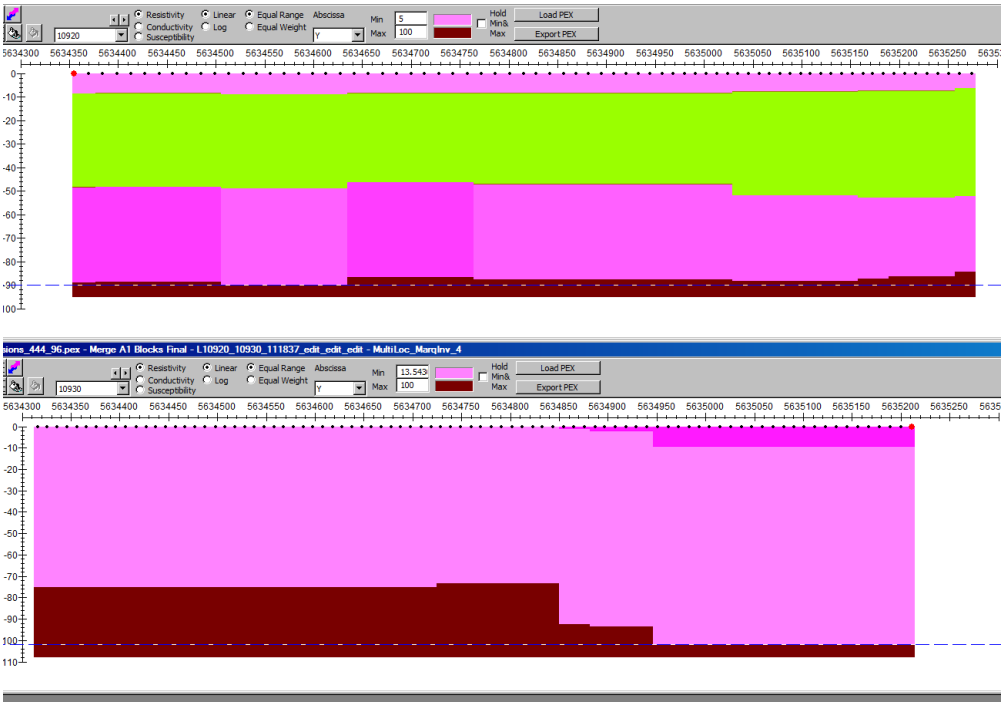

Figure 26: A focused southern section of Line 10920 on top with respect to ground level with L10930 on the bottom. Plotted in the same resistivity range. The well is just to the south of the shown areas.

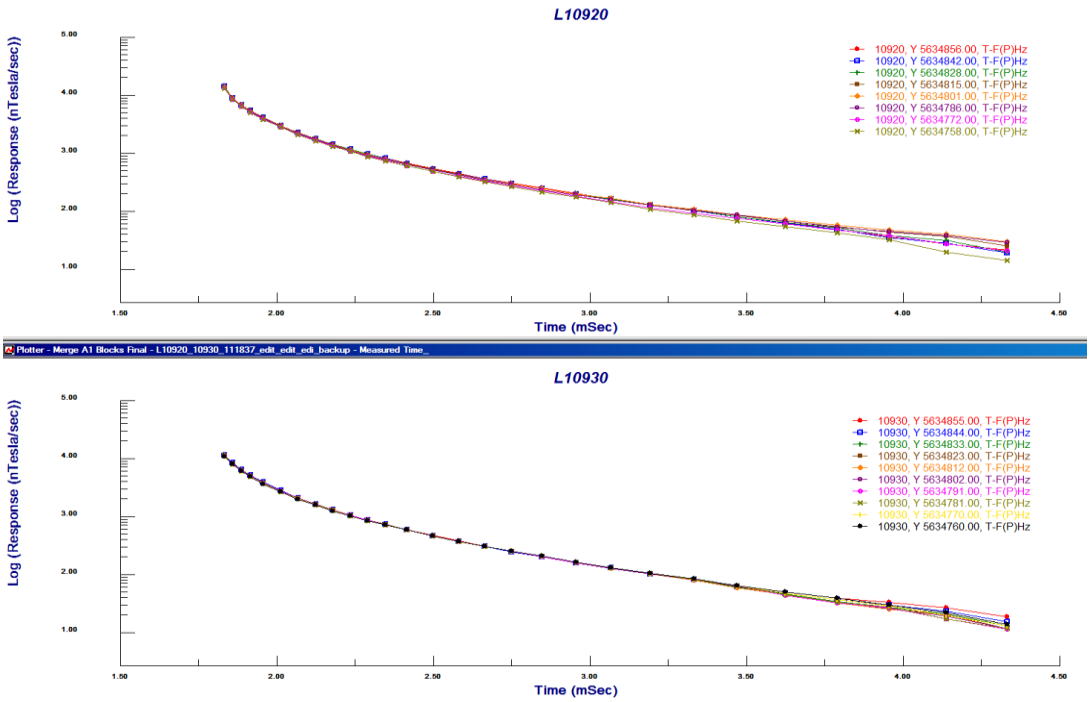

Figure 27: Data is shown at a group of stations covering approximately 100m over the central part of the focus area. Line L10920 at top and Line10930 at bottom.

6.1.2.1 Discussion of Inversion Settings for Area 1

Batch inversion settings for Area 1: Area 1 was inverted in large batch processing mode with channels 1-25 and a target misfit of 6% with a spatial weighting window of approximately 50m. It was generally chosen to utilize Channel 1 throughout the inversions as it provided shallow discrimination. A smaller misfit posed two problems: a) generally noise levels varied a great deal and attempting a smaller misfit in noisy errors provided problematic and b) time constraints generally would not have allowed us a smaller misfit as calculation times for each area extended from about 300 CPU hours to about 1200 CPU hours. A larger spatial weighting window proved difficult due to a) computation times and b) problems around man-made infrastructure.

Numerous inversions were performed over this area to examine the effects of:

1) Starting Model: All starting models contained 3 layers of varying thicknesses over a resistive basement of 100 Ohm m. All starting models consisted of a relatively conducting cover and a conducting third layer but the staring model for the second layer was either a resistive or a conducting layer.
2) Constraints on the layers. All top three layers were constrained to be between 2 and 70 Ohm m but for some tests the second layer was allowed to increase to 100 Ohm m.
3) Utilized time channels: Two main aspects were studied: a) the use of Channel 3 and the use of Channels 23 to 27.
4) Level of Misfit: The level of misfit was examined between 1% and 6%.

The most relevant factors were a) use of Channel 1 and the constraints on the second layer. The resistive layer could be produced on L10930 and as well it could be removed from L10920. Generally speaking, it is normal that a resistive layer wedged between two conductive layers is difficult to resolve. CDI techniques, for example, have great difficulty with this type of model as they depend entirely on decay rates and not amplitudes. With a proper inversion technique which utilizes both amplitude and decay rates generally the resolution of a wedged resistor is possible. However, it requires extremely reliable data in the appropriate time channels. In this case, Channel 1 is crucial as are the noise levels in Channels 3-10 which are not provided by this data.

As an example, we show the results of one inversion which does not utilize Channel 1 (**Figure** 28). In this case, the results are somewhat opposite. A thin slightly resistive layer is resolved on L10930 while a resistive layer is only slightly indicated on L10920. For this inversion, Channels 1 through 24 were used, a starting resistivity for layer 2 of 65 Ohm m which was allowed to increase only to 70 Ohm m, single station rather than spatial window, and a target misfit of 2%.

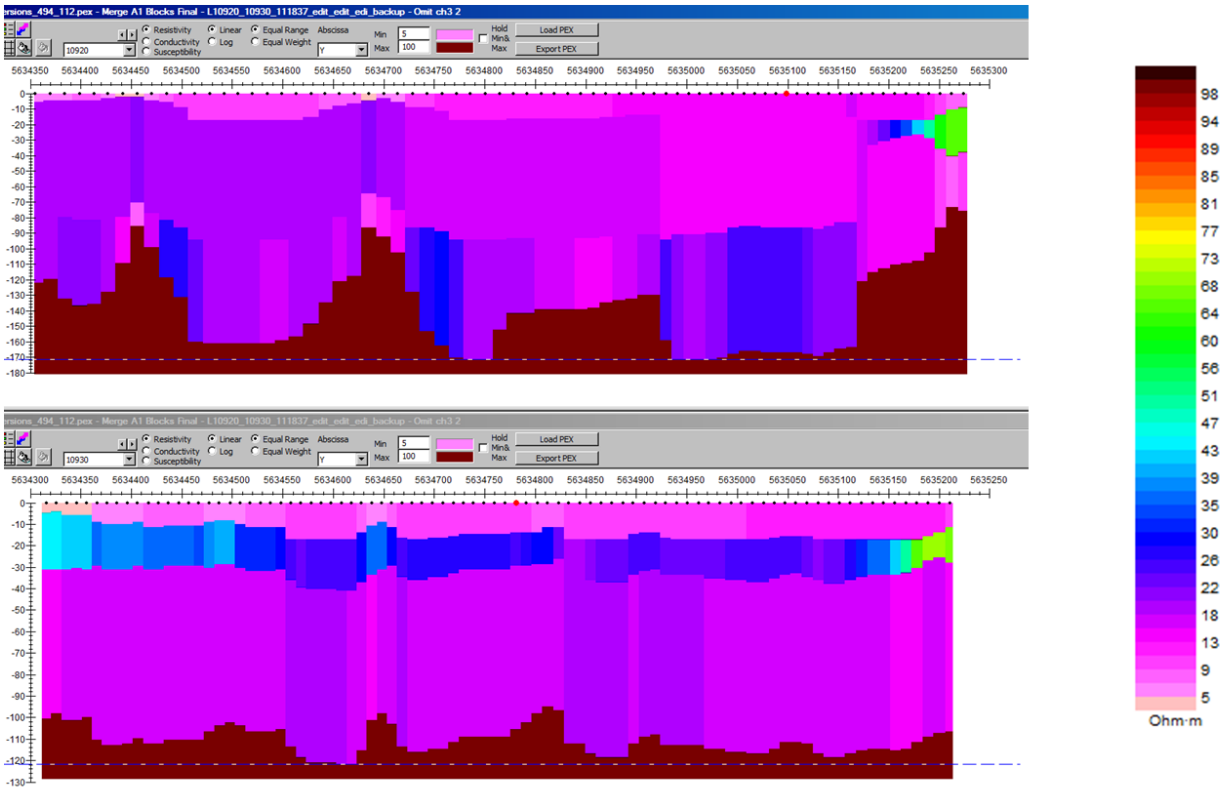

Figure 28: Inversion on Lines 10920-10930 without inverting Channel 1.

6.2 Area 2 (NE)

In this region, the basement is the sedimentary rocks below the drift. The geology is shown in **Figure** 29. Resistivity logs in the area were provided, and most of the geophysical logs are from the 1970's.

6.2. 1 Discrimination within the Basement

In this area, the upper basement formation is generally Horseshoe Canyon. Upon studying these logs in conjunction with down hole lithological picks, it was found that there was no discrimination between the different lithologies (sandstone, shale, siltstone) within the basement.

Furthermore, in two nearby holes, it was observed that there was little correlation between the lithologies in one hole and those in the other. In one hole (9239449), lithology between 20 m (thickness of cover) and 85 m depth is listed chiefly as siltstone, whereas in nearby hole 9239460, which is about 200 m away, the lithology is predominantly sandstone and shale at the same depths (**Figure** 30). Thus, it appears that the differences between these lithologies are subtle and identification depends largely on the interpreter. From this point of view, it is not surprising that they cannot be distinguished in the resistivity logs. Note: formations are not identified in lithological logs.

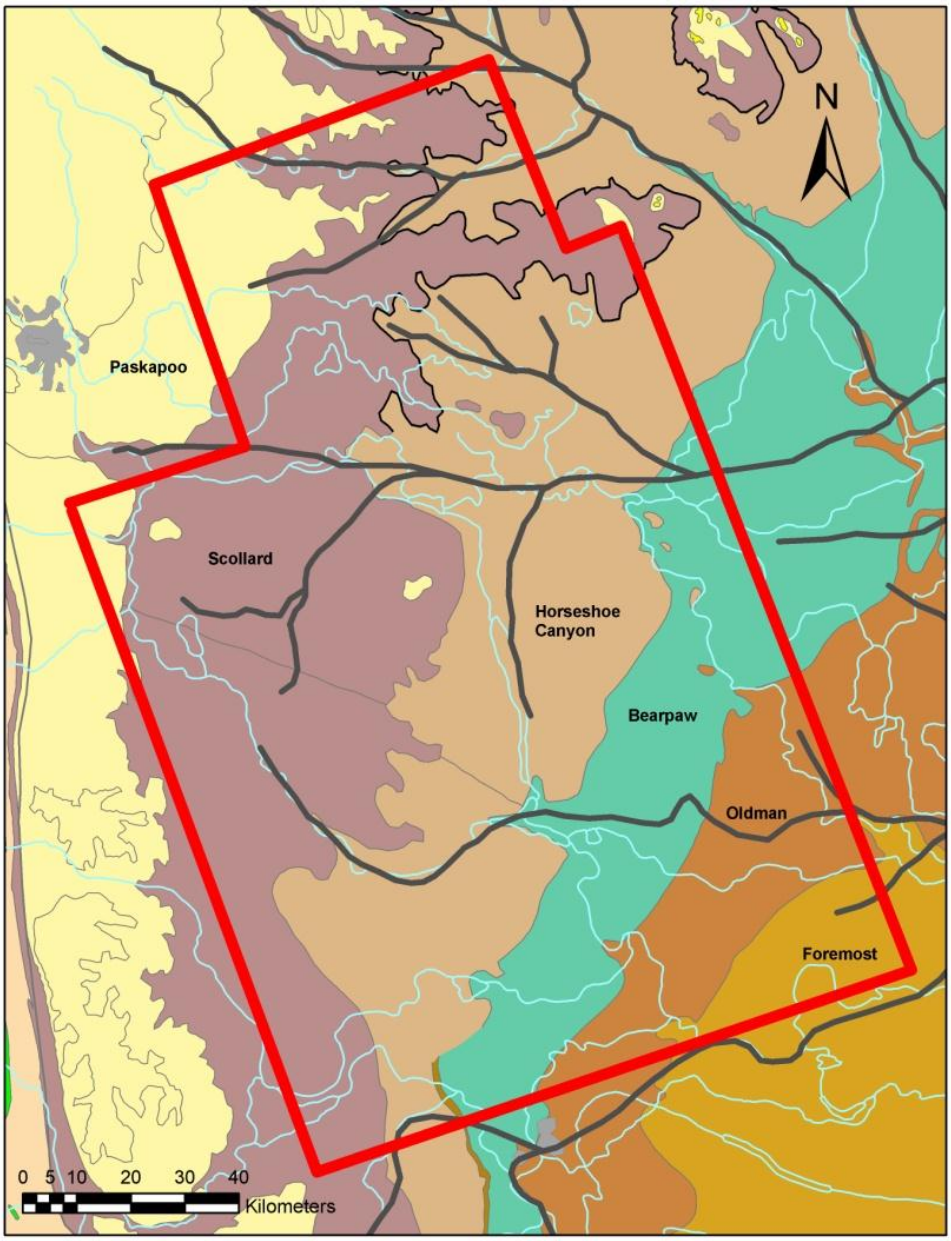

Figure 29: Map of the geology and paleochannels in the survey area. Geology from Hamilton *et al*, 1998.

9239460

Primary Lithology	Top (m)	Bottom (m)
Topsoil	0.0	1.7
Clay	1.7	12.2
Clay	12.2	13.9
Clay and Silt	13.9	15.7
Clay	15.7	19.8
Shale and coal	19.8	20.9
Siltstone	20.9	22.6
Shale	22.6	24.4
Siltstone	24.4	26.8
Shale	26.8	28.9
Shale	28.9	32.4
Shale	32.4	33.1
Sandstone	33.1	37.2
Sandstone	37.2	37.6
Sandstone	37.6	38.3
Siltstone	38.3	47.0
Sandstone	47.0	48.7
Shale	48.7	53.9
Sandstone	53.9	55.0
Shale and siltstone	55.0	59.2
Sandstone	59.2	60.6
Shale	60.6	64.4
Sandstone	64.4	66.1
Shale	66.1	69.6
Shale	69.6	69.9
Shale	69.9	80.0
Sandstone	80.0	81.8
Shale	81.8	92.2
Sandstone	92.2	94.0
Shale	94.0	95.7
Shale	95.7	97.4
Sandstone	97.4	102.7
Shale	102.7	104.4

9239449

Primary Lithology	Top (m)	Bottom (m)
Topsoil	0.0	16.0
Sand	16.0	19.8
Siltstone	19.8	39.0
Sandstone	39.0	46.3
Siltstone	46.3	52.9
Siltstone	52.9	65.4
Sandstone	65.4	71.0
Siltstone	71.0	73.1
Shale and siltstone	73.1	76.6
Siltstone	76.6	80.0
Siltstone	80.0	85.3

Figure 30: Comparison of lithological logs in nearby holes. Siltstone is shown as yellow, sandstone as red, shale as green, and sand/clay as blue.

In the inversion results, there is a resistor, typically at about 120 m, although it is not seen across the entire survey. (Although the 100 Ohm m layer's resistivity is fixed in the inversion, it is deep enough in some places that the response is not sensitive to it.) Upon examination of the drill hole lithologies, it is not clear to us what this resistor could represent. Note that such a resistor is not observed in the any of the geophysical logs examined; however few of these logs even reach a depth of 120 m. This resistor is observed across most of the survey area and a gradual trend across the area was not noted. This is surprising, given that the sedimentary sequence dips towards the northwest: a trend in the depth to the resistor from southeast to northwest would have been expected. Thus, the resistor does not appear to have a lithological significance. It is unclear whether this is an artifact of the data. The data may be filtered in such a way that a resistor is always observed in the late-time decays.

According to the Wheatland Regional Groundwater Assessment, the following bedrock aquifers are present in the county: Lower Lacombe, Haynes, Upper Scollard, Lower Scollard, Upper Horseshoe Canyon, Middle Horseshoe Canyon, and Lower Horseshoe Canyon. The available geophysical logs are mainly within Horseshoe Canyon, and suggest that discrimination within the Horseshoe Canyon using EM methods is not possible. The inversions of the AeroTEM data similarly do not show any differences between the southeast of Wheatland, where the Lower Horseshoe Canyon is the uppermost basement rock, and the center of Wheatland, where the Upper Horseshoe Canyon is the top of the basement. Thus, we conclude that the aquifers within the Horseshoe Canyon cannot be distinguished by the survey.

It is possible that some formations may be discriminated from others on the basis of resistivity, as the geophysical logs provided did not intersect all formations in the area. However, an examination of the depth slices over the Scollard and Paskapoo in Area 2 did not show any differences from the results over the Horseshoe Canyon.

In summary:
1) The inversions do not discriminate between different lithologies within the Horseshoe Canyon and indeed, geophysical logs support the fact that this cannot be discriminated on the basis of resistivity.

2) Similarly, the depth slices do not indicate that the Scollard and Paskapoo can be discriminated from the Horseshoe Canyon.

6.2.3.2 Depth-to-Basement

The inversions typically have an upper resistor (20-60 m thick) over a conductor, sometimes with an additional cover. It is thought that the resistor (typically about 60 Ohm m) is mostly likely the unconsolidated sediments over the basement. According to the lithological descriptions for the drill holes, the sediments are typically about 20 m thick. In some holes, the thickness of the sediments corresponds relatively well with the thickness of the resistor in the inversion model (e.g. 9239560). However, in many holes, they do not correlate as well with the resistor in the inversion model usually being thicker than that of the sediments (see **Figure** 31). The existence of this layer in the inversion results depends on the starting model used, as discussed for Areas 1.

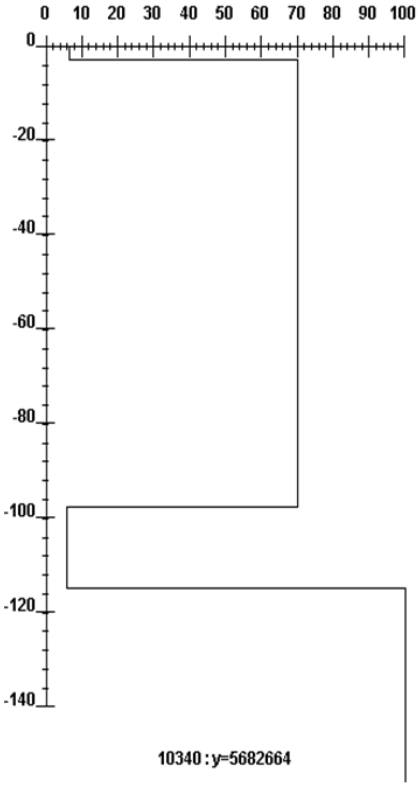

Primary Lithology	Top (m)	Bottom (m)
Clay	0.0	10.8
Gravel	10.8	13.9
Clay and Sand	13.9	20.9
Sand and coal	20.9	27.8
Sand and coal	27.8	33.4
Coal	33.4	34.1
Sand	34.1	37.2
Silt	37.2	41.8
Coal	41.8	42.8
Sand	42.8	52.2
Silt	52.2	60.6
Silt	60.6	74.8
Siltstone	74.8	81.8
Siltstone and coal	81.8	86.3
Sandstone	86.3	100.9
Siltstone	100.9	104.4
Siltstone	104.4	113.1
Coal	113.1	113.4
Siltstone	113.4	116.6
Sandstone	116.6	118.3
Siltstone	118.3	119.7
Sandstone	119.7	120.8
Coal	120.8	121.1
Sandstone	121.1	123.2
Siltstone and coal	123.2	125.3
Siltstone and coal	125.3	128.8

Figure 31: Comparison of lithology in 9228146 and nearby inversion result.

In the geophysical logs, the distinction between the sediments and underlying sedimentary rocks is mainly seen in the smooth variation in resistivity in the sediments versus the more rapidly-varying response in the underlying rocks (**Figure** 32), but there is not a clear increase or decrease in resistivity at the sediment-basement boundary. Thus, the lack of correlation between the inversion results and the depth-to-basement may be primarily a result of the lack of electrical contrast between the sediments and basement.

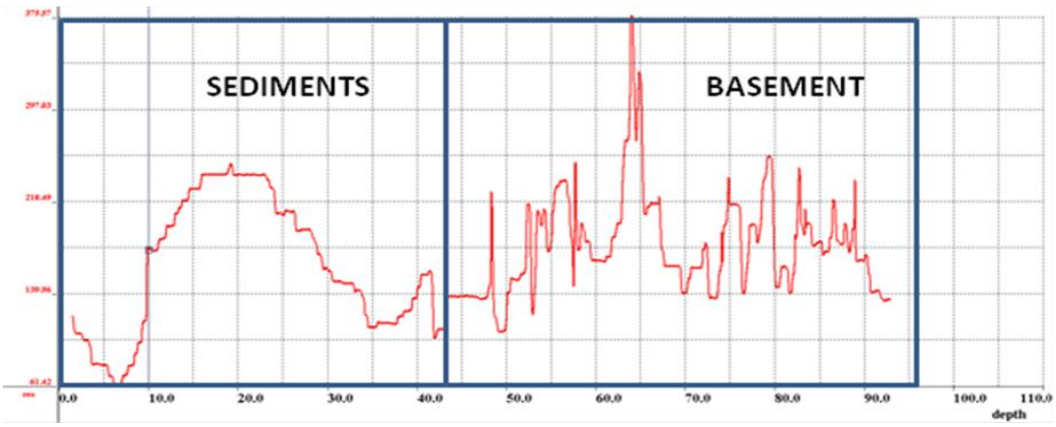

Figure 32: Resistivity log 9239476.

6.2.3.3 Resistivity Comparison (Logs vs. Inversion Results)

Above the 100 Ohm m resistor, the inversion results show resistivities of 6-70 Ohm m. Some of the logs show resistivities in a similar range; however, there is a significant variation in the resistivities observed in different holes. For example, hole 9329476 exhibits resistivities of about 180 Ohm throughout the hole, whereas 111006 has an average resistivity of 3 Ohm m. Some holes, such as 9239460, which has an average resistivity of about 17 Ohm m, do contain resistivities similar to those in the inversion results.

As a result of the significant differences in the resistivities in nearby holes, the amplitude of the resistivity is not considered reliable.

6.3 Area 3 (SE)

Area 3 is predominantly within Vulcan and Lethbridge counties. There is a Regional Groundwater Assessment for Vulcan, but such a report for Lethbridge cannot be found, and it is now known if it has been completed.

6.3.1 Analyses of Inversion Results

The shallow depth slices for Area 3 (0-35 m) show significant streaking, i.e., line-to-line effects. The 25 m depth slice is displayed in **Figure** 33.

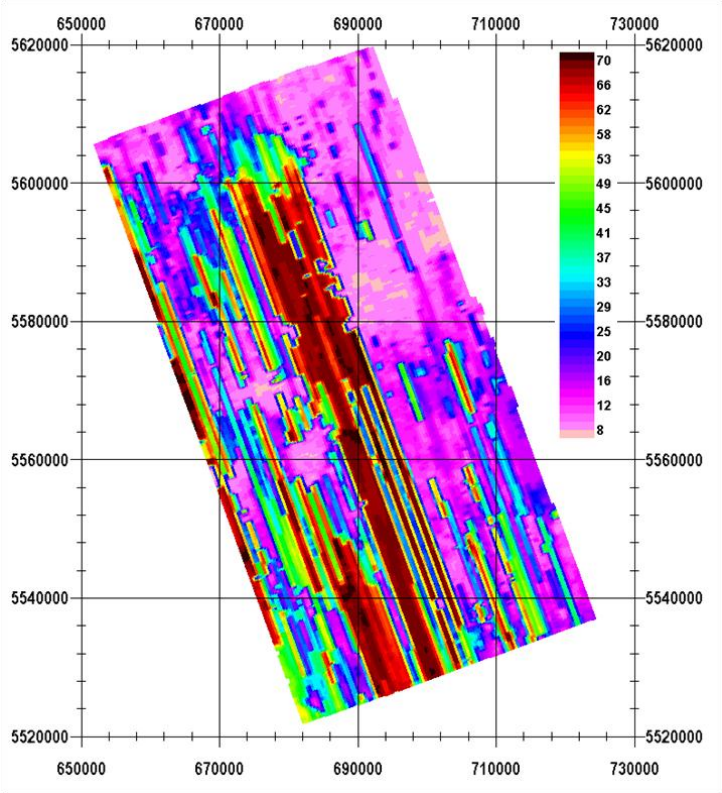

Figure 33: Depth slice at 25 m for Area 3.

It is noted that this has some correlation with the position of the channels after the end of the pulse. A map is shown in **Figure** 34. The position of the first channel relative to the end of the pulse varies between flights. Prior to running the inversions, some initial tests were performed on sample data from Area 1 using different window times (within the range observed in the data), and it was found that there was not a major difference in the inversion results between the correct windows for a line and the average window settings for the area.

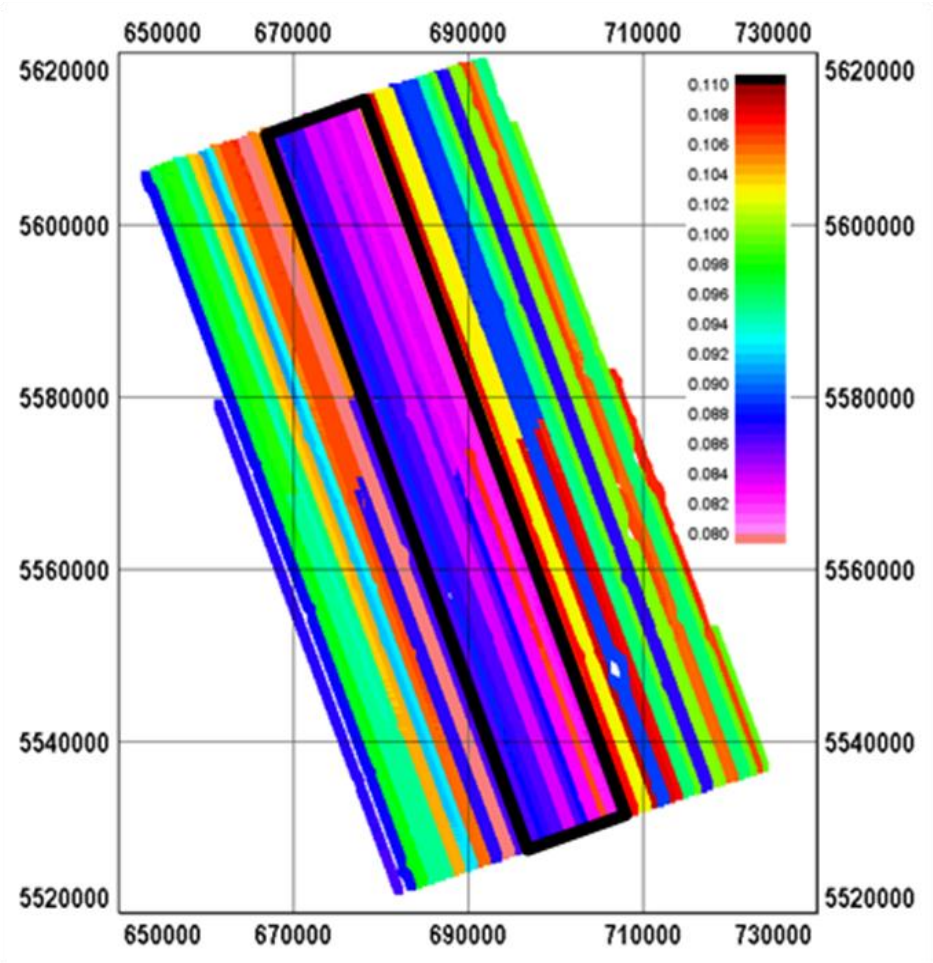

Figure 34: Time of Channel 1 after the end of the pulse.

However, an examination of the timing vs. the shallow depth slices (**Figure** 35) indicates that there is some correlation between them, with a higher shallow resistivity where the channels are closer to the end of the pulse.

A section of Lines 20240 (channels further from end of pulse) and 20250 (channels closer to the end of the pulse) was examined in further detail. This inversion results are compared in **Figure** 36: 20240 does not have a shallow resistor, but 20250 does.

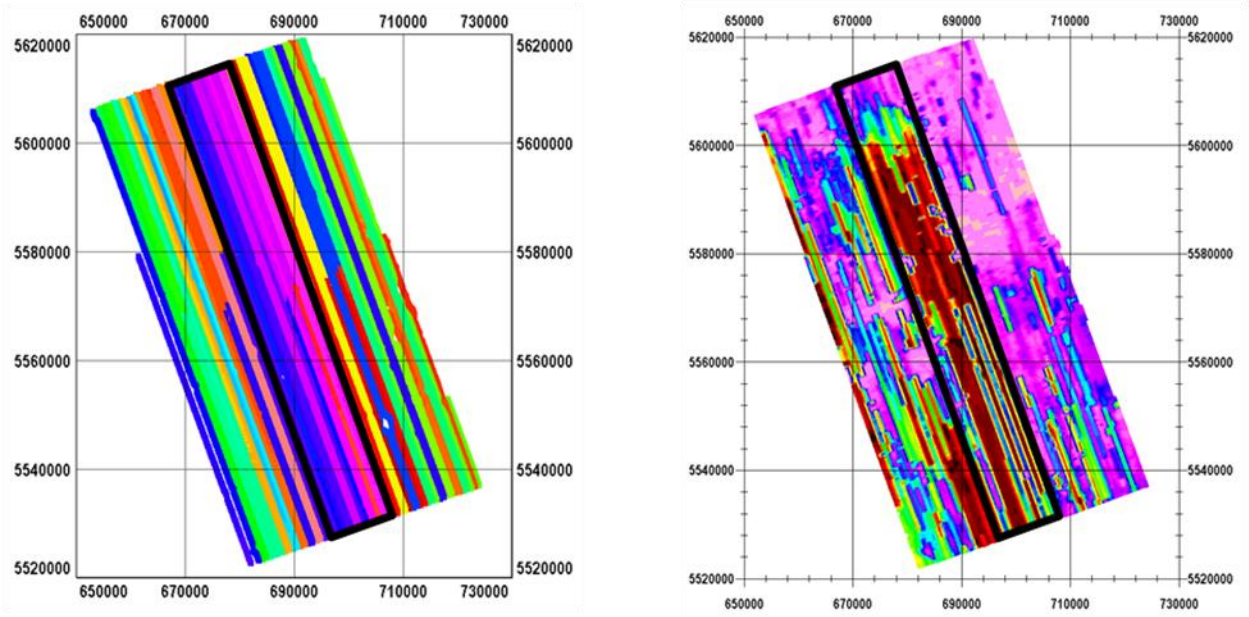

Figure 35: Comparison of the timing of Channel 1 (left) with the 25 m depth slice for Area 3. An area of high shallow resistivities in the depth slice and short delay to Channel 1 is marked in both figures by the black outline.

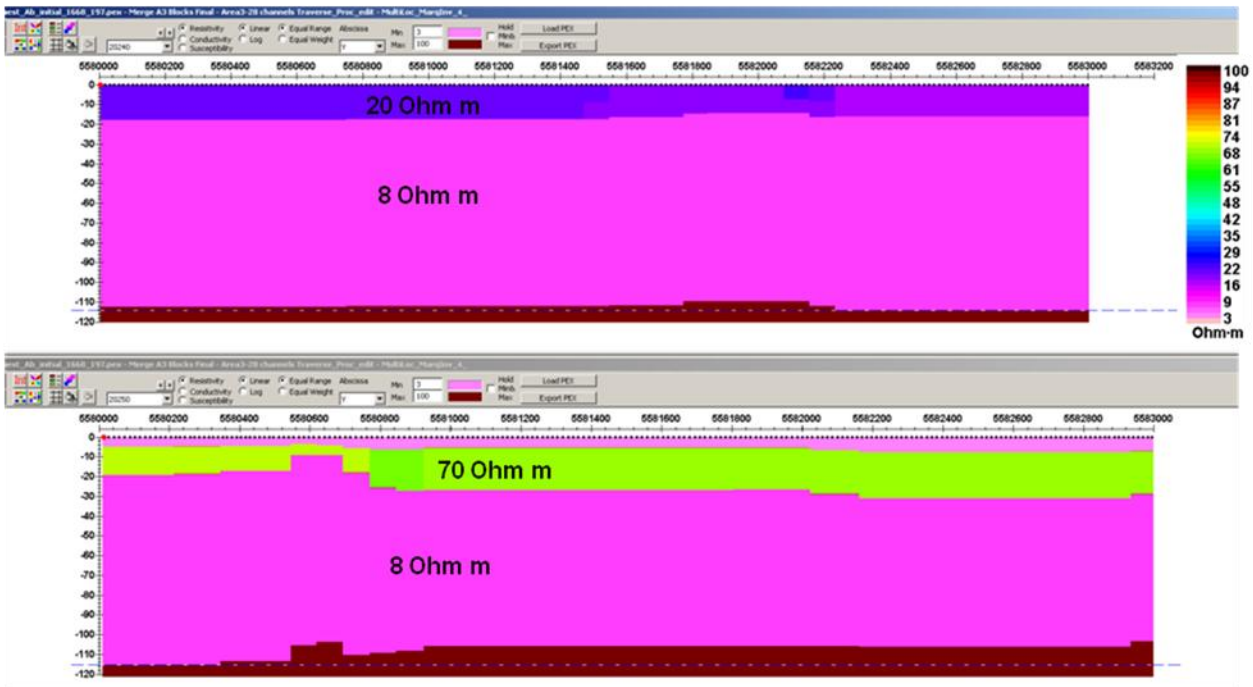

Figure 36: Inversion results along 3 km sections of 20240 (top) and 20250 (bottom).

Further inversions were run on both of these lines. The starting model was adjusted slightly so that the three layers above the 100 Ohm m resistor had the same resistivity, i.e. the resistor observed on Line 20250 was not present in the starting model. Inversions were run both with and without Channel 1, for the average time channel positions (as used in the full inversion) and the adjusted time channels for each line. (Note: the position of the end of the pulse is more or less constant across lines flown within a single flight.) For Line 20240 (**Figure** 37), all results are fairly similar to the initial inversion. There is a slightly resistive cover of 20 Ohm m or less, followed by a conductor. The thickness of this conductor is slightly less for the adjusted time channels, but all are fairly similar.

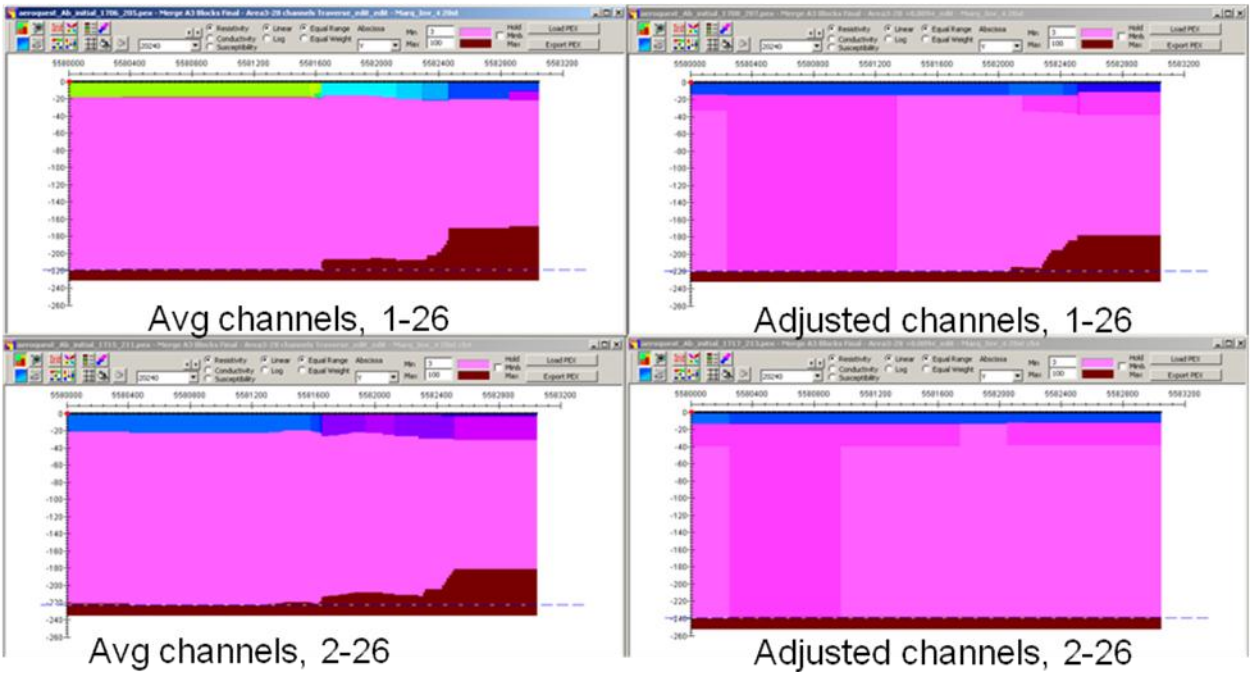

Figure 37: Inversion results along a 3 km section of 20240 for different time channel settings.

On Line 20250 (**Figure** 38), again the results are similar for all four inversions. There is a difference in the depth to the 100 Ohm m resistor at depth; however, all inversions indicate a depth of greater than 130 m to the resistor, and there is limited depth resolution by 130 m, so this is not considered significant. Interestingly, however, these results for Line 20250 do not have the near-surface 70 Ohm m resistor as in **Figure** 36. The main difference in these inversions versus the original was the starting model.

Further inversions were run in which the initial starting model (20 Ohm m, followed by 15 Ohm m over a 100 Ohm m half-space) was used. Again, this did not result in the same near-surface resistor despite the use of the same starting model as the original inversion. The reason for this is assumed to be that the inversion does not use this starting model at each station, but instead uses the model at the previous point along the line. Thus, presumably along Line 20250, the resistor was needed to fit stations closer to the beginning of the line, and therefore was the starting model by this section of the line. A further inversion on the subsection of Lines 20240 and 20250 was run, in which the resistor was included in the

starting model, was run. This results in a stronger resistor at surface on Line 20240 (50 Ohm m vs. 20 Ohm m) that is slightly thinner. On Line 20250, there is a resistor of similar resistivity, but it is overlain by a conductor. These results are the same whether or not Channel 1 is used.

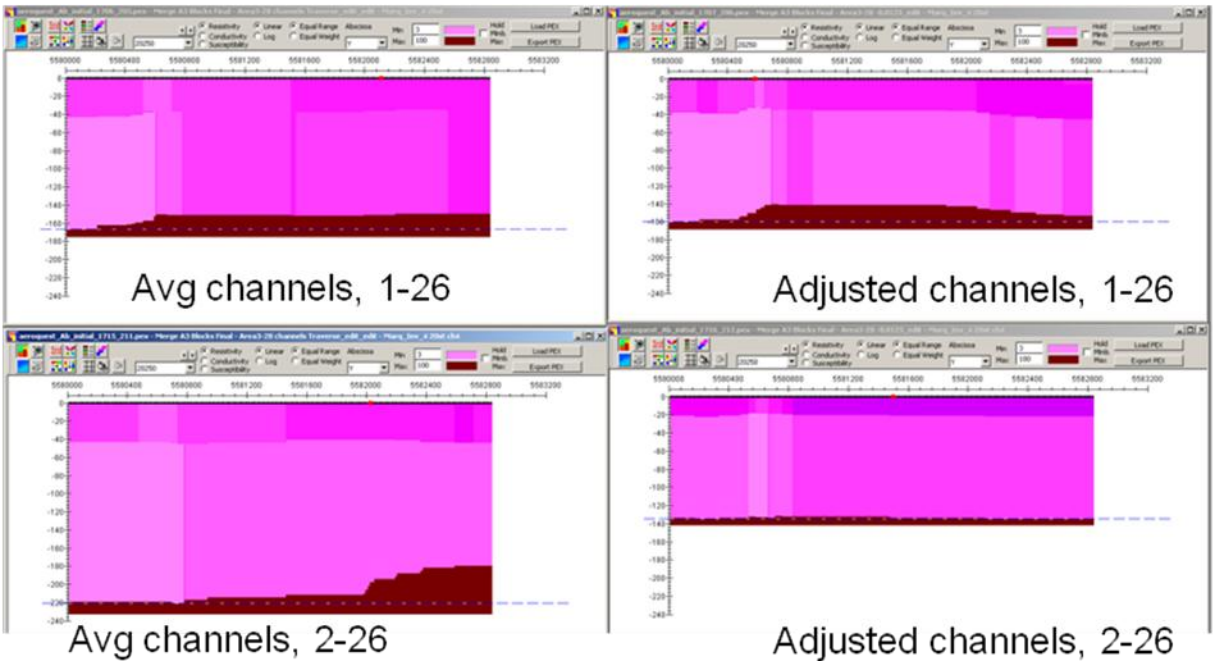

Figure 38: Inversion results along a 3 km section of 20250 for different time channel settings.

These initial results on a subsection, as shown in **Figure** 37 and **Figure** 38, do not show significant differences between the average and adjusted channels, and with and without Channel 1, although they do show significant sensitivity to the starting model.

Further inversions were run on a large section of Area 3: Lines 20210-20280(full lines) to see if on a larger scale, not inverting Channel 1 would result in more consistent inversion models between lines. Average channel times were used. Results on Lines 20210-20240 are similar for both inversions. Results on Lines 20250-20280 contain a near-surface resistor across most of the initial inversion, but only a small part of the new inversion without channel 3. Results on Line 20250 are shown in **Figure** 39. The new inversion, without Channel 1, does show a resistor over part of the line, slightly deeper than on Line 20250. This is observed over part of neighboring Line 20260 as well. It is thought that this resistor is real. Thus, preliminary results suggest that removing channel 1 from the inversion settings may improve consistency in the inversion results, removing the near-surface resistor across most of Lines 20210-20280 when it was absent in the starting model.

However, results are fairly sensitive to the starting model and constraints. If the resistor were present in the starting model, it is expected that it would be observed in the inversion results as well.

Furthermore, while the inversion without Channel 1 did not show a resistor across most of the survey, it does not mean that this model is necessarily correct, but more consistent across neighboring inversions. If Channel 1 is to be believed on the lines where it is closer to the pulse, then a conductor is needed to drive up the response of Channel 1. (Note: the elevated response of this channel could also be due to system response.

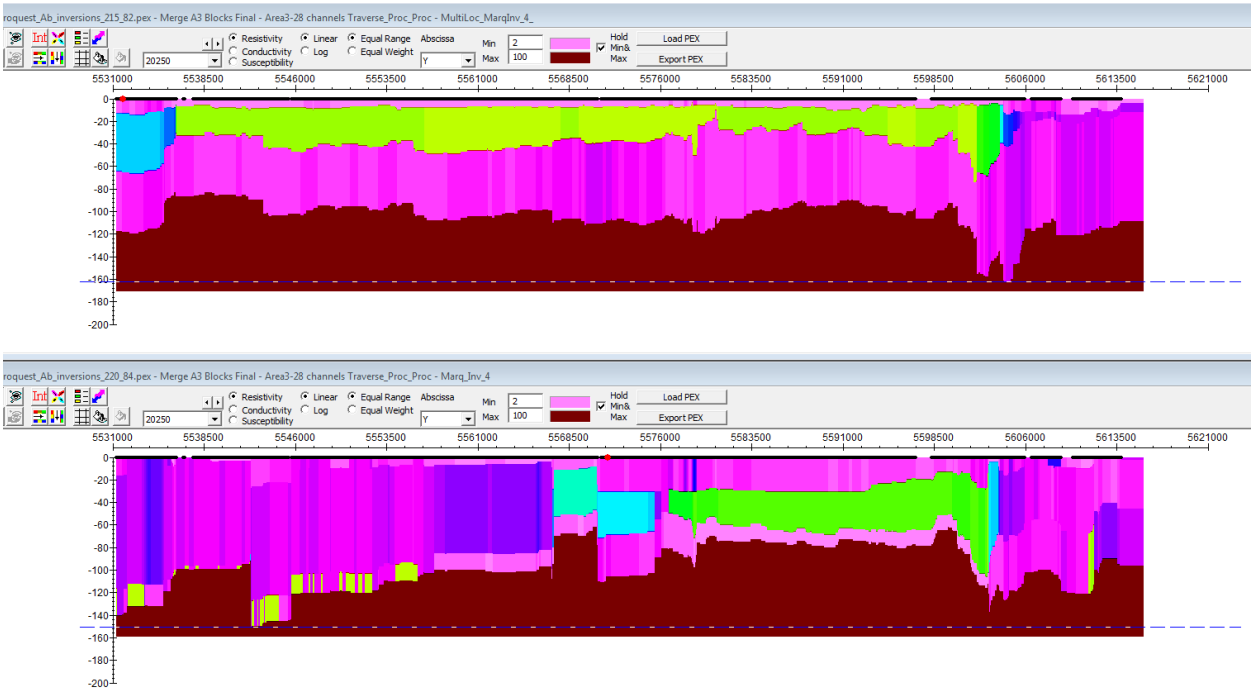

Figure 39: Inversion results along the length of 20250. Initial settings (top) and new settings without channel 1 (bottom).

6.3.2 Inversion Results and Geology

In Area 2, no correlation between the bedrock geology and the inversion results was observed. In contrast, the Bearpaw formation, which underlies the Horseshoe Canyon, has a slower mid-time decay and this corresponds to a lower resistivity in the depth slices, as seen in Area 3 and 4 (**Figure** 40). The Bearpaw is an aquitard. We do not have any drill logs for Area 3.

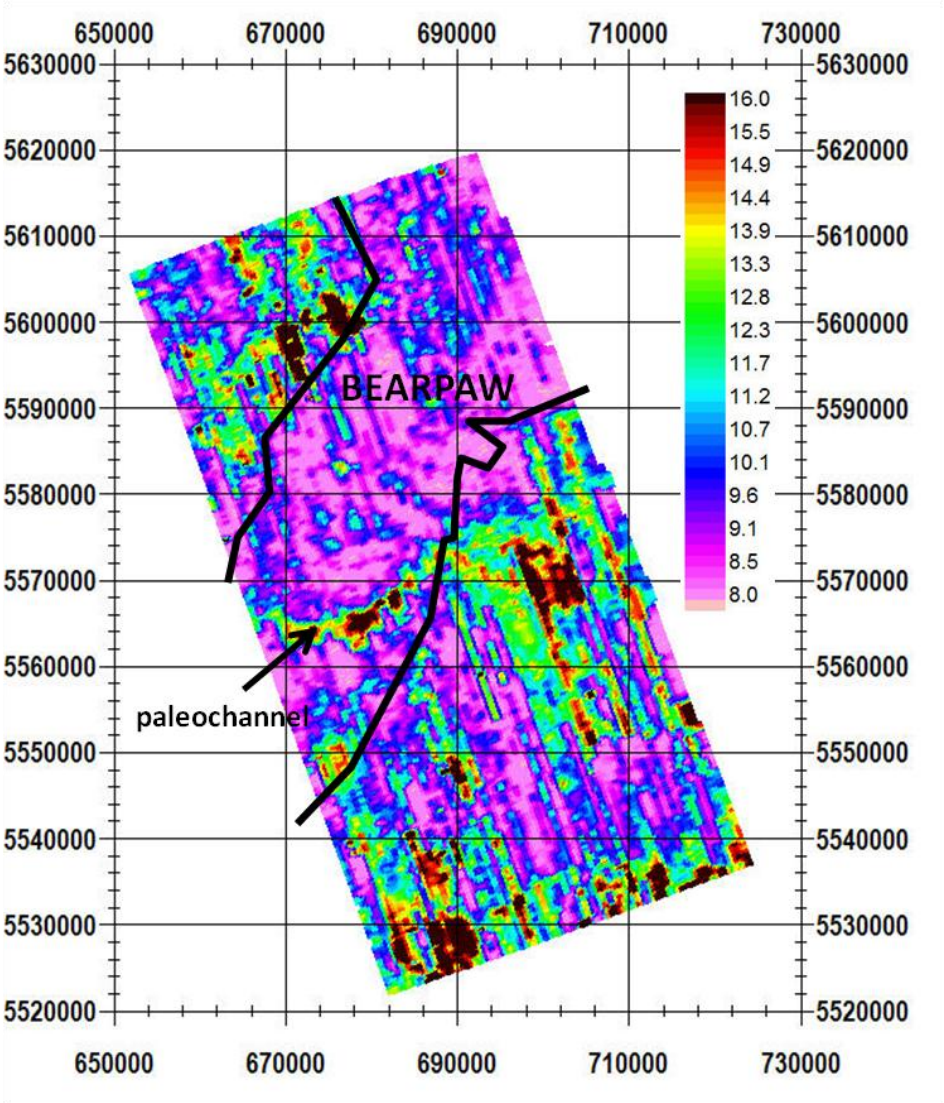

Figure 40: 75 m depth slice for Area 3, showing the boundaries of the Bearpaw Formation.

6.4 Summary of Results for Original Inversions

As discussed previously, numerous small groups of sites were examined via forward modeling. These exercises indicated to us that in general there were three strata of different resistivity above what was apparently a more resistive stratum. The resistivity of the bottom strata could not be resolved but would range at 100 Ohm-m and more. The top layer appeared to be thin and of relatively low resistivity (possibly unconsolidated sediments), the second layer was generally more resistive than the top layer and then there was a layer of lower resistivity before the bottom strata. It was therefore decided to perform the inversions with a 3-layer over a resistive lower strata. The constraints on the 3 top layers were wide enough to cover the ranges of resistivities found in our small group forward studies.

A summary of the results of these initial inversions are given:

1) Geophysical logs are available in Wheatland County. Detailed studies of these logs versus the inversion results generally indicated that the logs are not inconsistent with the AEM inversions but due to limited knowledge of the equipment used and variable resistivities in different holes, these logs are insufficient for calibration of the system.

2) Inversions show significant line-to-line variation in the depth to the 100 Ohm m half-space. Given the line-to-line differences in the decays and the inconsistency of the late-time data, this is not surprising. The significance of this layer is not known, and it is possible that the late-time resistor is a result of processing procedures for the data. Ground data would greatly assist in determining its significance.

3) Inversions also show “streaking” or strong variations between neighbouring lines at shallower depths. In our opinion, this variation in shallow models between lines is a result of a) noise in the mid-time data b) variations in the response at Channel 1 and c) non-uniqueness of models that fit the data. This latter result is at least in part a result of the noise in the data. Removing Channel 1 from the inversions may improve consistency of inversions line-to-line.

4) The data is unable to resolve the basement geology, with the exception of the Bearpaw formation, which is slightly more conducting and has a more uniform resistivity than the other formations.

6.5 New Shallow Inversions

Through analyses of the initial inversion results, as detailed in Sections 6.1-6.3, it was observed that on some lines, a shallow resistor was imaged in the inversion model under a thin conductor whereas on other lines there was little variation in the resistivity of the top three layers. These two distinct model types are observed in all four areas often on neighboring lines. For example, compare the results on Lines 10920 and 10930 in Area 1 in Section 6.1. As a result, streaking is observed in the depth slices, particularly above 35 m (for example, see Figure 33), as the shallow inversion results vary from one line to another. These features may or may not be true but with the line spacing, quality of the data and

lack of calibration information whether by resistivity logs or ground TEM data, it is not possible to determine.

The original inversion was performed with four layers, three layers over a half-space, the top layer being a thin cover, as such a model was fit the data best in some areas. However, in the inversion results on some lines, as described above, the top three layers are essentially blended into a single layer.

We believe that the shallow resistor is present, at least over part of the survey, but it cannot be adequately resolved due to the data quality issues, described in Section 3.0. In particular, it is related to variations in the early time amplitude. In Section 6.3, it was shown that there is some correlation between the timing of Channel 1 and the streaking in the depth slices. We believe that the amplitude of Channel 1, which is affected by variation in the timing of this channel from the end of the pulse, has some bearing on the streaking in the slices. As described in Section 6.1.2, where various tests on the inversion settings were described, whether or not Channel 1 is used in the inversions was an important factor in the results. However, the streaking is not entirely due to the first off-time channel. (Note that the timing has little effect on the amplitude of the response beyond Channel 1, and further issues with the early-time data are not likely related to timing issues.) The inconsistent results line-to-line are also a result of noise and amplitude issues in other channels.

The difference in response between the two model types (conductor-resistor-conductor and moderate conductor-resistor) is slight and very clean data in the early channels is required to distinguish between them (see Section 6.1.2). Through our examinations of the decays and the depth slices, we believe that the data cannot distinguish between them in many areas. In such cases, the starting model, i.e., whether or not it contains the intermediate resistor can affect the result. In other cases, minor aspects of the decay may cause the inversion to favor one model over the other, although the differences in the data may be a quality issue and not actually reflective of the ground. Thus, we conclude that we are unable to satisfactorily resolve the top two layers in the large regions of the data. The streaking in the inversion slices may be improved if we do not attempt to discriminate these two layers thus producing depth slice maps that are more palatable. However, we still hold that for the cross-sections, the original inversions are more accurate.

A second set of inversions were thus performed with the goal of improving the appearance of the inversions (i.e. to decrease the streaking in the shallow inversion results). Rather than using three layers over a half-space, two layers over a half-space were used so that the inversion was not allowed to discriminate a thin conductor over a resistor at surface. Thus, the top layer in the new inversions was a combination of the two uppermost layers in the original inversions. Although we believe that the shallow resistor is present, the data is such that it cannot be resolved, and so it was not attempted to resolve it in the second inversion process.

For the second inversion process fewer time channels were utilized. Channels 2-18 were used rather than Channels 1-26. Channel 1 was not used in the inversion as it was somewhat affected by timing differences between flights (Section 6.3), although timing is not necessarily the sole cause of the variability in this channel. This channel was frequently difficult for the inversion to fit, and appeared inconsistent with the rest of the decay in some areas. As such, the removal of Channel 1 from the inversions also significantly reduced the computational time. Each area could now be inverted in 48hours rather than the previous 96-120 hours.

The latter time channels (19-26) were removed from the second inversions because the decays were not considered reliable, particularly in the Mike data (see section 3.0). There is significant variation in the late decays on reflies and at tie line intersections. Maps produced of decays also shows inconsistencies in the decay rate on certain lines. These channels were used in the original inversion to maximize depth resolution where the data quality was good.

The shallow, smooth inversions significantly improved the esthetic appearance of the depth slices at shallow depths for Areas 1, 2, and 3. For example, see both 30 m depth slices for Area 2 in **Figure 41**. The inversion at this depth is very similar to a simple grid of the data (**Figure 42**), although it is slightly smoother. Generally, the original inversions did not contain interpretable results until at least 35 m depth, whereas the second shallow inversions contain apparently mode consistent results if not from the surface, than from 5 or 10 m depth. The depth slices for Area 4, which generally had the poorest-quality data, were not improved as significantly at shallow depths as the other three areas. However, the Area 4 depth slices are still appeared somewhat cleaner in the second set of inversions.

Below about 50 m, the original inversions and new shallow inversions show fairly similar features but there is generally less streaking in the new inversions (**Figure 43**) and in some regions, there is better discrimination within resistive features. This is at least in part due to the later (and noisier) channels not being used in the inversion, but may also be related to there being more consistent shallow models. **Figure 43** presents a general comparison of the new shallow and original inversions, but more detailed comparisons, with reference to particular features, are presented in the interpretation section that follows.

The fact that some streaking remains in the new shallower inversions, particularly in Area 4, is reflective of the inconsistencies in the early-time amplitudes. If the data were inverted in smaller sections, some adjustments could be made to resolve this issue, and that may result in cleaner depth slices.

We believe that the original inversions are a more accurate reflection of the amplitude and decays in the data. However, the new shallow inversions resulted in cleaner depth slice images because the channels that contained the greatest inconsistencies in the data were not used in the inversions, and we did not attempt to resolve the shallow structure. Indeed, the fact that these inversions are more interpretable supports our conclusions regarding the data quality.

Despite the problems in the data outlined in Section 3.0, we believe that the AeroTEM data and depth slices contain considerable information on the subsurface, as will be detailed in Section 7.0. Many features observed in the inversions correspond to known structures, and possible structures of interest are mentioned. More detailed comparisons of the two sets of inversions are also made over particular features. The above discussion of the results for the new inversions is a general overview. The specifics of the comparisons vary somewhat between the four areas and the following section provides further detail.

To our knowledge, the GeoTEM data previously collected for AENV was not exhaustively examined for data quality. Although our findings are somewhat critical of the quality of the AeroTEM data, based on our experiences with GeoTEM data in the past and the information contained in our AeroTEM inversions, we believe the AeroTEM system was more suitable for this survey.

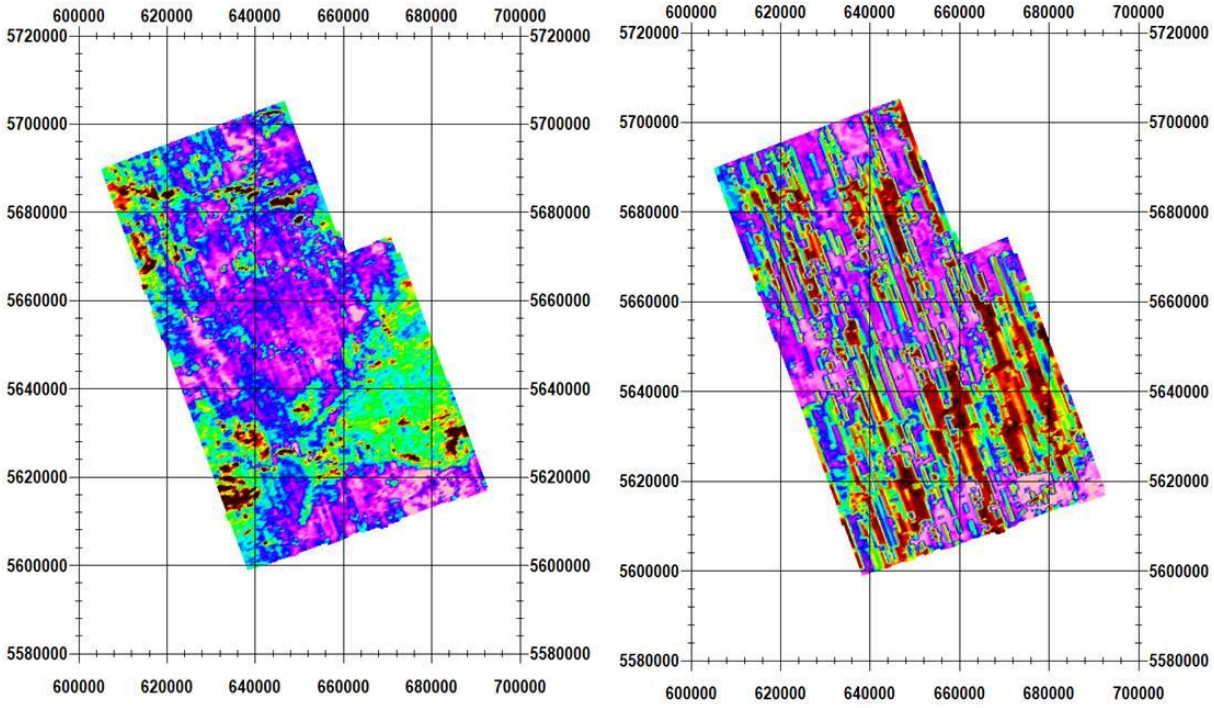

Figure 41: comparison of 30 m depth slices for Area 2: new shallow inversion (left) and original (right).

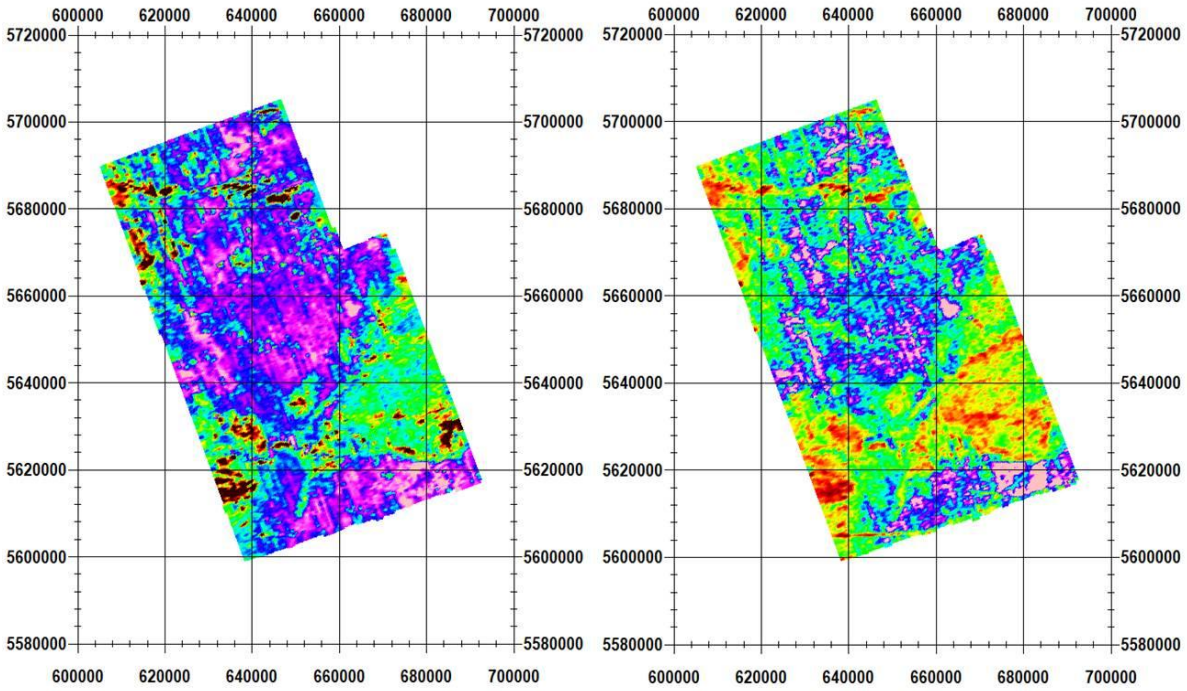

Figure 42: 30 m depth slice for shallow inversion (left) and Channel 8 data (right). Red-yellow is low amplitude in the data and high resistivity in the depth slice; pink-blue is high amplitude in the data and low resistivity in the depth slice.

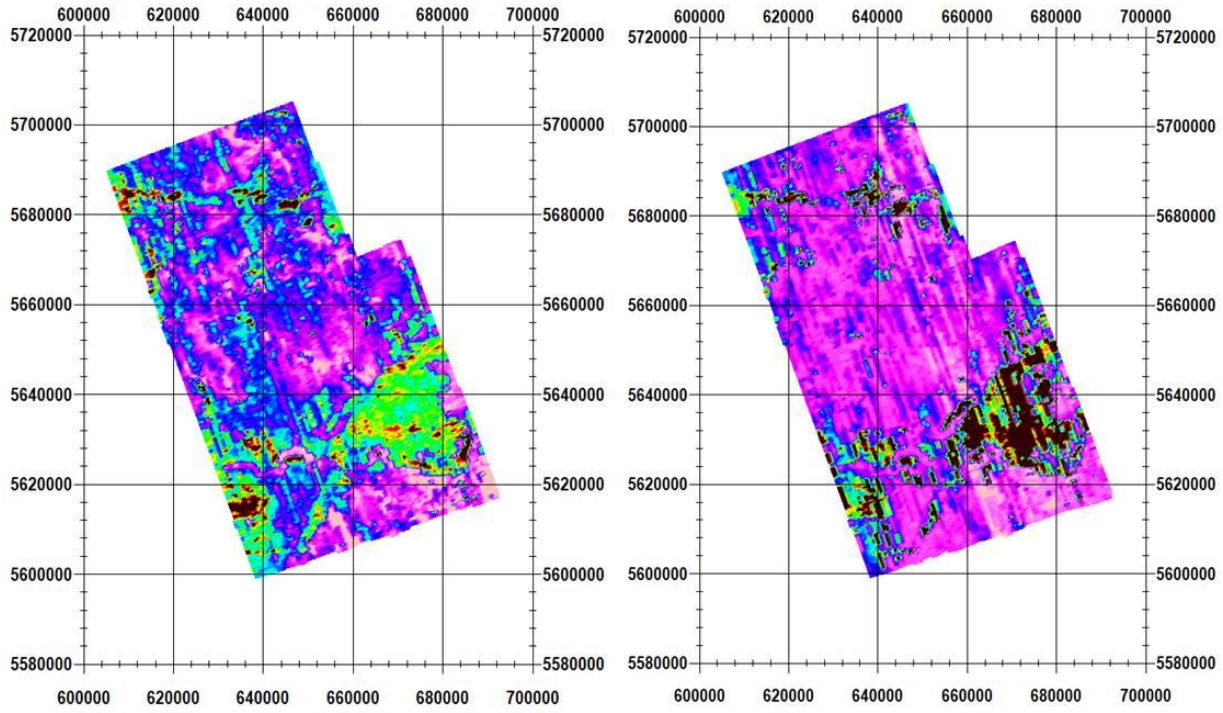

Figure 43: comparison of 60 m depth slice for Area 2: new shallow inversion (left) and original (right).

7.0 Preliminary Interpretation by Area

Below is a preliminary interpretation of each of the four survey blocks (see **Figure** 16) presented individually. The correlation between the data and known man-made structures as well as rivers and topography is discussed. Maps of the rivers were obtained as vector data from Aeroquest and also from the provincial geology map (Hamilton *et al*, 1998). The former appears to be more detailed and better correlates with the digital terrain model, but does not include as many rivers as the later. Comparisons are also made between the data and known paleochannels (Pawlowicz *et al*, 2007) and areas of further interest are noted.

In our own research of aquifers in this area, we found no information as to resistivities of the different types of aquifers and indeed very little in regard to the composition of the aquifers. In our initial analyses of the data with comparisons to the available maps and paleochannels, it was observed that a large number of rivers appeared conductive at shallow depths and then relatively resistive at greater depths. Many of these deeper resistive zones correlating roughly with the path of the rivers also were consistent with interpreted paleochannels.

It is therefore assumed that the aquifers are coarse sediments or gravels and they are thus resistive compared to the formations surrounding them. There is also some correlation between areas of higher resistivity in the inversions and known sand/gravel aquifers in Wheatland and Vulcan counties. The resistivity of gravel/sand depends on several factors including the water content and the distribution of grain sizes. The solubility and composition of the sand/gravel could affect dissolved ions in the water, which in turn would affect the resistivity. Thus, the resistivity of sand and gravels is quite variable. We were unable to find any information as to what range of resistivities to expect from these deposits. The well logs that we examined were not helpful in this regard.

Additionally, the amount of water flow along and into these deposits and the sediment content of the flow will affect resistivity. As the flow rate can control the amount of sediment settling in the deposits. The type of sediments contained in the water flow thus affect the resistivity of these settlings as does the amount of particles in suspension in water in these deposits.

7.1 Area 1 (NW)

Results for the original inversions and the smooth, shallow inversions are presented separately.

7.1.1 Effect of Known Features

7.1.1.1 Infrastructure

Figure 44 displays the Area 1 (channel 4) data, cleaned of very noisy areas, with a map of the major highways. Only the main TransCanada highway appears to have any effect upon the data. Low amplitude would be expected over a major highway due to increased altitude of the system.

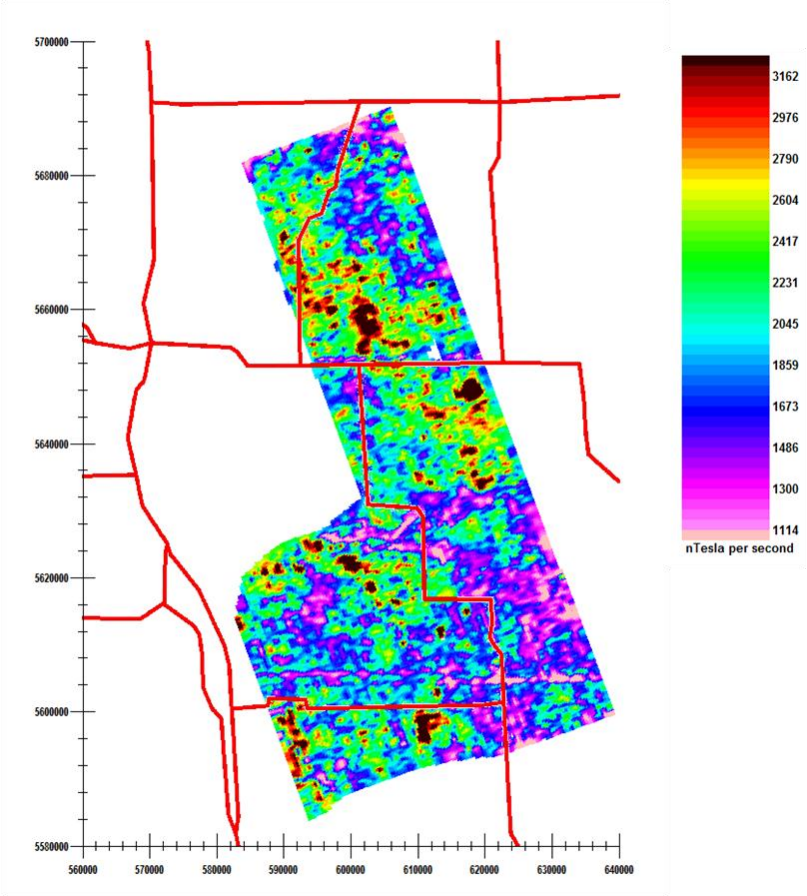

Figure 44: Effects of Highways on Area 1 data. Channel 4 cleaned of noisy areas is shown. Highways are in red.

The data is compared with known railways, power lines, and pipelines in **Figure** 45. There is no portion of the data which displays any great correlation with the railways. Only one section of power line indicates a clear correlation with the data (A)-(A'). The power line indicator channel provided with the survey data indicated a power line along this line segment and data stations were removed which had a significant power line indicator. However, there still remains an apparent correlation along this one segment of power line. There is also indication a power line continues west along the same angle which is not shown in the map of infrastructure. Low amplitudes may be expected at power lines due to

increased altitude of the system. A map of the altitude is shown in **Figure** 46. Altitude suggests an extension of the power line (A)-(A') to the west. Higher altitudes over the Bow River agree with a topography drop shown later. There is a general increase in elevation on the east of the survey.

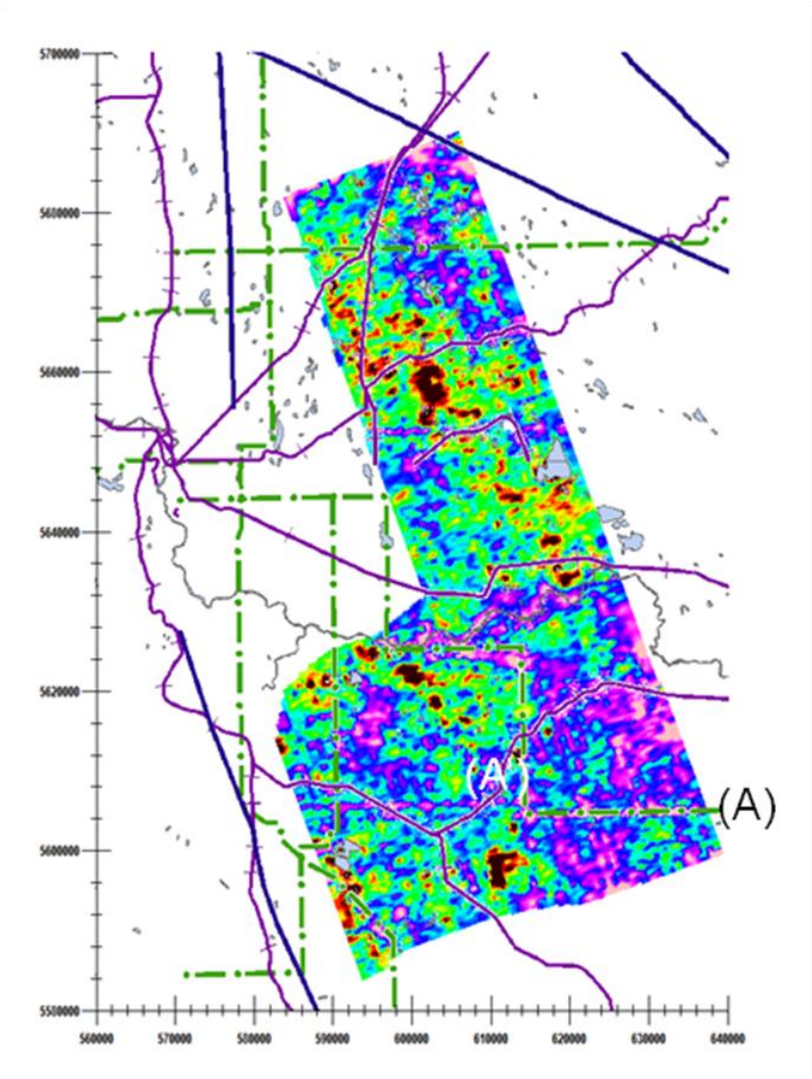

Figure 45: Effects of Other Infrastructure on Area 1 data: Railways in purple, pipelines in dark blue, and power lines in green are shown. Only one section of power line indicates a clear correlation with the data (A) – (A').

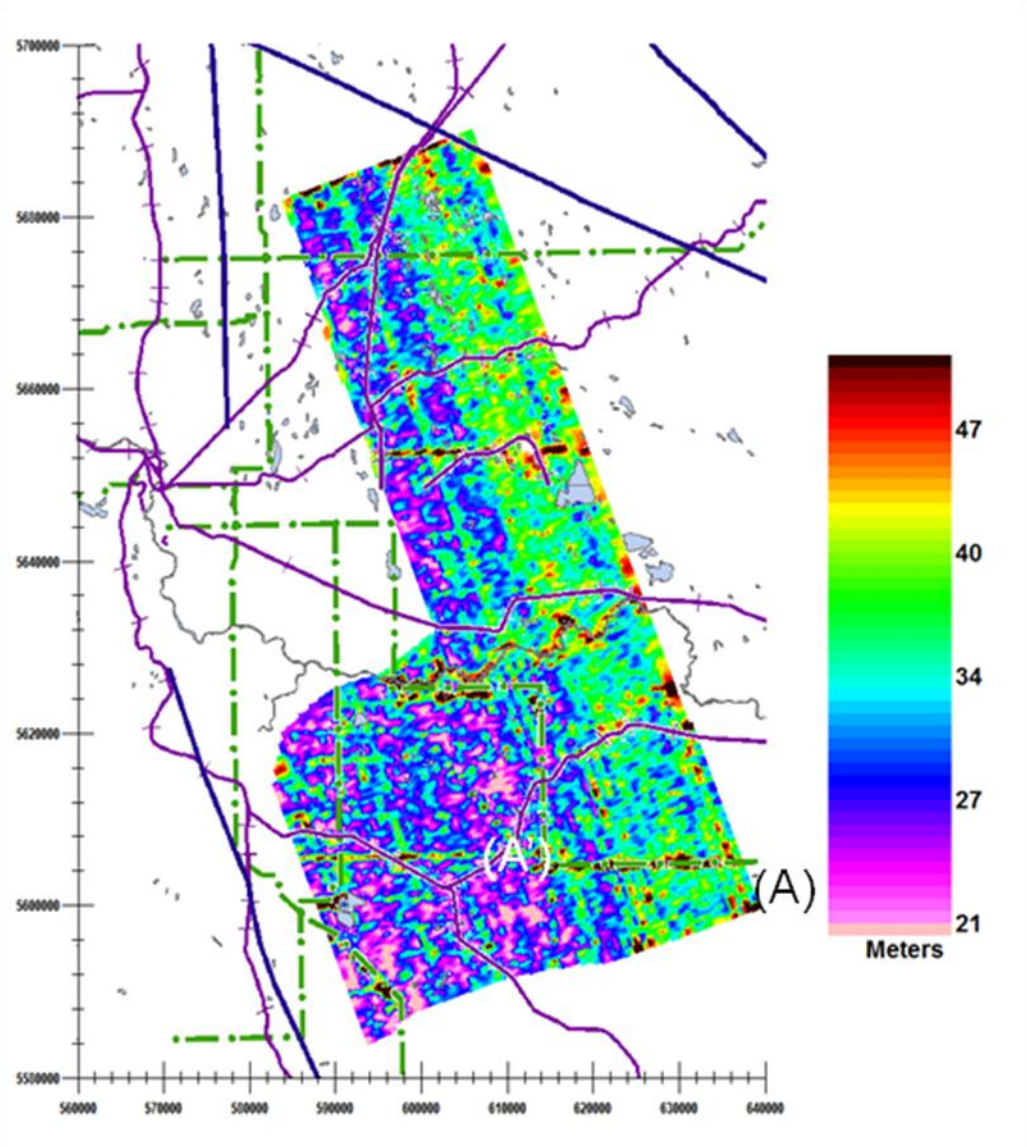

Figure 46: Height of bird over Area 1.

7.1.1. 2 Topography and Rivers

Figure 47 compares the Channel 4 data over Area 1 with the digital terrain model. The only areas where there appears a correlation with the topography are where there are topographic lows. Specifically, this refers to areas (A)-(C) as well as along a section of the Bow River where the topography is low. A close-up along the Bow River is presented in **Figure** 48.

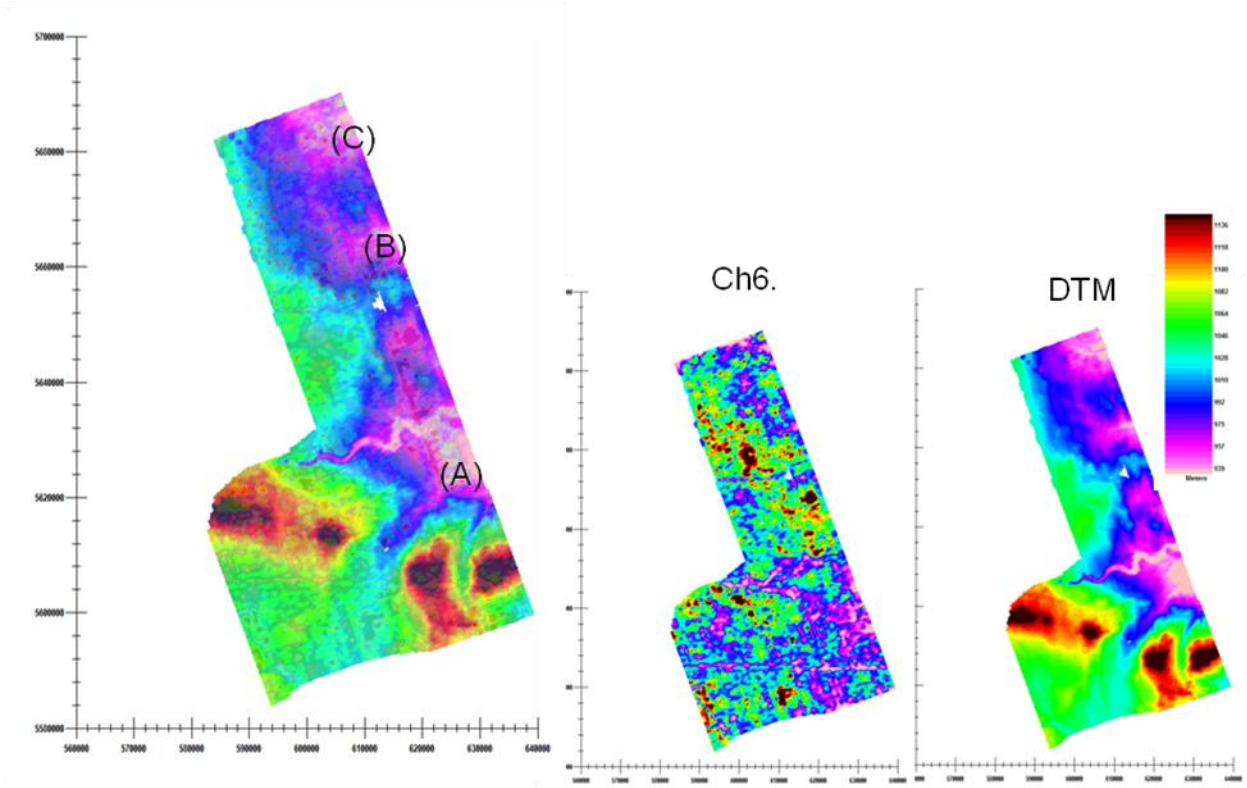

Figure 47: Effects of Topography for Area 1. Correlations are noted where there a topographic lows, e.g. areas (A)-(C) as well as along a section of the Bow River where the topography is low.

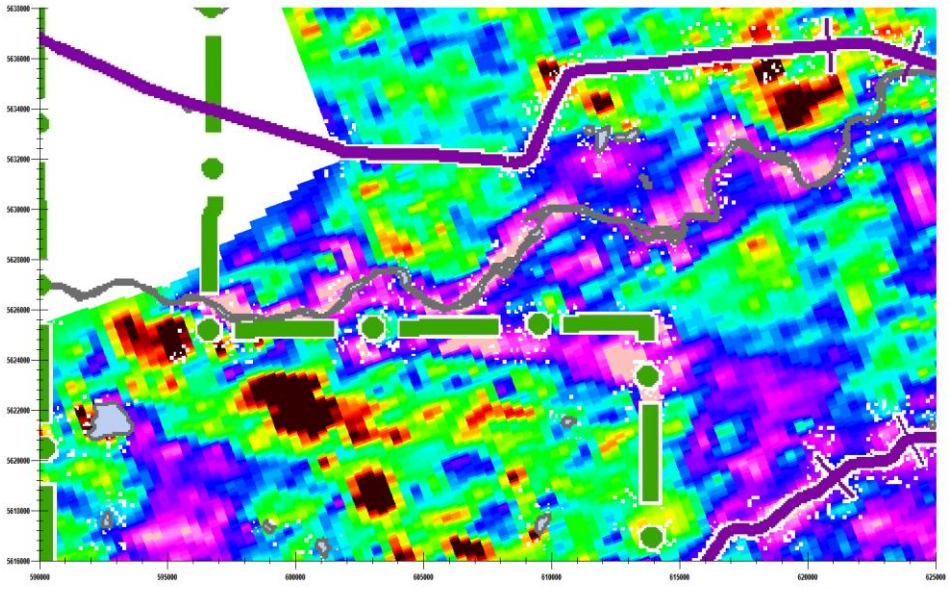

Figure 48: Effects of Rivers for Area 1. The only strong area of correlation between the rivers and the data is along the Bow River (grey). The approximate location of the power line is shown in green.

7.1.2 Interpretation of Original Inversions

The first depth section that reveals structure is at 35m. **Figure** 49 compares the depth slice with rivers and known paleochannels. There is some correlated resistive structure along the Bow River (A), a cohesive spatial resistive structure at (B) as well as a possible resistive structure at (C).

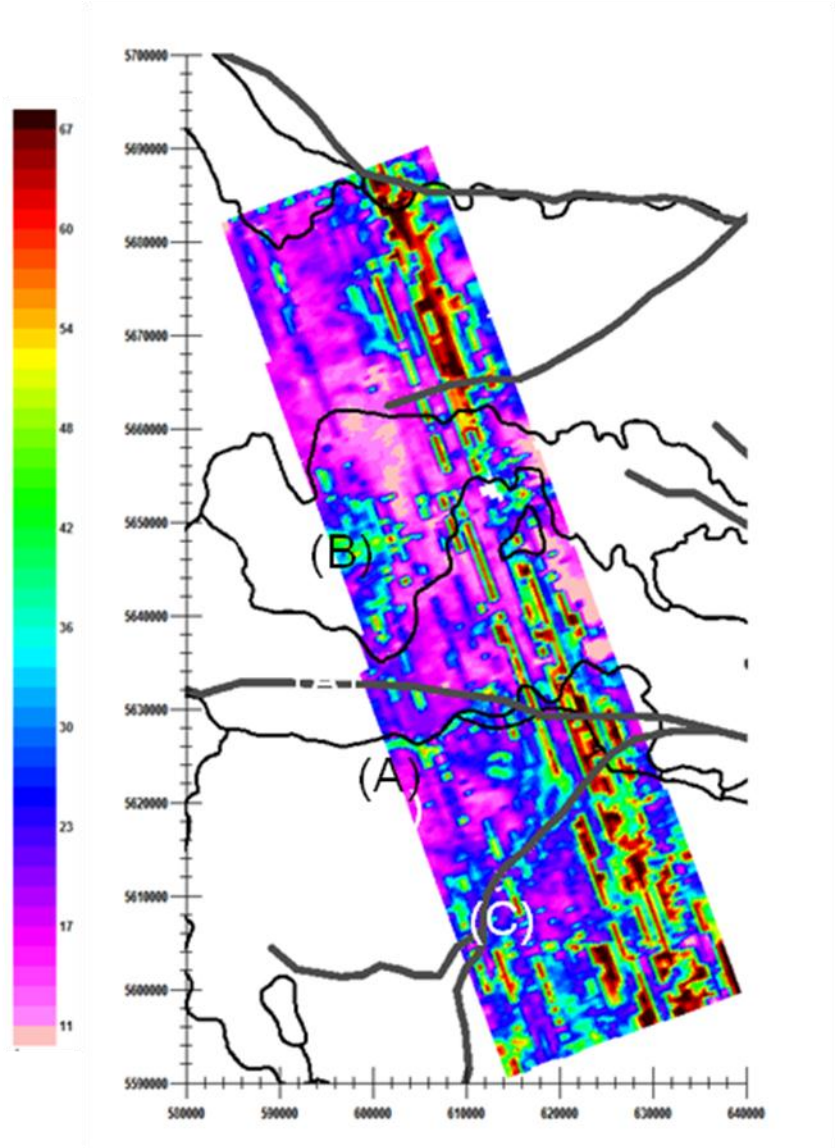

Figure 49: Area 1 east, 35 m depth slice. River geometries are shown in thin black while paleochannels are shown in grey. There is some correlated resistive structure along the Bow River (A), a cohesive spatial resistive structure at (B) as well as a possible resistive structure at (C).

The 65 m depth slice is shown in **Figure** 50. At this depth, the three structures are still visible. Area (C) appears to be a quite large spatial area of low resistivity extending to the east. Area (C) appears correlated with a paleochannel.

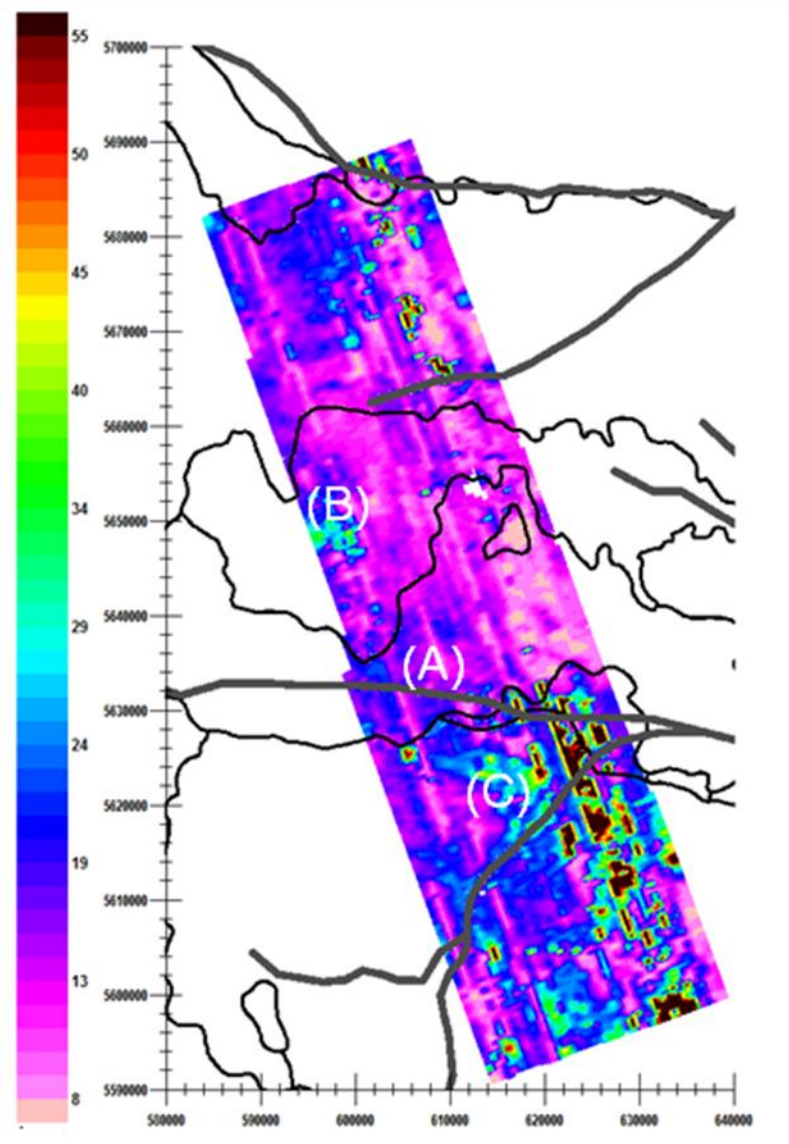

Figure 50: 65 m depth slice for Area 1. Area (C) appears to be a quite large spatial area of low resistivity extending to the east. Area (C) appears correlated with a paleochannel.

At 75m depth (**Figure** 51), there appears no correlation with the paleochannels. However, large areas of resistive material are to be seen which could indicate more coarsely grained sediments. These somewhat more resistive areas continue well below 100m when then begin to merge into the resistive substructure.

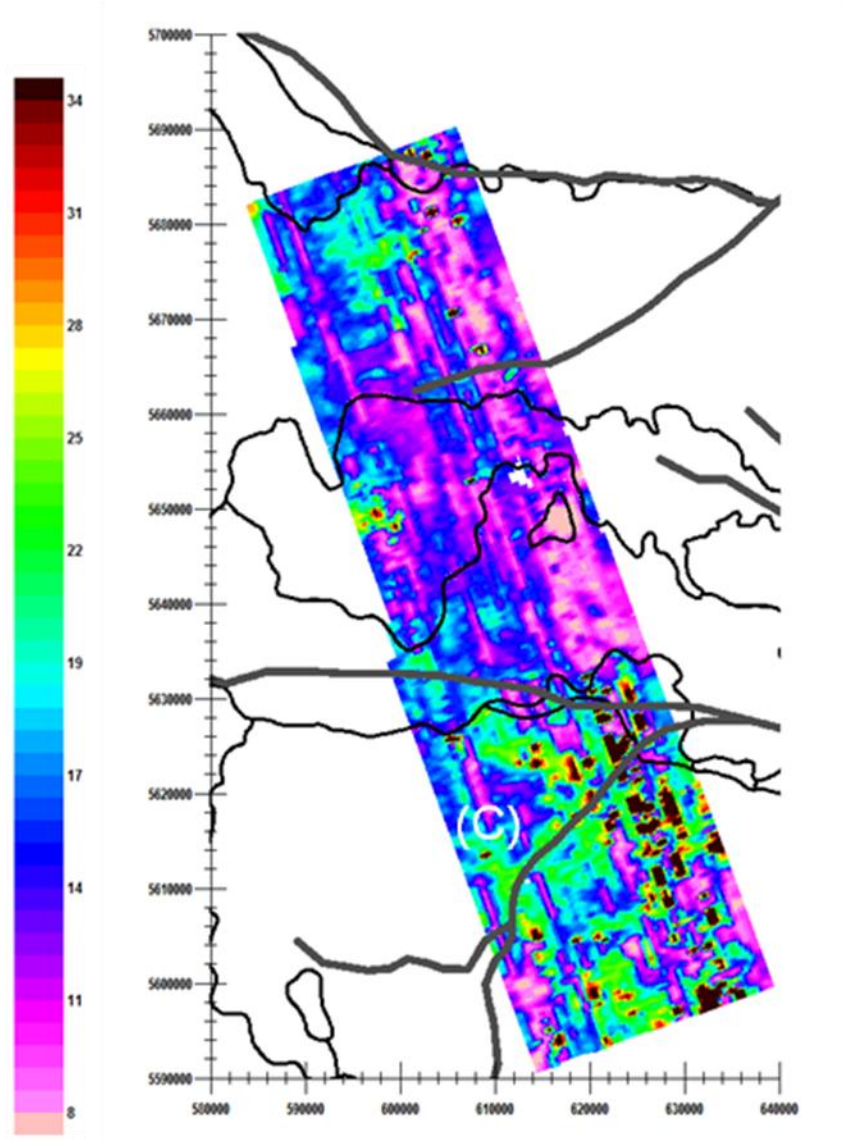

Figure 51: 75 m depth slice for Area 1.

7.1.3 Interpretation of Smooth, Shallow Inversions

In this section, figures showing the depth slices for the shallow inversions between 10 m and 60 m are presented. These are compared with known infrastructure and also maps of the rivers and paleochannels. Little correlation is noted between the infrastructure and the inversion results. Some correlation with rivers and paleochannels is observed, as are other features of interest.

The second set of inversions is more interpretable than the original inversions. The shallow inversions for Area 1 are much cleaner from the shallowest depth slice when we do not attempt to resolve the shallow resistor. As mentioned in Section 6.5, this supports our conclusions regarding the quality of the very early and the mid-late decays. While some of the same features are noted in both sets of inversions, additional structures are observed in the shallow inversions, and a discussion of these features is provided.

In **Figure 52**, a resistivity depth section is shown at 10m below surface for the shallow inversion approach. Major highways are shown as dark red lines. No significant effects of the major highways are evident.

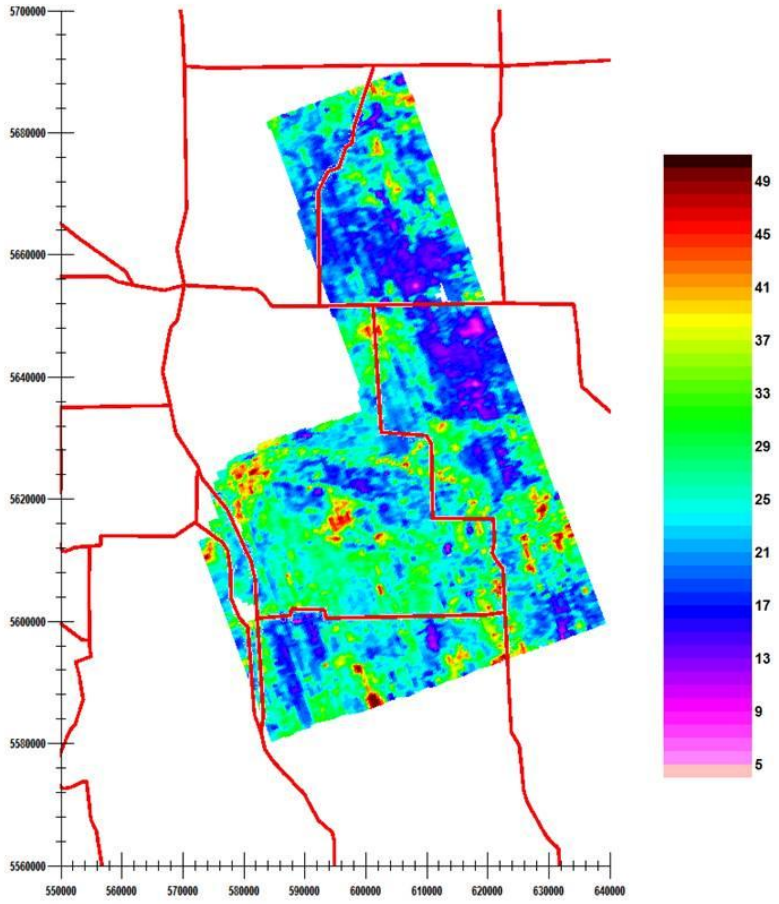

Figure 52: Highways on Area 1 depth slice at 10 m below (shallow inversion).

Similarly, no significant effects of major power lines are evident in the depth slice at 10 m, as shown in **Figure 53** except possibly at (A), (B), and (C).

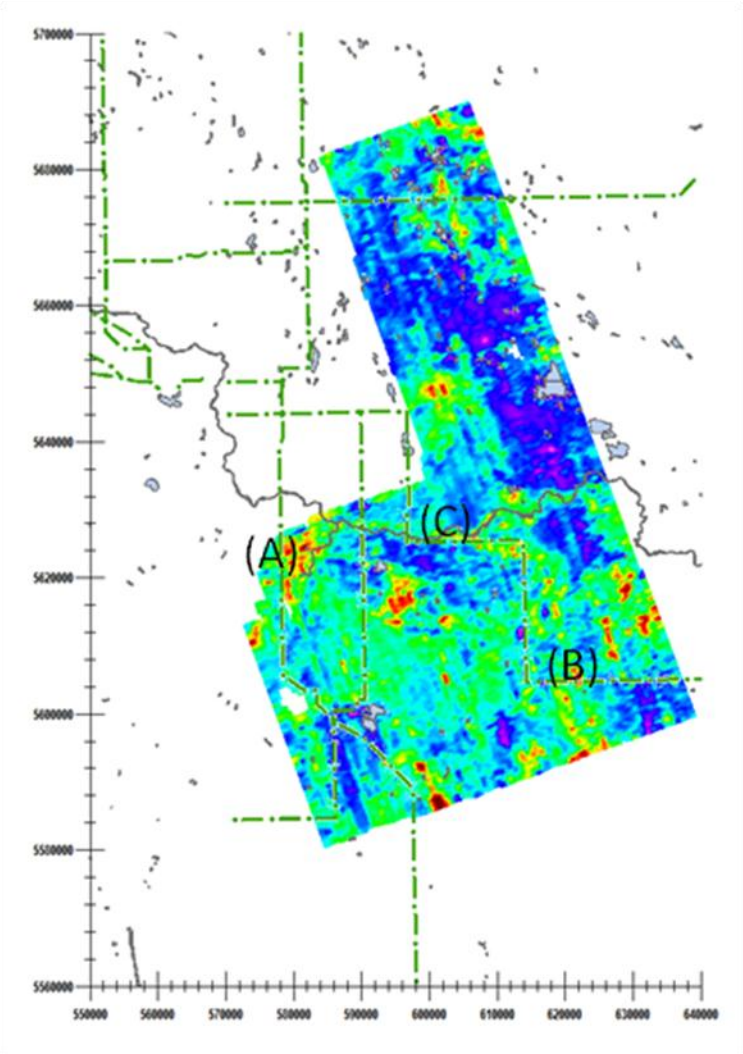

Figure 53: Depth section at 10 m for Area 1. Major power lines are shown as broken green lines.

In **Figure 54**, the same resistivity depth section is shown with rivers and paleochannels marked. Four structures are marked:

(A) - Some correlation with the interpreted paleochannel.

(B) Low resistivity area correlated with 2 rivers and 2 paleochannels.

(C) Possible correlation with river but also appears to be an area of population.

(D) - (D') - appearance of an unknown structure

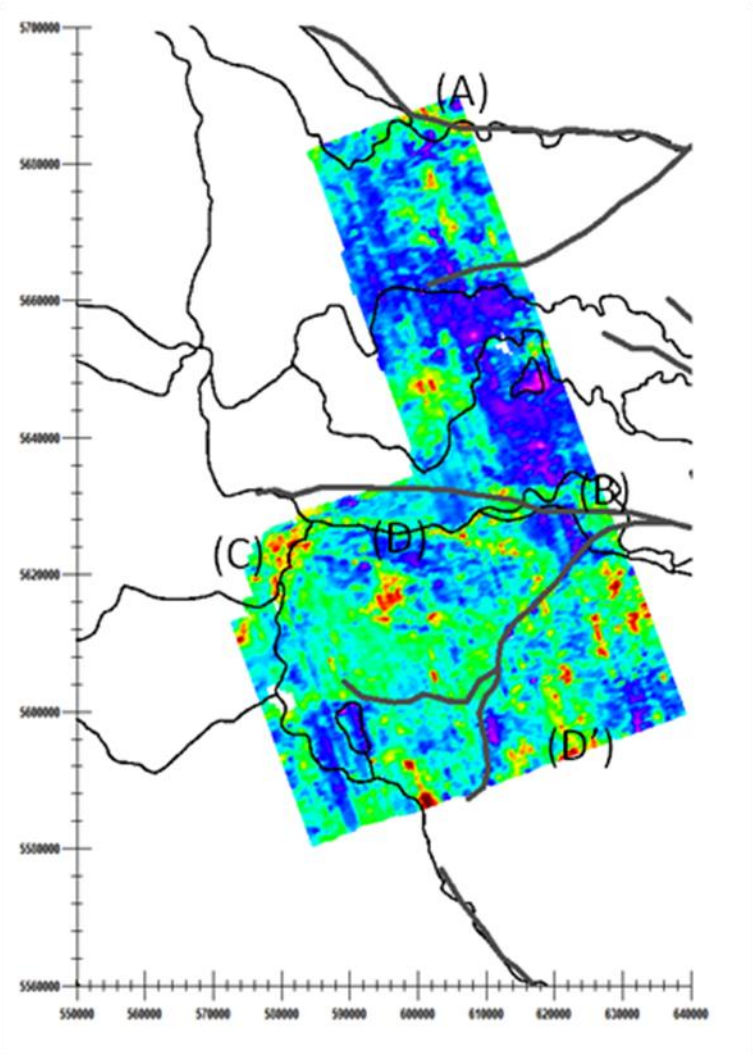

Figure 54: Depth section at 10 m for Area 1 (shallow, smooth inversion). Rivers are shown as thin black lines and paleochannels by thicker grey lines.

A deeper slice, 30 m, is displayed in **Figure 55**. Important features are described below:

(A) – some correlation with the interpreted paleochannel.

(B) – (B') Low resistivity area correlated with 2 rivers and 2 paleochannels.

(C) Possible correlation with river and possible gravel bed but also appears to be an area of population.

(D)- (D') - stronger appearance of an unknown structure

In addition to these items, there appear to be several areas of low resistivity or possible gravel beds.

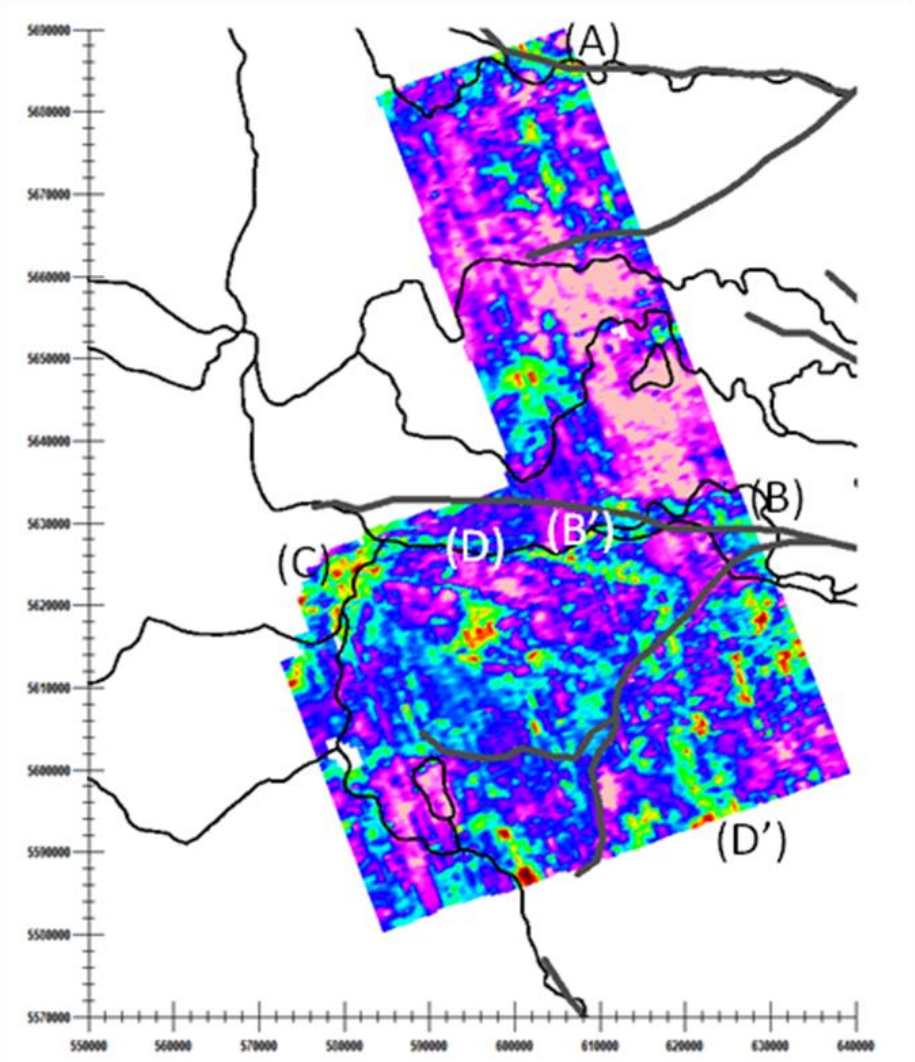

Figure 55: Depth section at 30 m for Area 1 (shallow, smooth inversion). Rivers are shown as thin black lines and paleochannels by thicker grey lines.

The 40 m depth slice for the shallow Area 1 inversions is shown in **Figure 56**. The following are observed, as marked on the figure:

(A) – Continued correlation with the interpreted paleochannel.

(B) – (B') Low resistivity area correlated with 2 rivers and 2 paleochannels.

(C) Possible correlation with river and possible gravel bed but also appears to be an area of population.

(D)- (D') - continued appearance of an unknown structure

(E) Apparent correlation with interpreted paleochannel

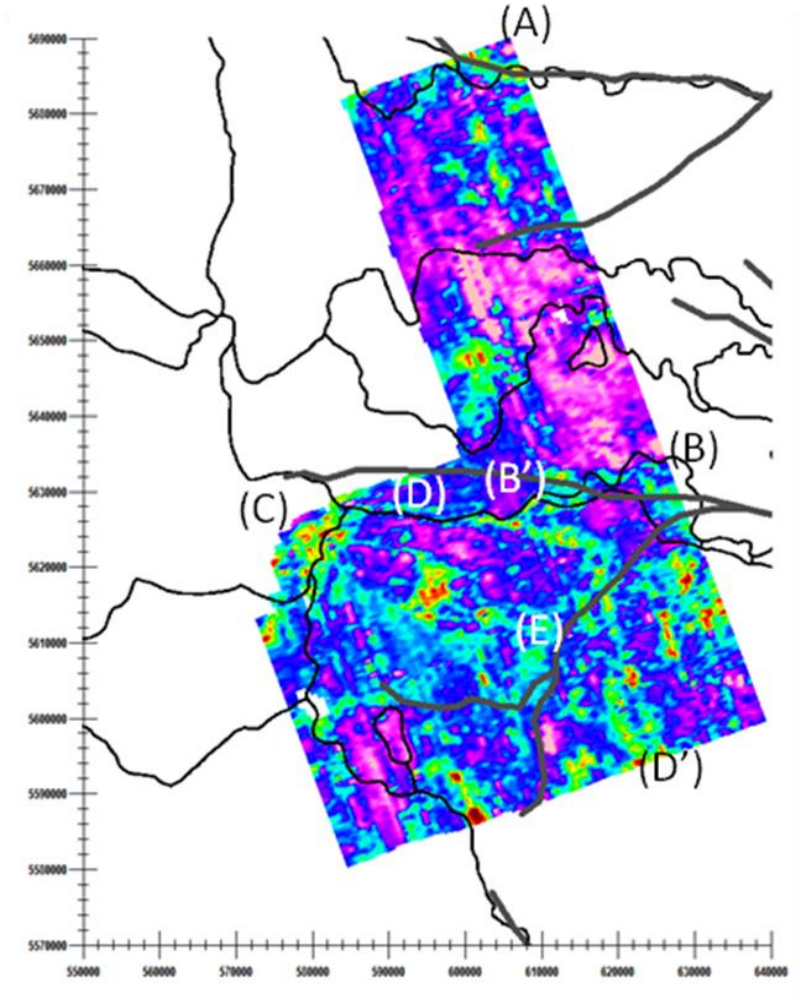

Figure 56: Depth slice at 40 m for Area 1 (shallow, smooth inversion). Rivers are indicated as thin black lines and paleochannels by thicker grey lines.

The 40 m depth slice is shown again in **Figure 57,** but with a different color range to emphasize the resistive areas. Based on the results, the position of the south paleochannel has also been adjusted and is shown in grey-blue.

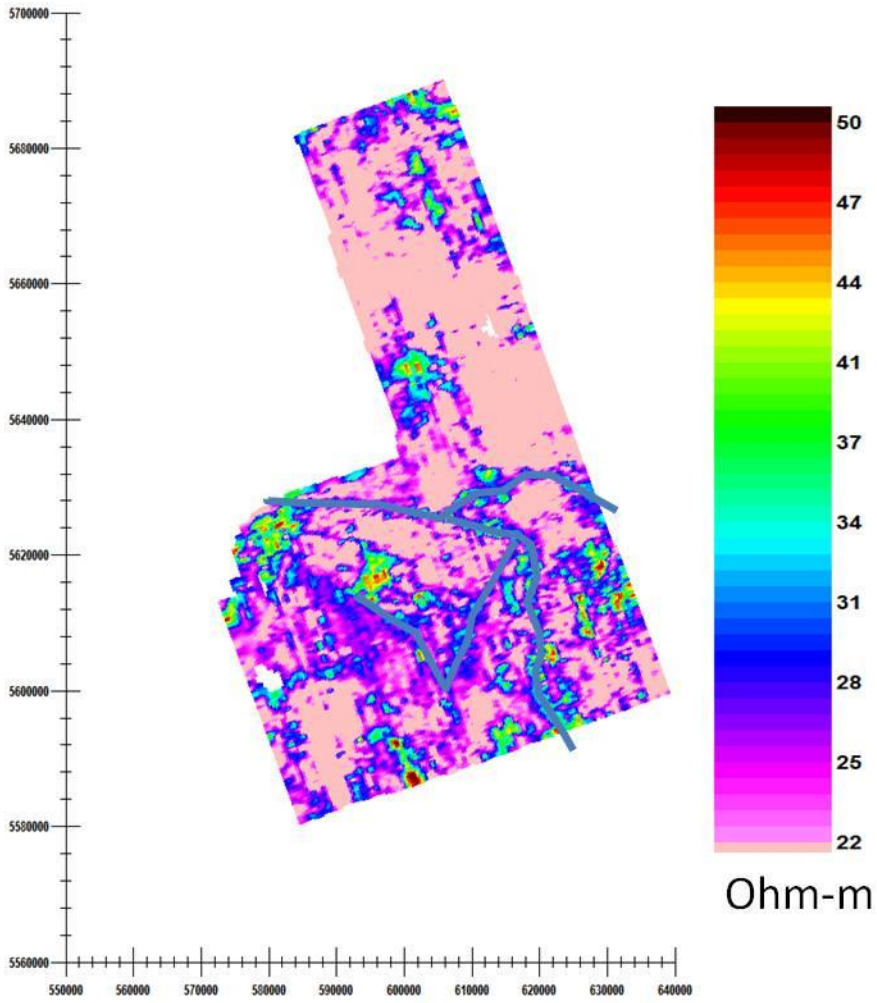

Figure 57: Depth slice at 40 m for Area 1 (shallow, smooth inversion). A suggested revision to the southern paleochannels is marked in grey-blue.

The 50 m depth slice for the shallow inversion is displayed in **Figure 58**. There are several features of interest:

(A) Continued correlation with the interpreted paleochannel.

(B) – (B') Low resistivity area correlated with 2 rivers and 2 paleochannels.

(C) Possible correlation with river and possible gravel bed but also appears to be an area of population.

(D)- (D') - continued appearance of an unknown structure but weaker

(E) Apparent correlation with interpreted paleochannel

(F) Some correlation with paleochannel

(G) Some correlation with paleochannel

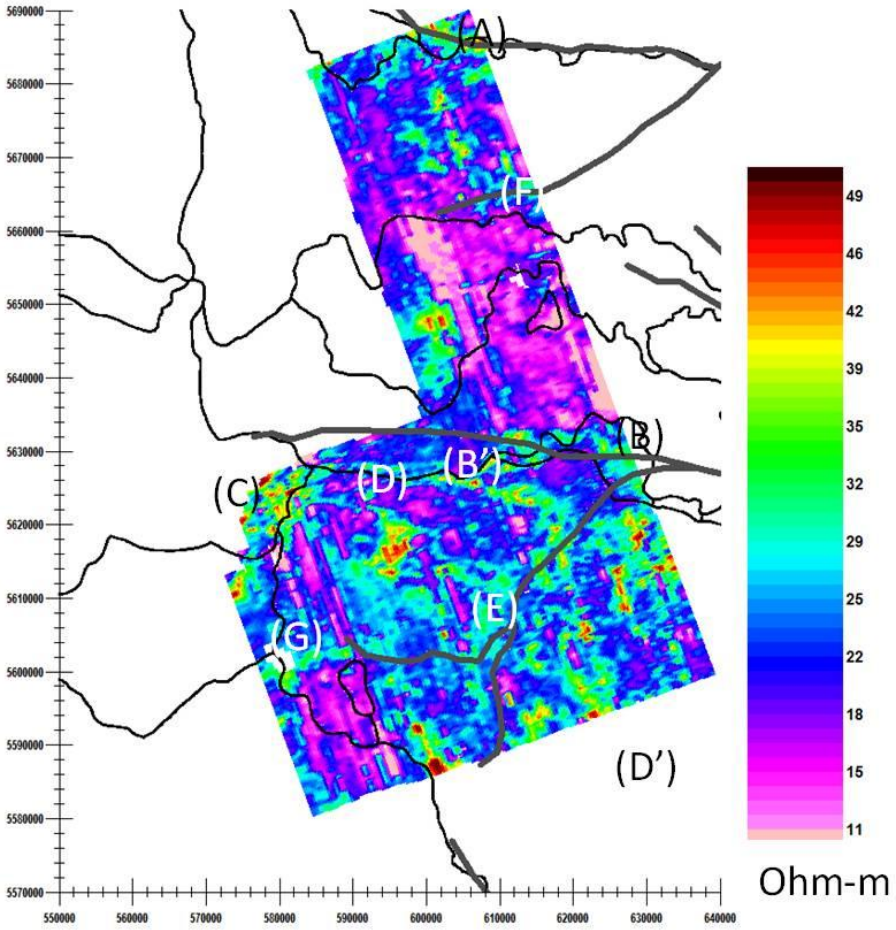

Figure 58: Depth slice at 50 m for Area 1 (shallow, smooth inversion). Rivers are shown as thin black and interpreted paleochannels by thick grey lines.

The 60 depth slice for Area 1 is displayed in **Figure 59.** Of note:

(A) Continued correlation with the interpreted paleochannel.

(D)- (D') - continued appearance of an unknown structure but weaker

(E) Apparent correlation with interpreted paleochannel

(F) Some correlation with paleochannel

(G) Some correlation with paleochannel

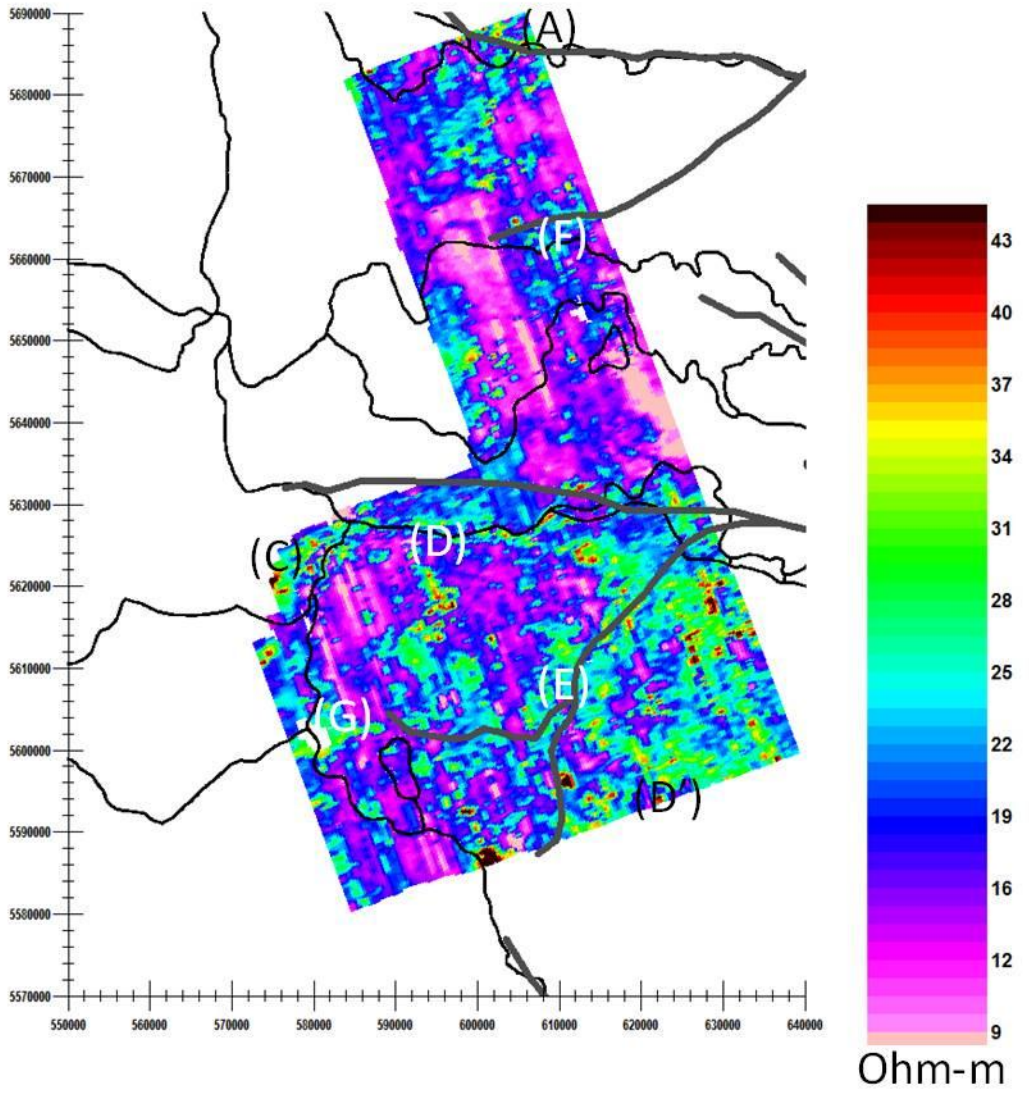

Figure 59: Depth slice at 60 m for Area 1 (shallow, smooth inversion). Rivers are shown as thin black and interpreted paleochannels by thick grey lines.

7.2 Area 2 (NE)

7.2.1 Effect of Known Features

7.2.1.1 Infrastructure

No correlation with the major highways is noted in the Area 2 data.

Figure 60 displays the Channel 4 data with a map of the railways, pipelines, and major power lines in the area. One major power line to the south corresponds to a low in the data. No other strong correlation with manmade structures is noted.

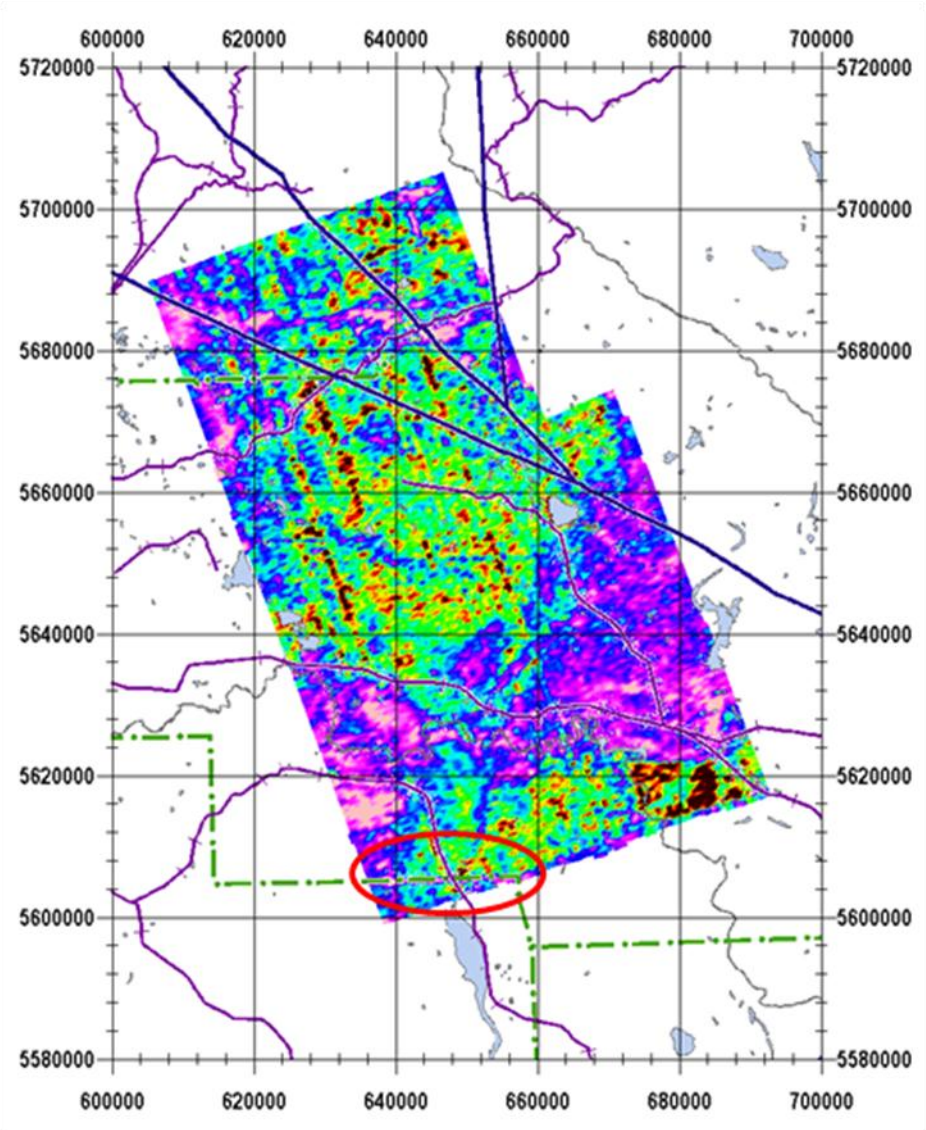

Figure 60: Channel 4 data for Area 2 with pipelines (dark blue), railways (purple), power lines (green), lakes (light blue) and rivers (grey) shown.

7.2.2.2 Topography and Rivers

Figure 61 compares the data with rivers and known paleochannels. Two rivers are observed as lows in the data, and a further river appears as a boundary between a lower response to the east and a higher response to the west. Sections of both of the rivers that appear as lows in the data are also topographic lows (see **Figure** 62) over all or part of their length. Also of note in comparing the digital terrain to the data is that the topographic low to the southeast approximately correlates with a low in the data.

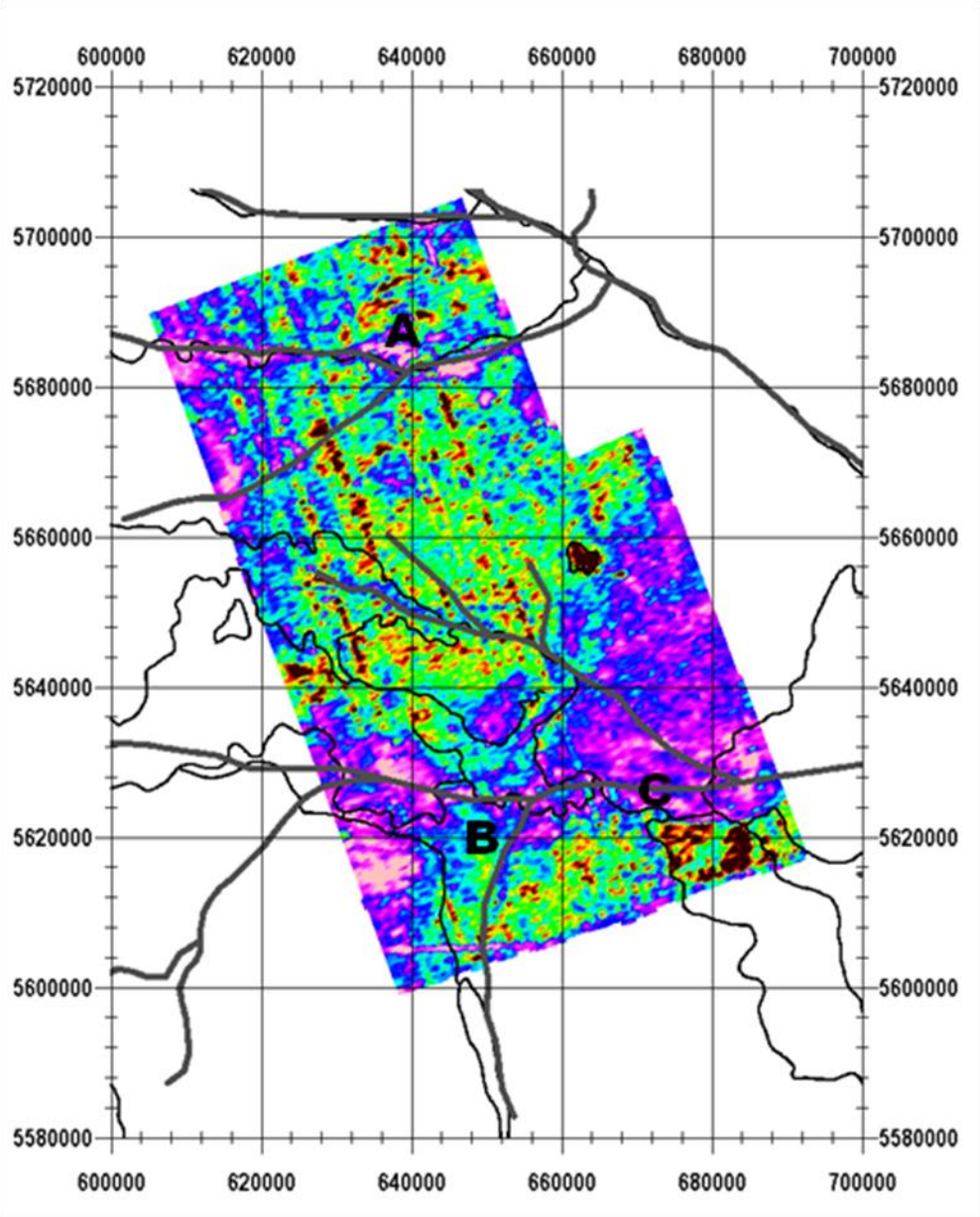

Figure 61: Channel 4 data for Area 2 compared with rivers (thin black lines) and paleochannels (thicker grey lines. Some rivers are along paleochannels. Significant correlation between rivers and a low amplitude is noted at two locations (A and B), and the river in (C) is along a boundary in the response.

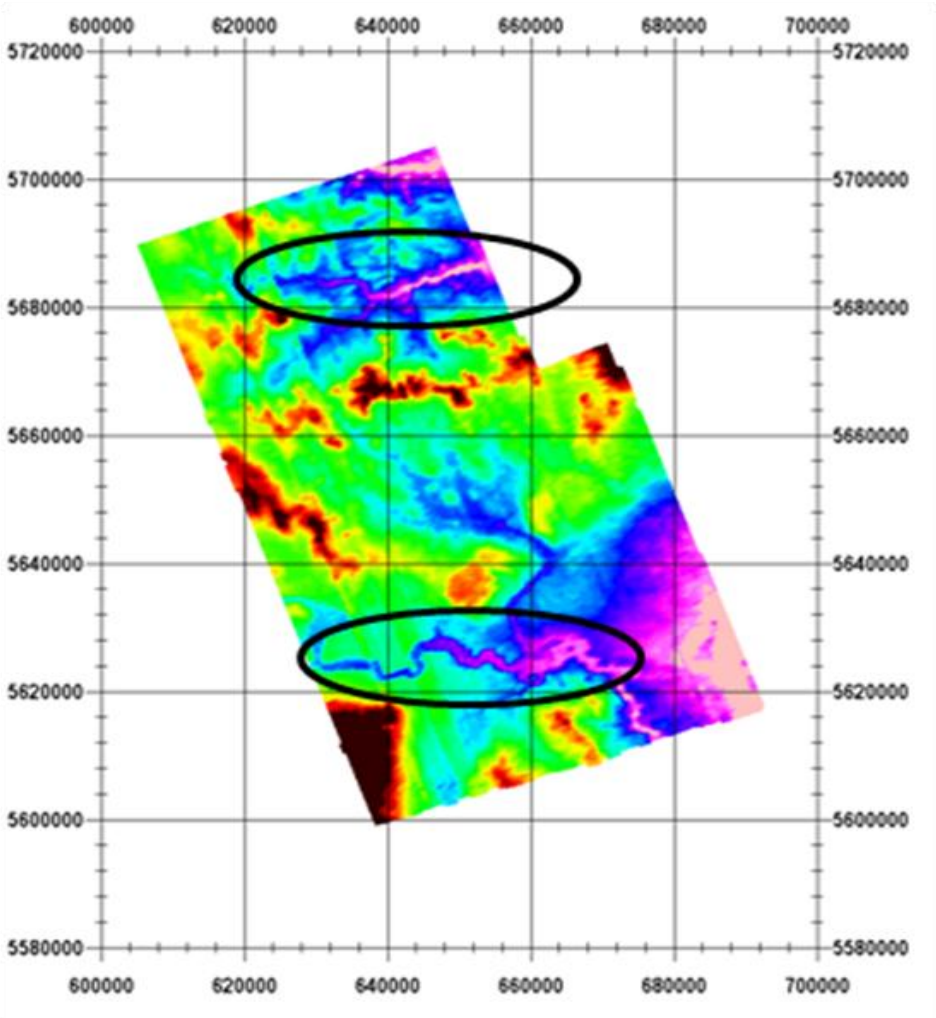

Figure 62: Digital terrain model for Area 2. Rivers are circled.

A close-up of the north river in Area 2 is shown in **Figure** 63 both with the Channel 4 data and the digital terrain model. The position of the river in black (from the Alberta geology map) corresponds fairly closely with the digital terrain model, with some minor differences. This approximately corresponds to a linear low in the data, as noted previously; however, there are some differences in the position of the river and the low in the data.

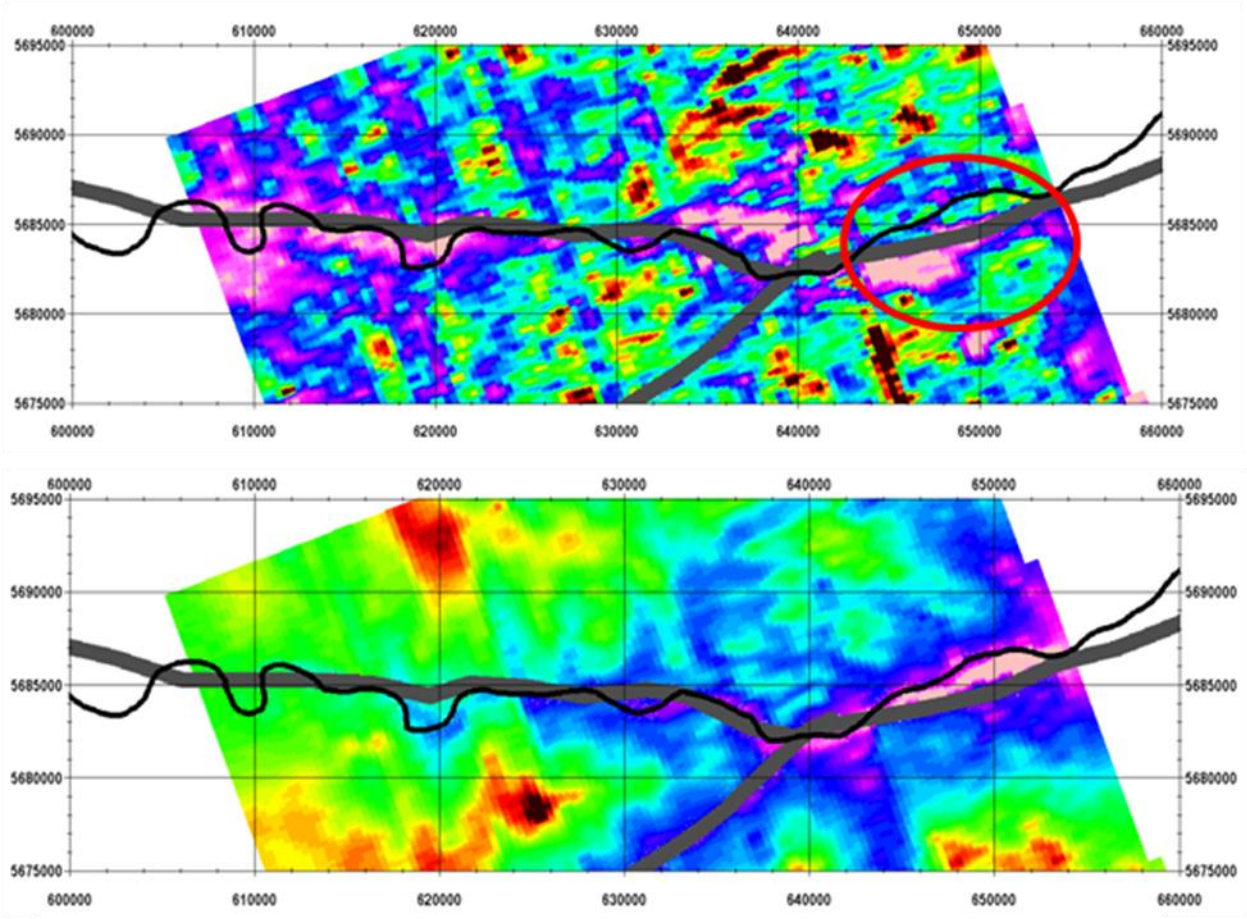

Figure 63: Comparison of north section of Area 2 with location of river (black) and paleochannel (grey). Channel 4 is shown on top and the digital terrain model is shown below.

7.2.2 Interpretation of Original Inversions

7.2.2.1 Paleochannels

In evaluating the ability of the survey to meet the objectives of AENV, the depth slices were compared with known paleochannels. A map of the paleochannels and depth slice of the Area 2 inversion at 60 m is shown in **Figure** 64. (Area 2 is the survey block with the most known channels.)

In the north, a single paleochannel to the east (1) branches into two channels (2, 3) in the west. These are observed in the depth slice as resistors, with the exception of a section of the southern branch (3). Further south, (4) and (5) are also observed as resistors, and the inversion suggests that (5) continues to the northeast (see Section 7.0). (6) cuts through an area of elevated resistivity but the channel itself is not resolved. (6) branches into (7), (8), and (9), which do not have any clear association with the resistivity distribution in the depth section. In addition to the known paleochannels, it appears that (6) extends to the northeast, as marked in **Figure** 64.

Note that the paleochannels are most readily observed in the depth sections between about 45 m and 65 m. However, some channels are also observed as shallow as 30 m and as deep as 80 m in the depth slices. No information on the true depth of these paleochannels is available for comparison.

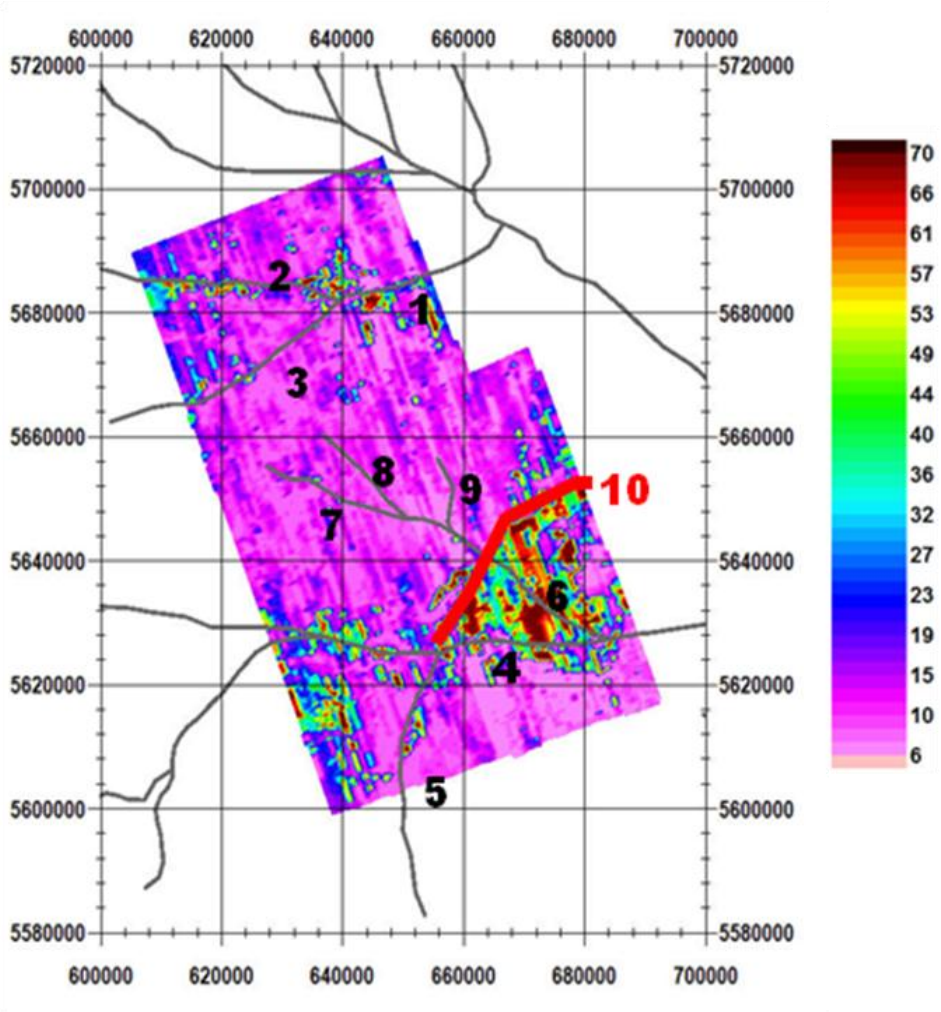

Figure 64: 60 m depth slice for Area 2 showing known paleochannels in grey, labeled 1-9. Paleochannels 1-5 correlate with resistors in the depth slice. (10) is a possible extension of (5) based on the inversion results.

These results show that the inversions are able to highlight some of the known paleochannels. Features with similar characteristics in the depth slices that are not correlated with known channels may be of interest. It is not known why some of the channels are not observed in the depth slices. Some possibilities:

1) Lack of resistivity contrast between the background and the fill material. The fill material in these undetected channels (7,8,9) may be different than that of the other channels.

2) Greater depth to top of paleochannel. The detected paleochannels were seen in the depth slices around 50 m depth. If (7,8,9) are significantly deeper, the survey may have insufficient resolution to see them.

These comparisons suggest that the AeroTEM survey is able to resolve some paleochannels, and potential paleochannels may be found in examination of the inversion depth slices, but that the survey is not able to resolve many of these channels. While this may be in part due to the data quality, it is thought that the properties of some of the channels make them difficult to detect with an AEM survey. This is based on the fact that certain channels in Area 2 (where data quality is comparatively good) are not seen in the inversion results but are observed in the data. Paleochannel 7, in fact, is observed in the shallow inversions (Section 7.2.3).

7.2.2.2 Comparison with Sand and Gravel Deposits

The majority of the survey area is within the following counties: Vulcan and Wheatland. Regional Groundwater Assessments, performed by Hydrogeological Consultants Ltd., are available for both of these counties. These reports contain information on aquifers, as determined from a large sample of drill logs. Both contain maps of sand and gravel aquifer thickness. Most of Area 2 is within Wheatland, and the area of high resistivity to the southeast generally corresponds to greater thickness of sand and gravel aquifers (**Figure** 65). Note that this is observed most clearly in the depth slices between 40 m and 60 m, although it is assumed that these aquifers would be close to surface.

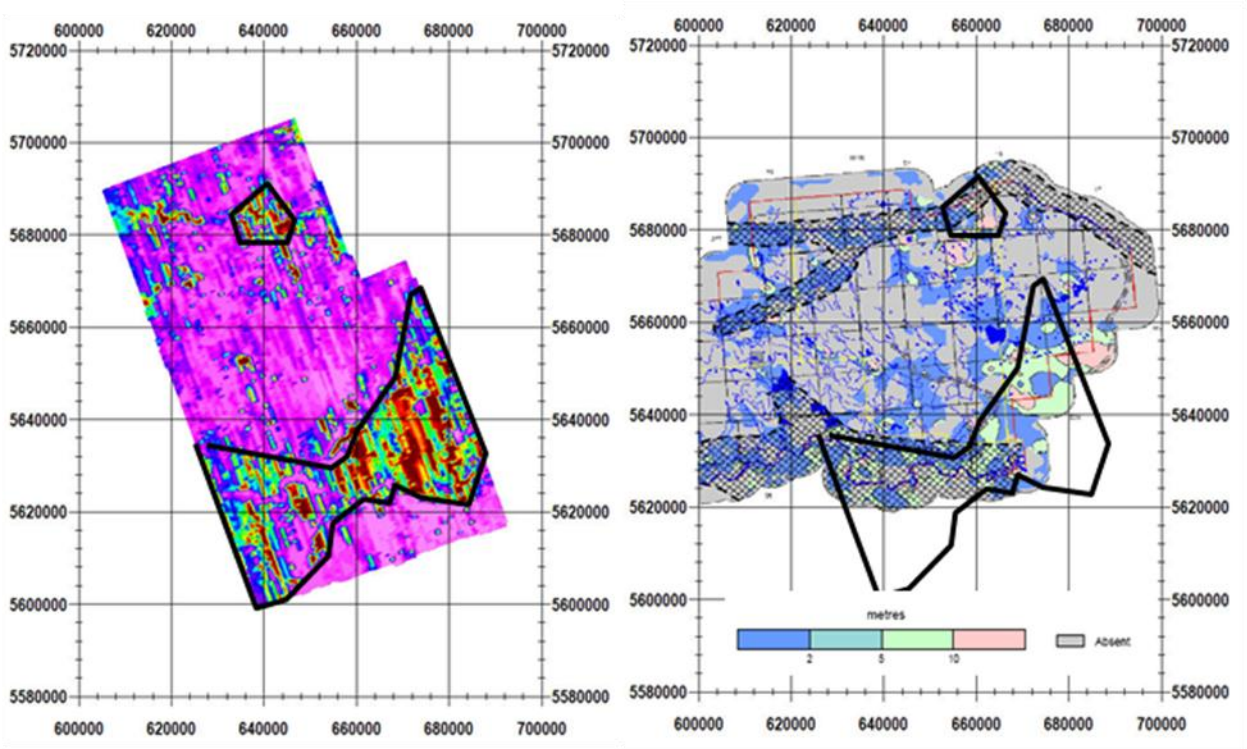

Figure 65: 50 m depth slice for Area 2 and map of sand and gravel aquifers (from HCL, 2003) with area of high resistivity in the depth slice marked.

7.2.3 Interpretation of Shallow, Smooth Inversions

Figure 66 shows the shallow inversion depth slice at 20 m. Several features are of note:

(A) – Linear resistor, corresponds to paleochannel. This was also noted in the original inversions, but was not observed at a shallow depth

(B) – Linear resistor, corresponds to paleochannel. Possible extends to B'.

(C) – Area of high resistivity. Possibly sand/gravel.

(D) – Linear resistor, though not as clear as (A) and (B). This was not observed in the original inversions.

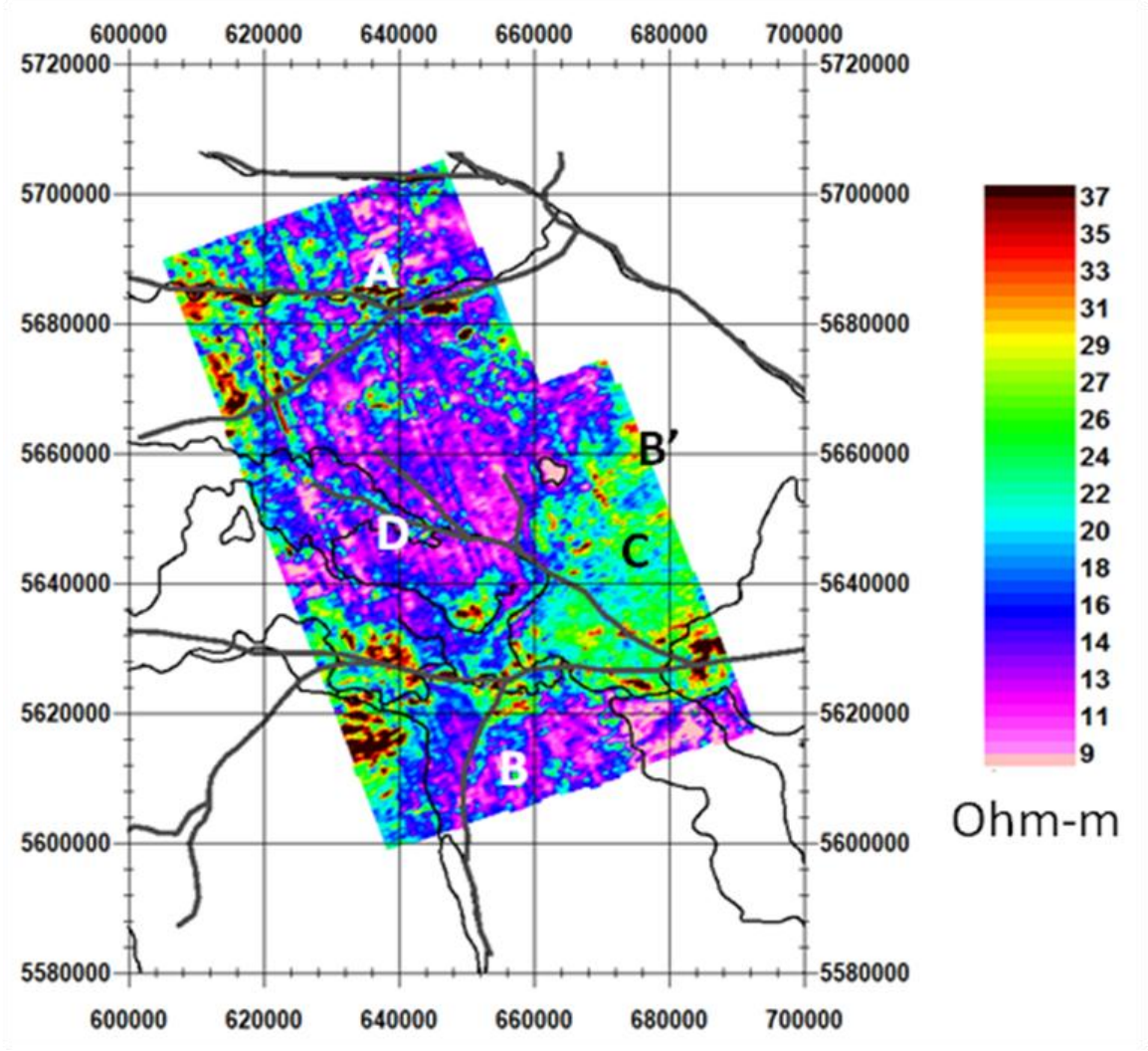

Figure 66: Depth slice at 20 m for Area 2 (shallow, smooth inversion). Rivers are shown as think black and interpreted paleochannels by thick grey lines.

Below is the 40 m depth slice for the shallow Area 2 inversions. It is quite similar to the 20 m depth slice, although the paleochannel at (B) is defined more clearly.

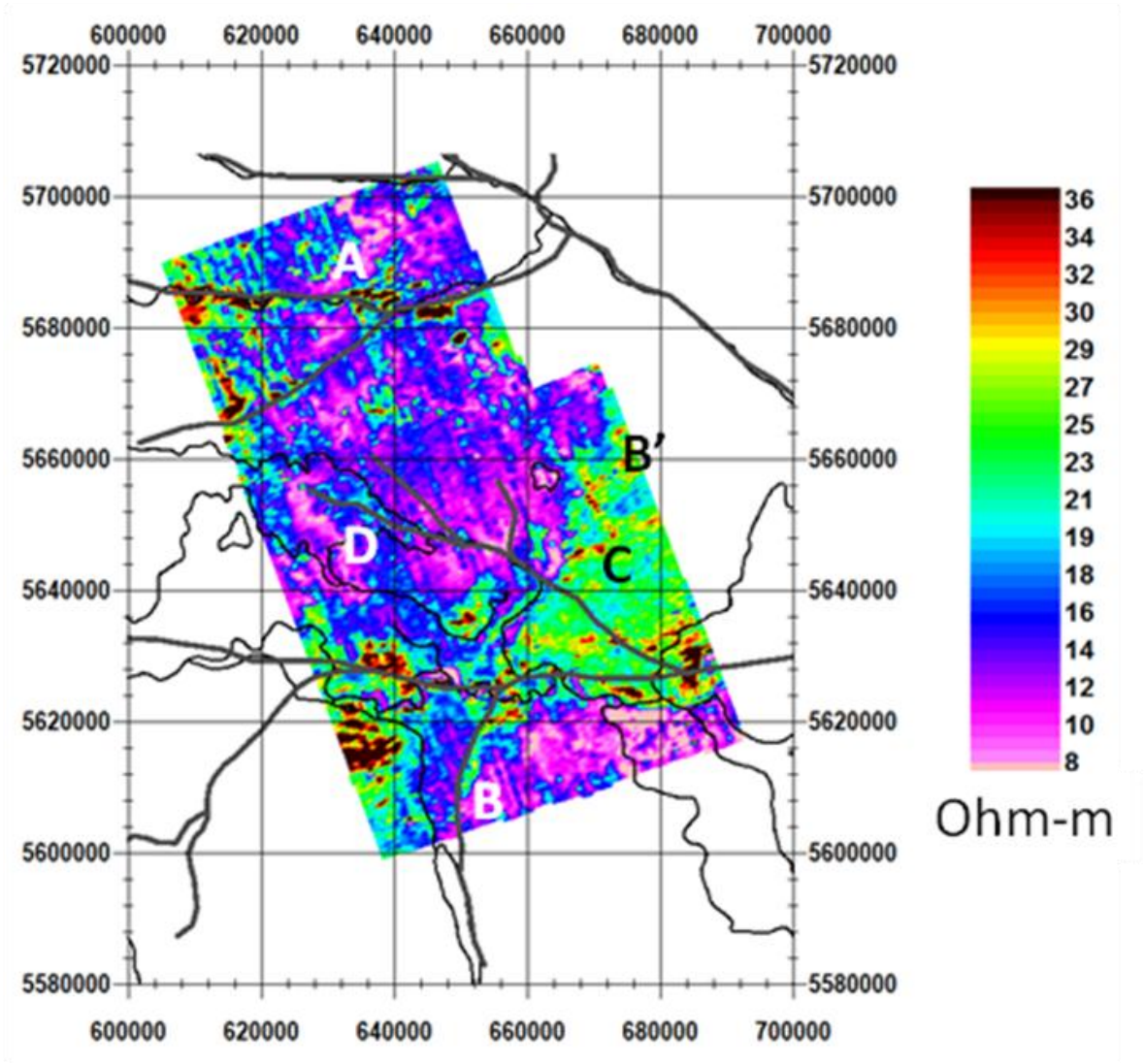

Figure 67: Depth slice at 40 m for Area 2 (shallow, smooth inversion). Rivers are shown as think black and interpreted paleochannels by thick grey lines.

Results for the new shallow inversions are shown for a depth of 60 m in **Figure 68**.

(A) – Still clearly observed at this depth; corresponds with paleochannel and river.

(B) – Greater resistivity contrast than at 20 m.

(C) – Resistive area is not as broad as at shallower depths.

(D) – While this paleochannel is still observed, it is not as clear as at shallower slices.

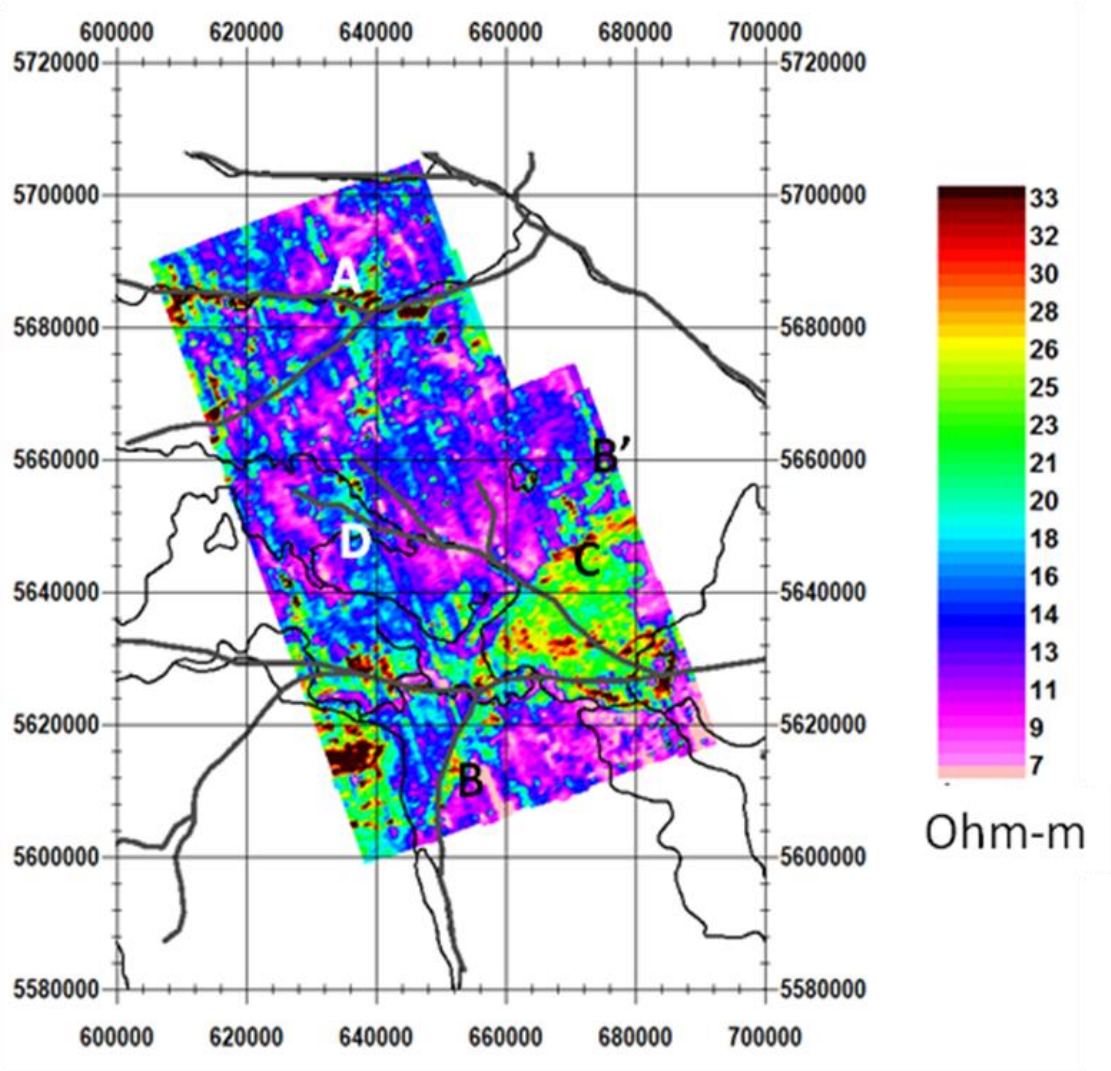

Figure 68: Depth slice at 60 m for Area 2 (shallow, smooth inversion). Rivers are shown as think black and interpreted paleochannels by thick grey lines.

A close-up of the 60 m inversion result near (A) for both the original and the shallow inversion is presented in Figure 69. This feature is observed clearly in both results although resistivities differ slightly.

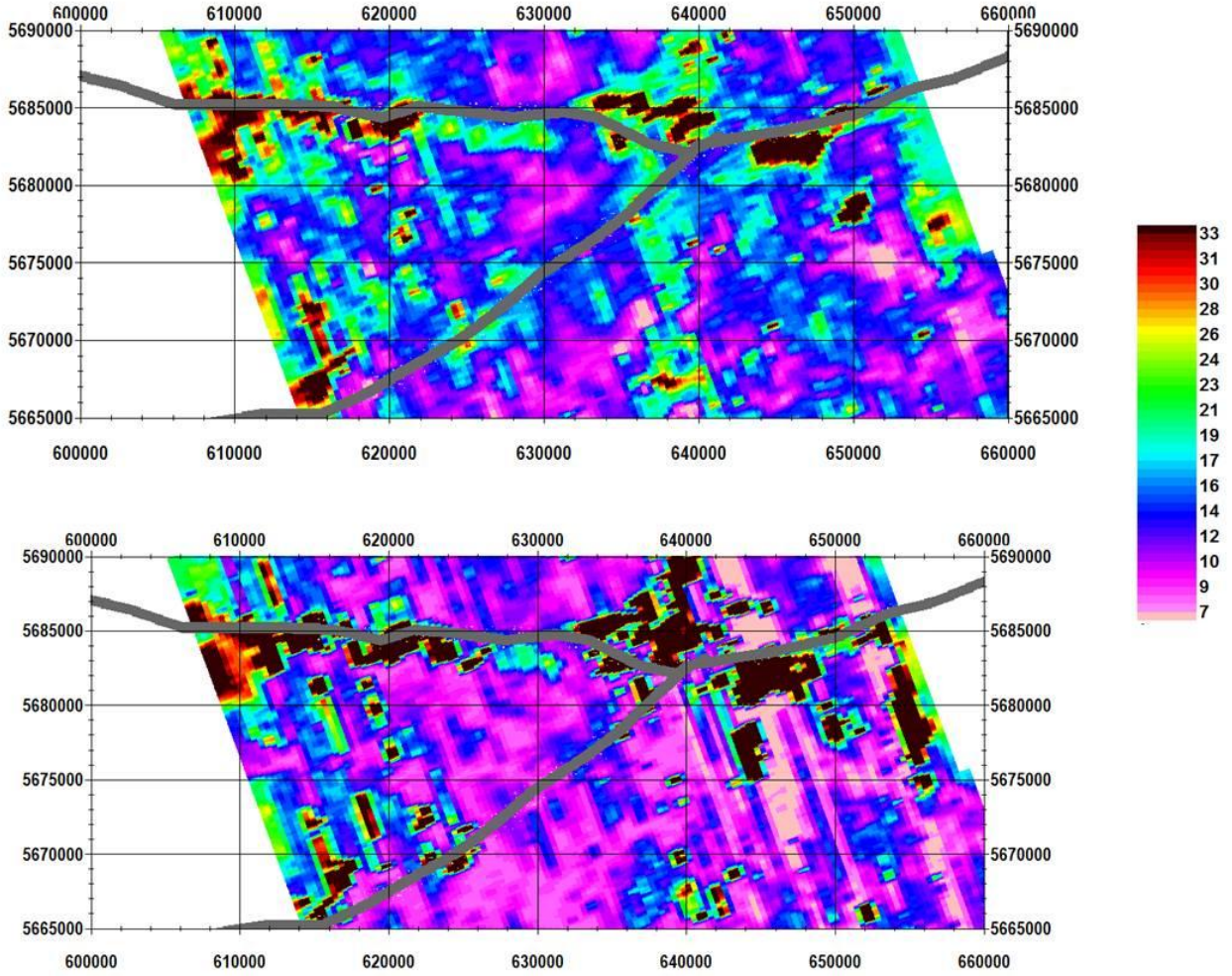

Figure 69: Comparison of original inversion (bottom) with shallow inversion (top) in the north part of Area 2. Paleochannels are shown.

A close-up of the south section of Area 2 at 60 m is displayed in **Figure 70** for both the original and the new shallow inversions. Paleochannels (thick lines) and rivers (thin black lines) are also marked. Both inversions show the same general areas as having high resistivity, although the range of resistivities within these structures is somewhat different. Some of these areas correspond to known sand/gravel deposits, as noted in Figure 65, and others may be potential aquifers.

The river near 5626000 N is more clearly observed in the shallow inversion, although its shape does not correspond precisely to that of the river map.

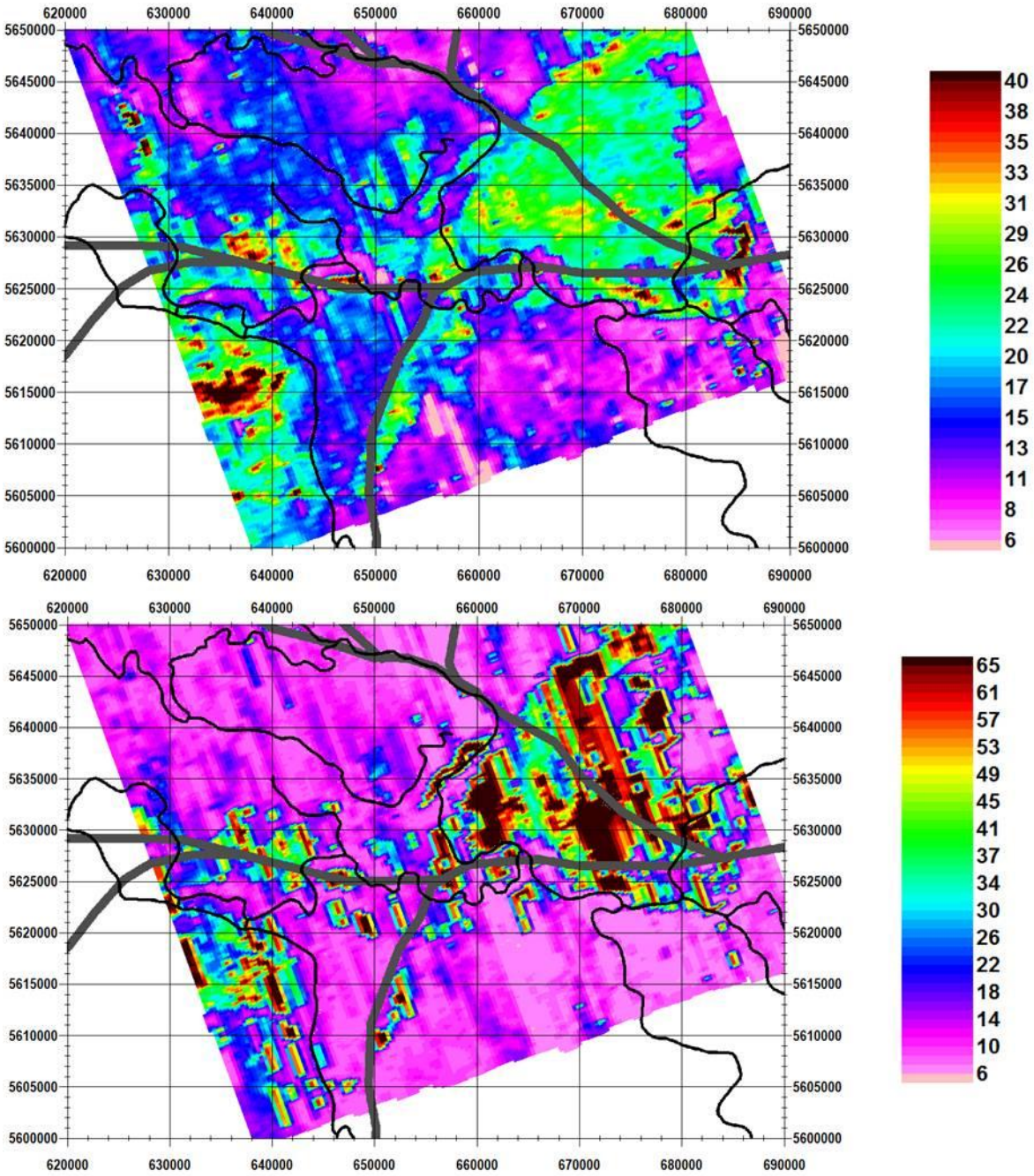

Figure 70: 60 m depth slices for original (bottom) and new shallow (top) inversions in the south section of Area 2. Paleochannels (thick) and rivers (thin) are also marked.

Figure 71 shows the depth slice at 80 m for Area 2.

(A) – Still observed at 80 m, although resistivity contrast is slightly less.

(B) – Clearly observed, and extension to (B') is most clear at this depth.

(C) – Extent of this resistive area has shrunk. It is thought that this is a sand/gravel deposit whose extent narrows at depth.

(D) – This paleochannel is no longer readily observed in the inversions by this depth.

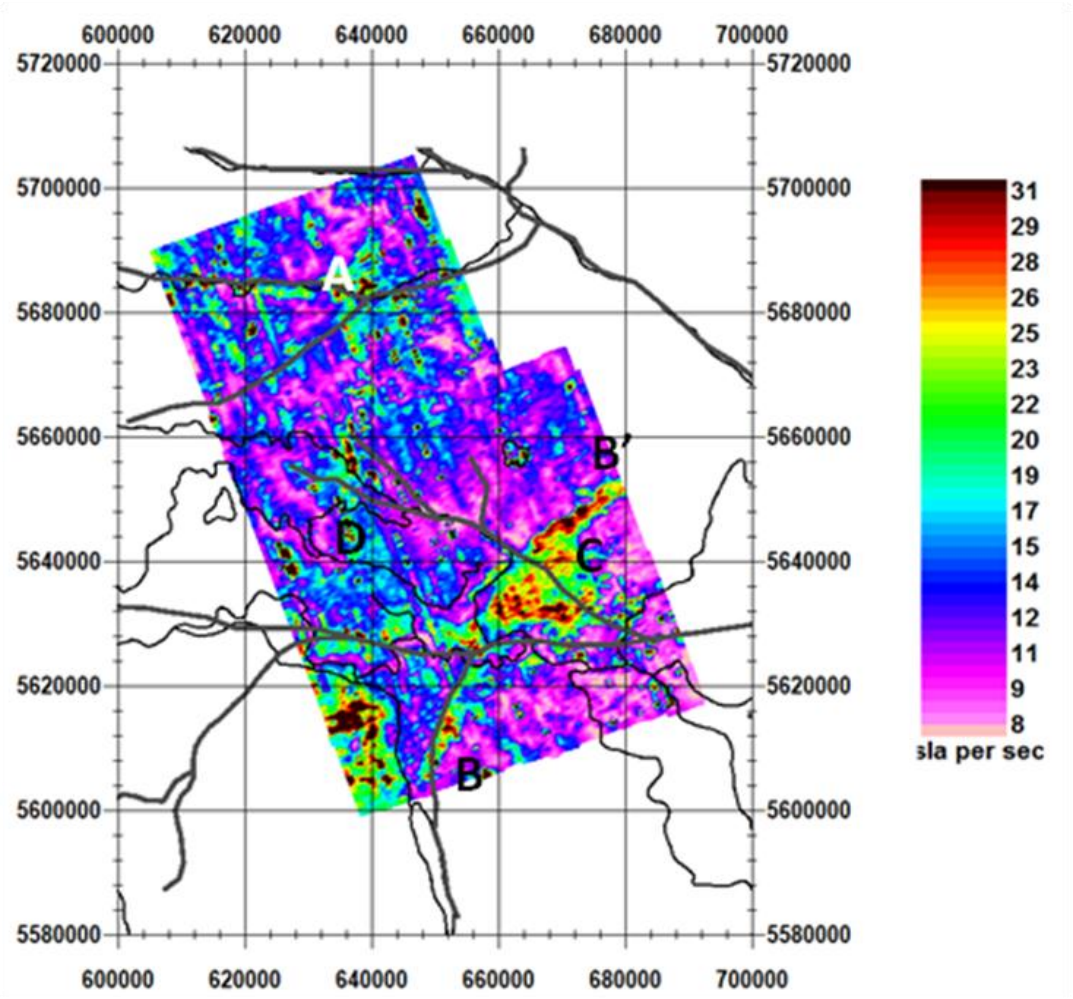

Figure 71: Depth slice at 80 m for Area 2 (shallow, smooth inversion). Rivers are shown as think black and interpreted paleochannels by thick grey lines.

7.3 Area 3 (SE)

7.3.1 Effect of Known Features

7.3.1.1 Infrastructure

Figure 72 displays the infrastructure against the Channel 4 data for Area 3. The major power line in the north corresponds with a drop in the AEM data amplitude. A second feature, parallel to this and assumed to be another power line, is noted further north. No correlation with major highways is observed.

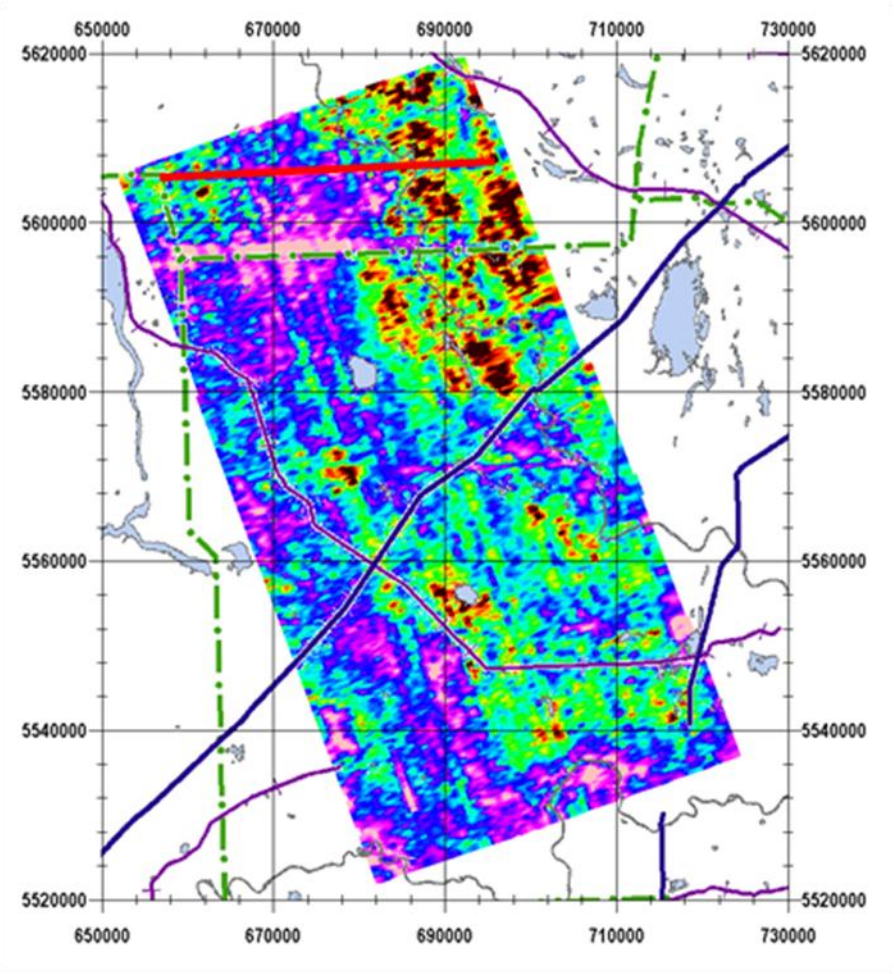

Figure 72: Channel 4 data for Area 3 with pipelines (dark blue), railways (purple), power lines (green), lakes (light blue) and rivers (grey) shown.

7.3.1.2 Topography and Rivers

Figure 73 displays the digital terrain model of the area. No significant correlation between the data and the terrain is noted. Some of the rivers appear as topographic lows in the digital terrain model. Note that the rivers used are from the province-wide AGS geology map, and it appears that there are minor

discrepancies between the position of the river and the minimum of the topographic lows. It is thought that this is because the river GIS information is a rough map of the rivers in the province, and details may not be accurate. The transformation of the data to the 10TM coordinate system in ArcMAP may also be a source of error.

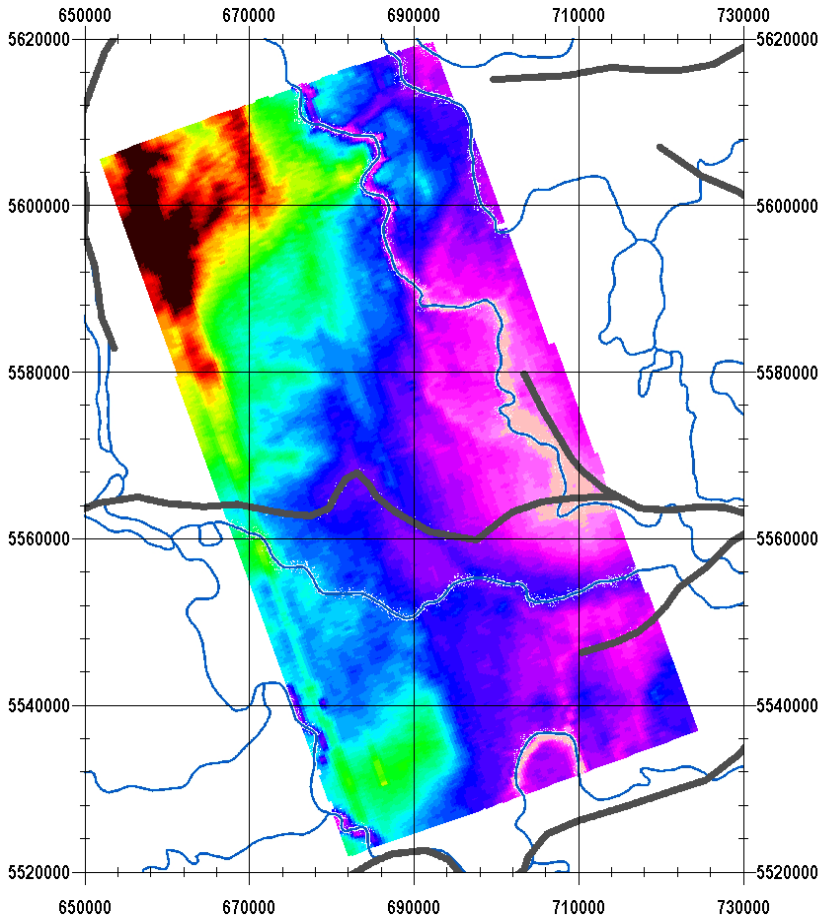

Figure 73: Digital Terrain model for Area 3 showing known paleochannels in grey and rivers in blue.

Figure 74 displays the data with known paleochannels and rivers. Unlike in other areas, no correlation is noted between the rivers and the AEM response.

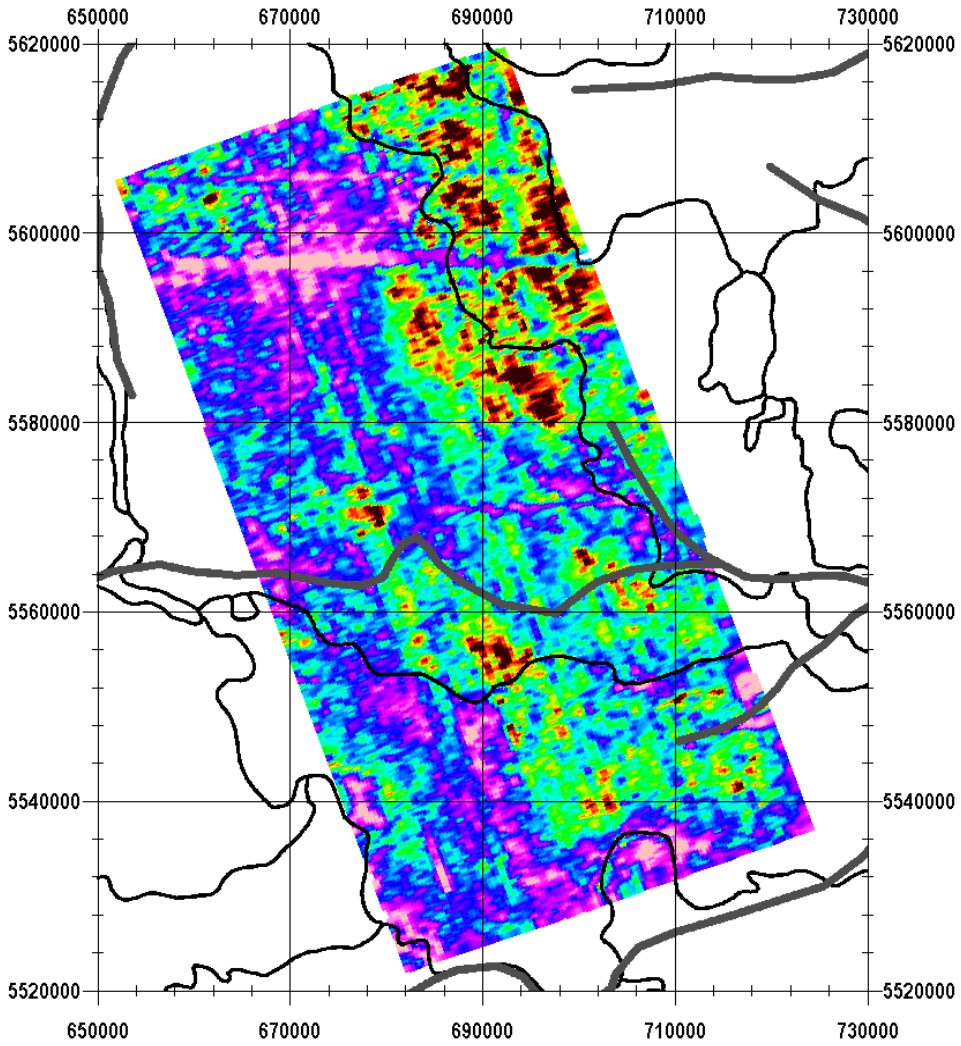

Figure 74: Channel 4 data for Area 3 with known paleochannels (grey) and rivers (black).

7.3.2 Interpretation of Original Inversions

7.3.2.1 Paleochannels

Figure 75 displays the known paleochannels and depth slice at 65 m for Area 3. The west side of (1) correlates strongly with a resistor in the depth slice. This is observed in the depth slice between 45 m and 100 m. The east and central sections of this paleochannel do not have a strong correlation with the depth slice. Based on the depth slice, it appears that where (1) bends towards the south, there is another extension further north, which is marked by (4) on the figure. This is based on the observation of a linear, resistive structure in the depth slice.

Paleochannel (2) is roughly parallel to the survey lines. While it roughly correlates with a resistor in the depth slice, it could also be streaking in the inversion results, caused by inconsistent data on multiple

lines. (3) does not show any clear association with the inversion results. Other than (4), no further structures are identified as possible paleochannels.

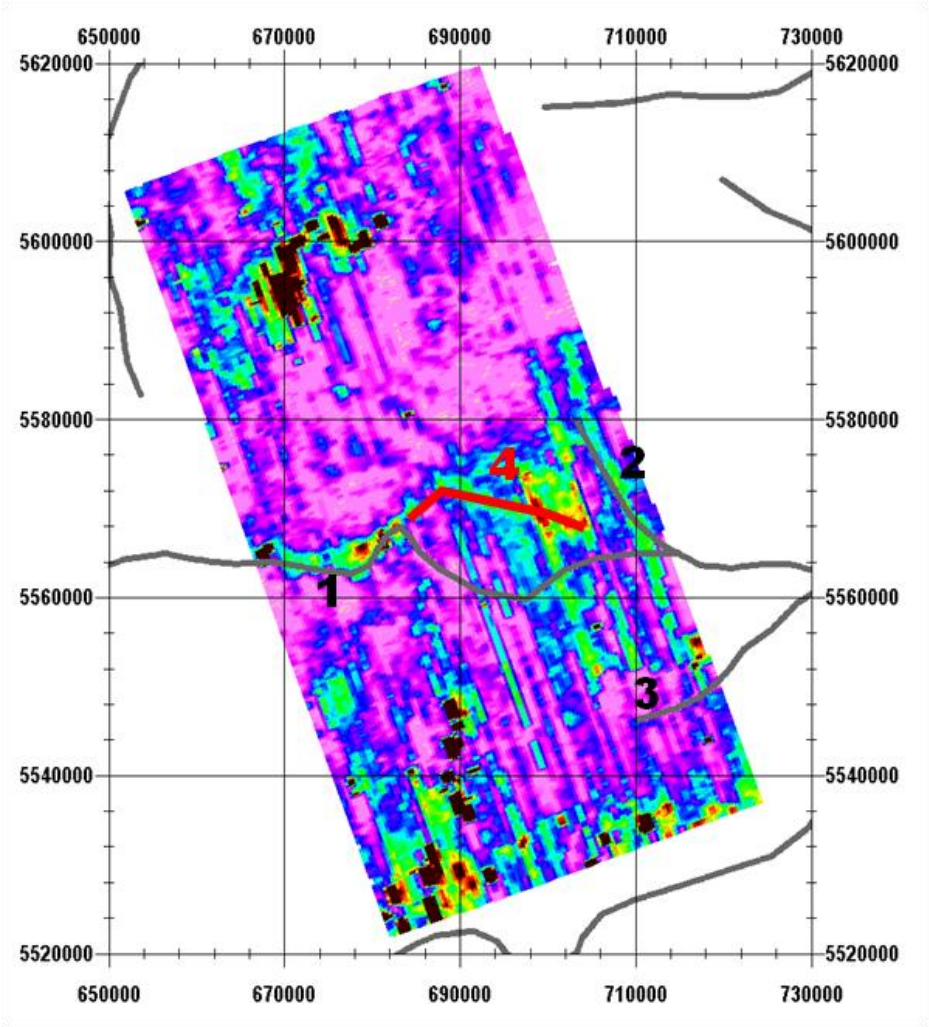

Figure 75: Area 3 depth slice at 65 m with paleochannels.

7.3.2.2 Comparison with sand/gravel aquifers

Figure 76 compares the sand and gravel aquifers in Vulcan Country (HCL, 2007) with two depth slices. The thickest sand/gravel aquifer (1) also correlates with the location of paleochannel (1) described in the previous section. The resistive structure in the inversion correlates with the paleochannel, and lacks the extent of the sand/gravel aquifer.

Two other areas of thick sand and gravel aquifers, (2) and (3), roughly correlate with areas of elevated resistivity at both depths. A fourth, smaller aquifer does not show any significant correlation.

Other areas of interest are noted at 5-7, where an increase resistivity is noted in the depth slice.

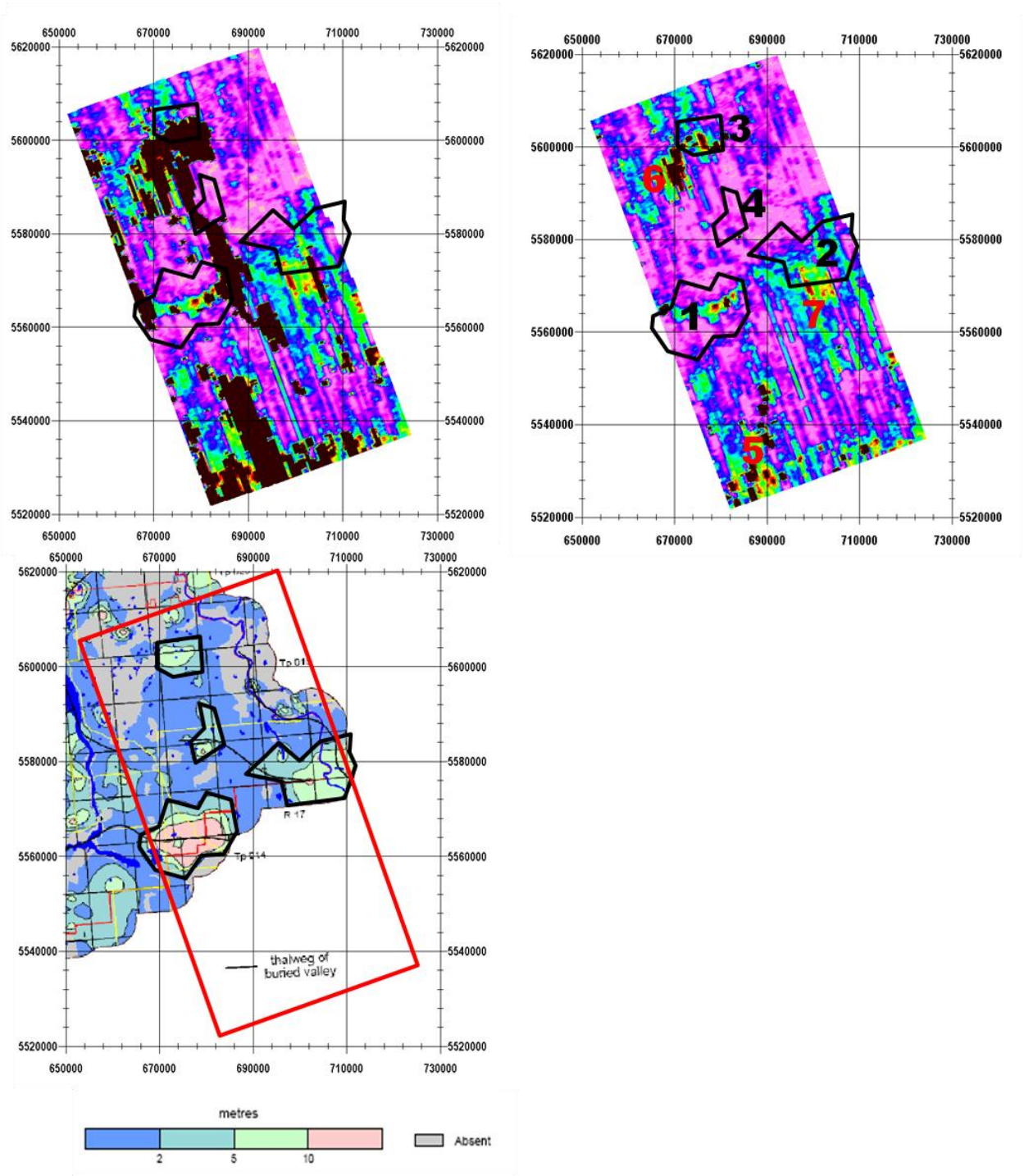

Figure 76: Comparison of known sand/gravel aquifers (bottom) from (HCL, 2007) with depth slices and 45 m (left) and 65 m (right) for Area 3.

7.3.3 Interpretation of Shallow, Smooth Inversions

A shallow depth slice, at 20 m for Area 3 is presented in **Figure 77**. There is some streaking at this depth, but some resistive features are observed.

(A) – Approximately corresponds to marked paleochannel, but not clearly observed at this step.

(D) – Area of high resistivity to the north.

(E) – Area of high resistivity to the south.

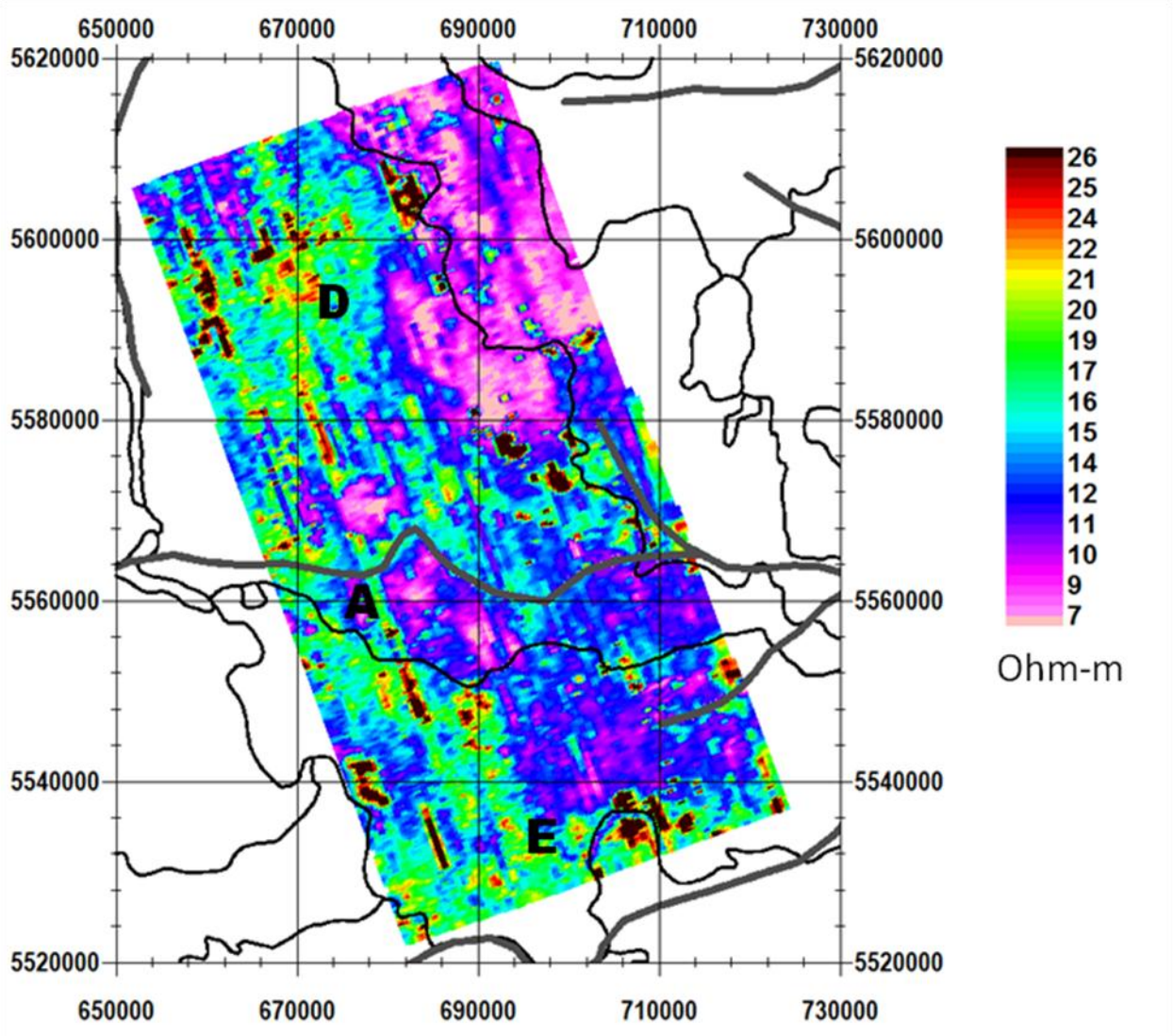

Figure 77: Depth slice at 20 m for Area 3 (shallow, smooth inversion). Rivers are shown as think black and interpreted paleochannels by thick grey lines.

Figure 78 is the depth slice at 30 m.

(A) – Linear resistive structure now clearly corresponds to paleochannel, although shape differs slightly.

(B) – Area of elevated resistivity to the northeast of A.

(C) – Area of elevated resistivity to the east of A.

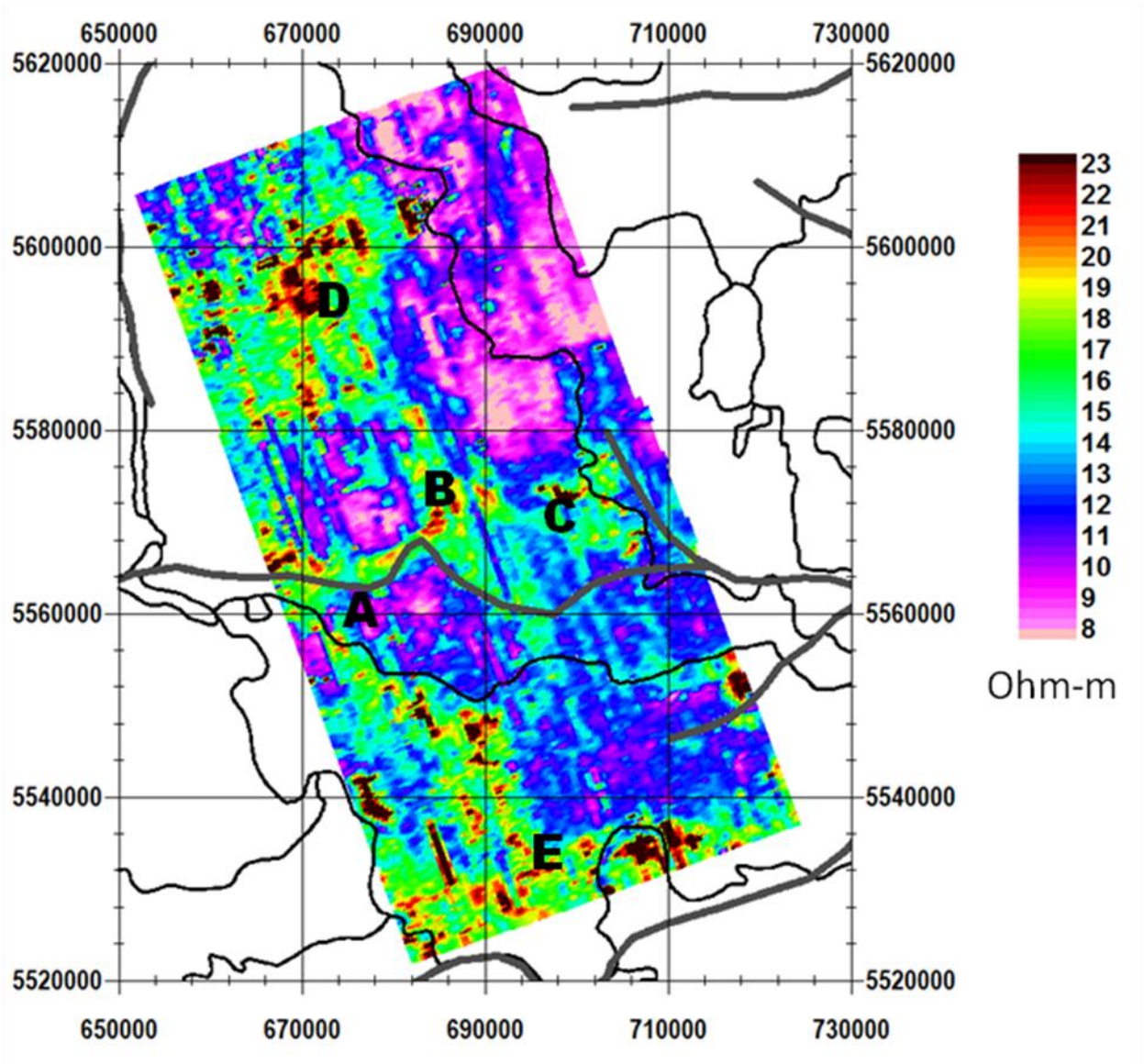

Figure 78: Depth slice at 30 m for Area 3 (shallow, smooth inversion). Rivers are shown as think black and interpreted paleochannels by thick grey lines.

The depth slice for the new shallow inversion at 44 m for Area 3 is presented in **Figure 79**. Similar to the 30 m depth slice, but resistivity is more uniform near (D). It is thought that (A) branches into (B) and (C), marked by red lines.

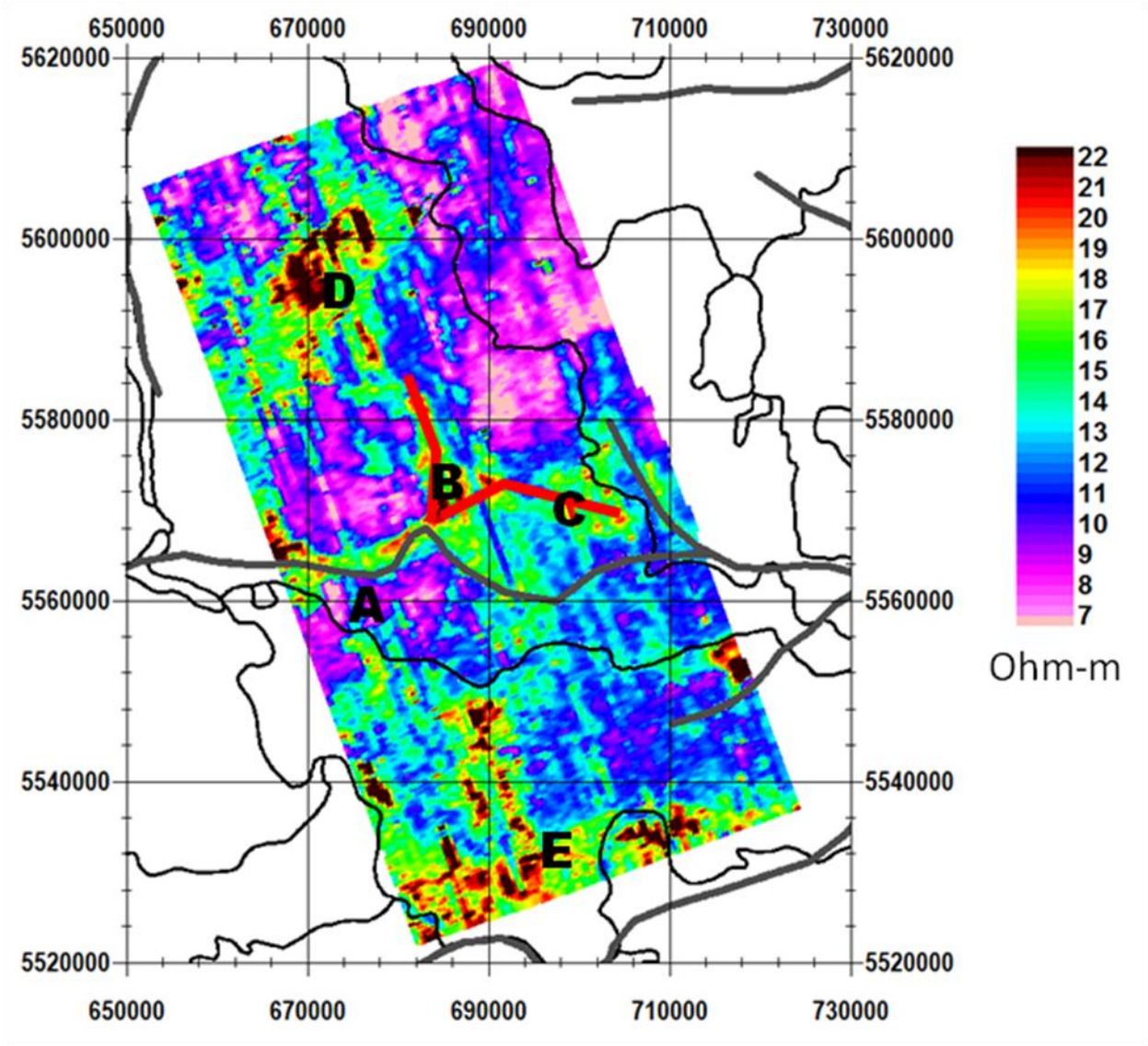

Figure 79: Depth slice at 44 m for Area 3 (shallow, smooth inversion). Rivers are shown as think black and interpreted paleochannels by thick grey lines.

Figure 80 is a depth slice at 66 m. The apparent extension of (A) into (B) is clearer here.

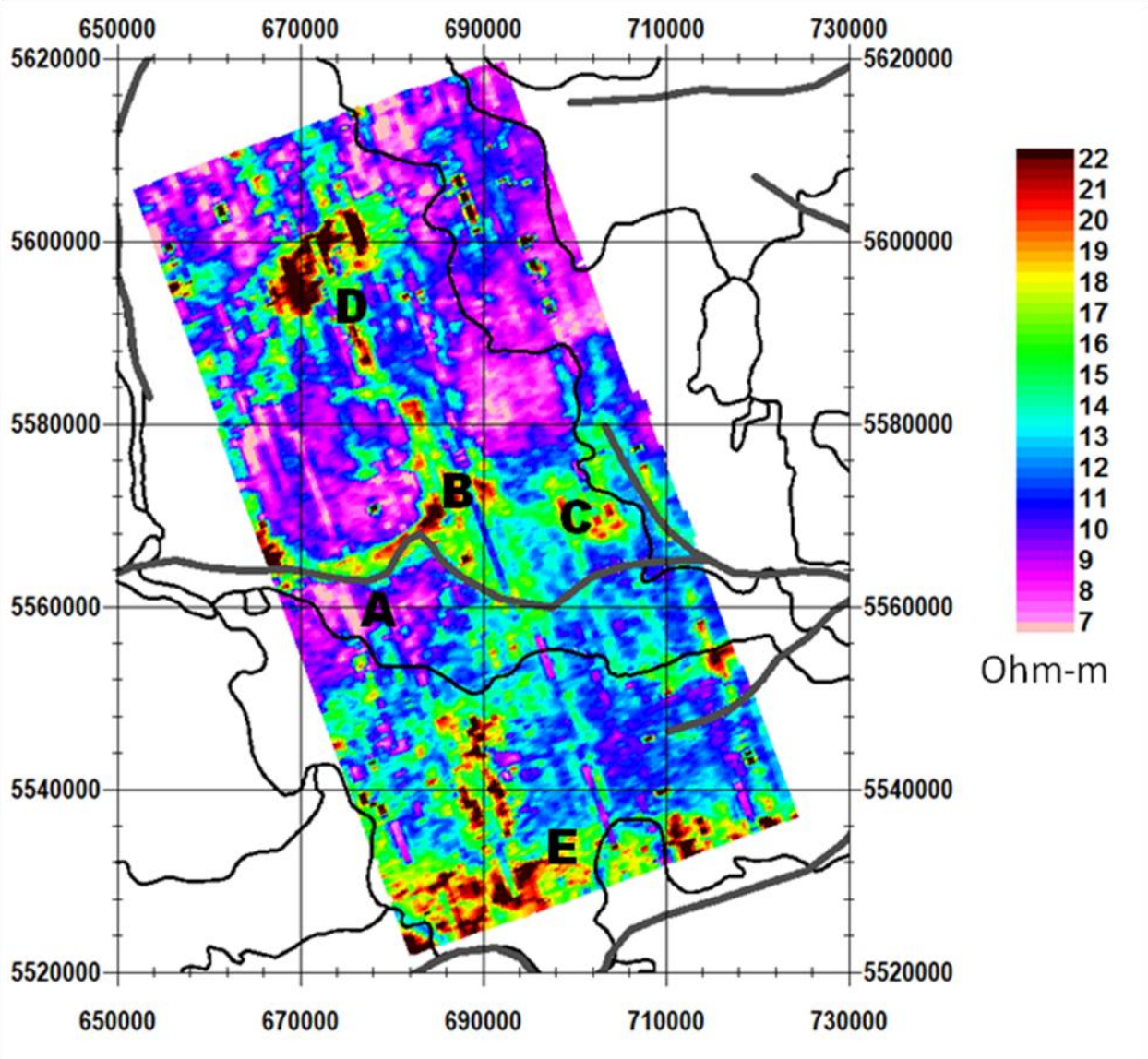

Figure 80: Depth slice at 66 m for Area 3 (shallow, smooth inversion). Rivers are shown as think black and interpreted paleochannels by thick grey lines.

A close-up is shown in **Figure 81** in the vicinity of (A, B, C). It is thought that the old inversion more clearly delineates boundaries, but it does not strongly indicate the presence of (B), although this is some to some extent in the original inversion at shallow depths.

Note that the paleochannel to the west (A) curves a bit further south than the resistor marked in either inversion result. The reason for this is not known. One possibility is the accuracy of the paleochannels map.

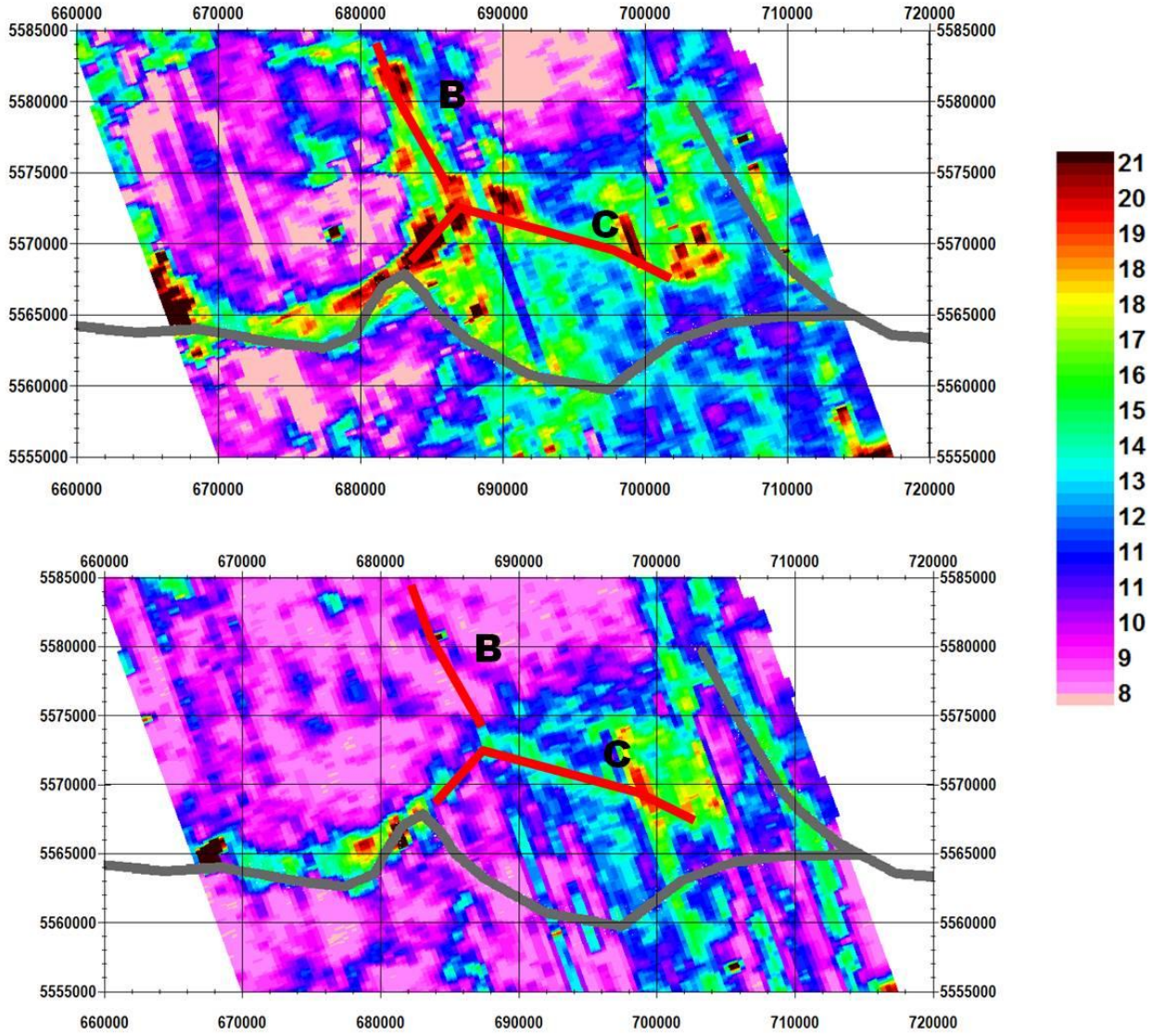

Figure 81: Close-up of the middle of the new Area 3 depth slice (top) and the original inversion (bottom). Depth is 66 m.

7.4 Area 4 (SW)

7.4.1 Effect of Known Features

There is a correlation with the data almost near the power lines along almost all the extent of the power lines. However, the width of the effect is quite small (see **Figure** 82).

The rivers are associated with lows likely caused by drops in topography and thus higher elevation of the system above the ground but could be associated with the river beds if they are highly graveled. One long thin lake in the centre-east is associated with an amplitude low whereas two lakes (NE and south central) are associated with amplitude highs.

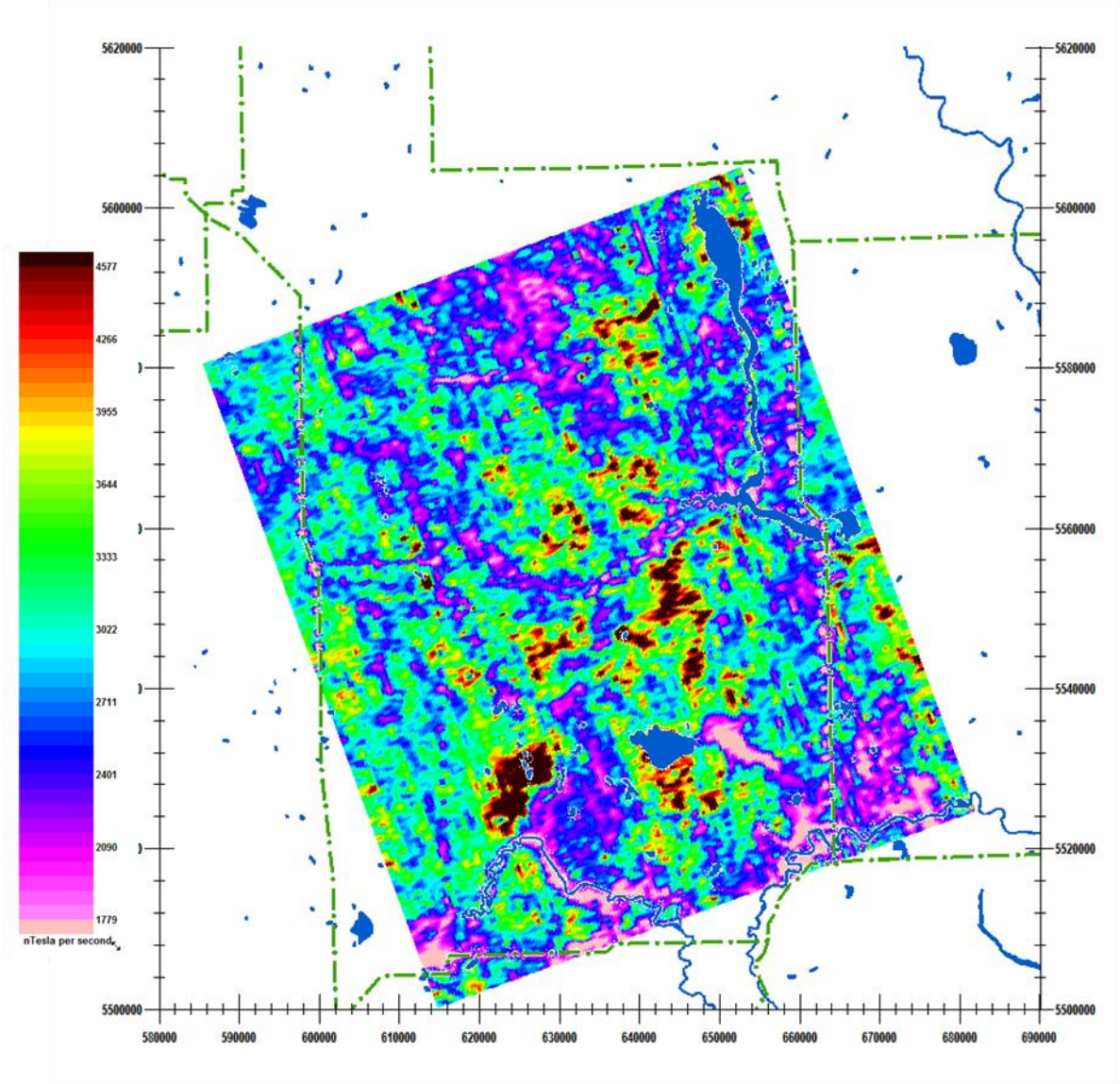

Figure 82: Channel 5 data for Area 4 with rivers, lakes, and power lines overlaid.

In **Figure** 83, there are more rivers shown (dark blue) and lakes outlined in dark blue. The river maps don't agree exactly between these last two figures, however again there is a strong correlation between the rivers and amplitude lows. (The rivers in **Figure** 82 are from GIS information from Aeroquest and the rivers in **Figure** 83 are from the Alberta geology map.)

Generally, the paleochannels are following along the amplitude lows and thus under the topographic lows.

In addition, to the possibility of a paleochannel extensions at 1) and 2) and 3) is the feature (A) which appears to be an extensive area of resistivity lows fed by at least 2 surface water sources.

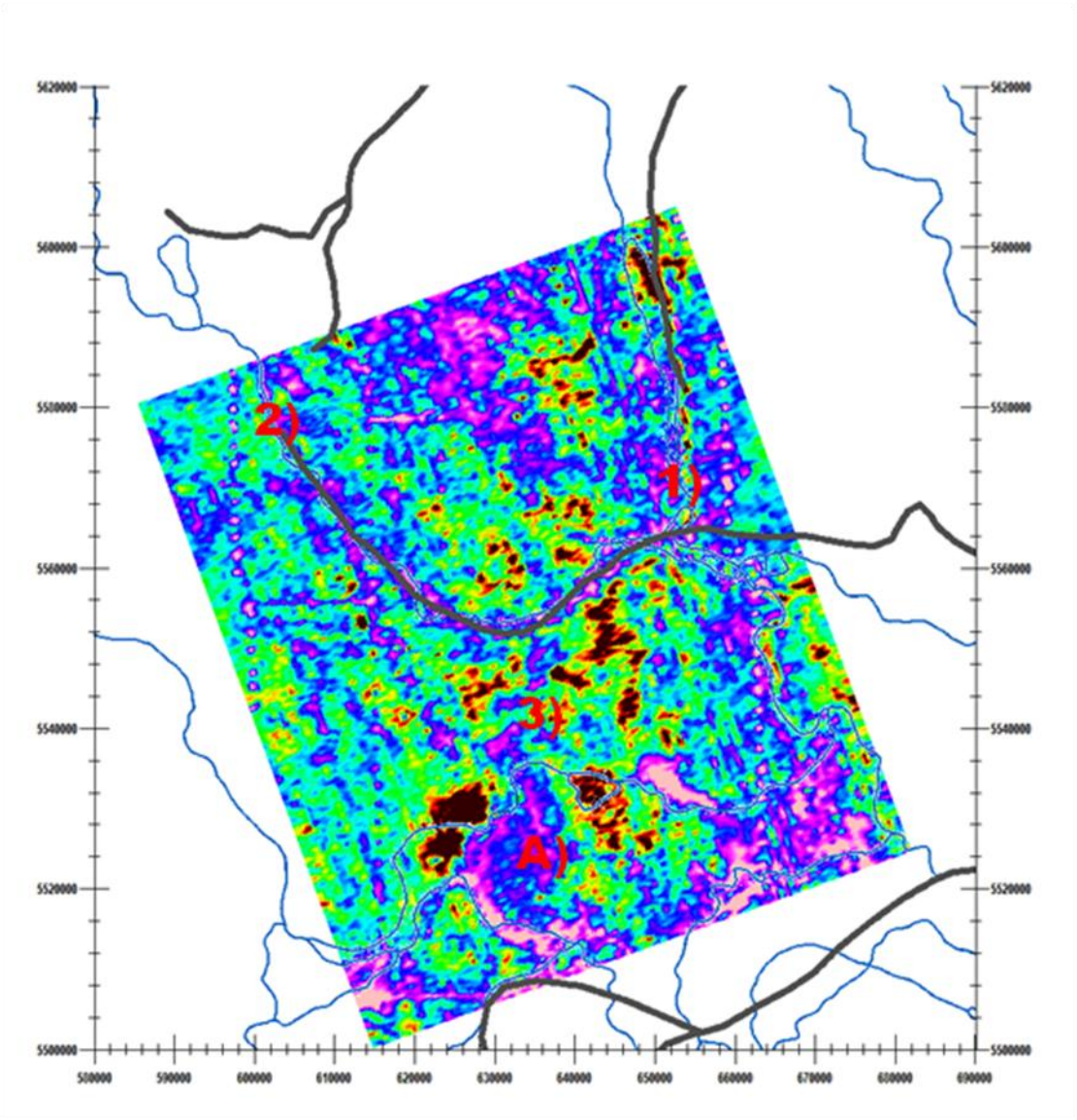

Figure 83: Channel 5 data for Area 4 with rivers, lakes, and paleochannels overlaid.

A map of the bird height is shown in **Figure** 84. The power lines can be seen clearly in this displays (1-4) as well as some other linear structures which had to be flown over. Note that 1-3 were not clearly defined by the power line monitor and so the data were not removed in processing of the data. Generally, the rivers appear as altimeter highs indicating short drops in topography. The lakes are sometimes altimeter highs but also altimeter lows.

The rivers generally follow topographic lows and thus are associated with early time amplitude lows (**Figure** 85). The placement of lakes and the rivers in this overlay map appear to be slightly in error.

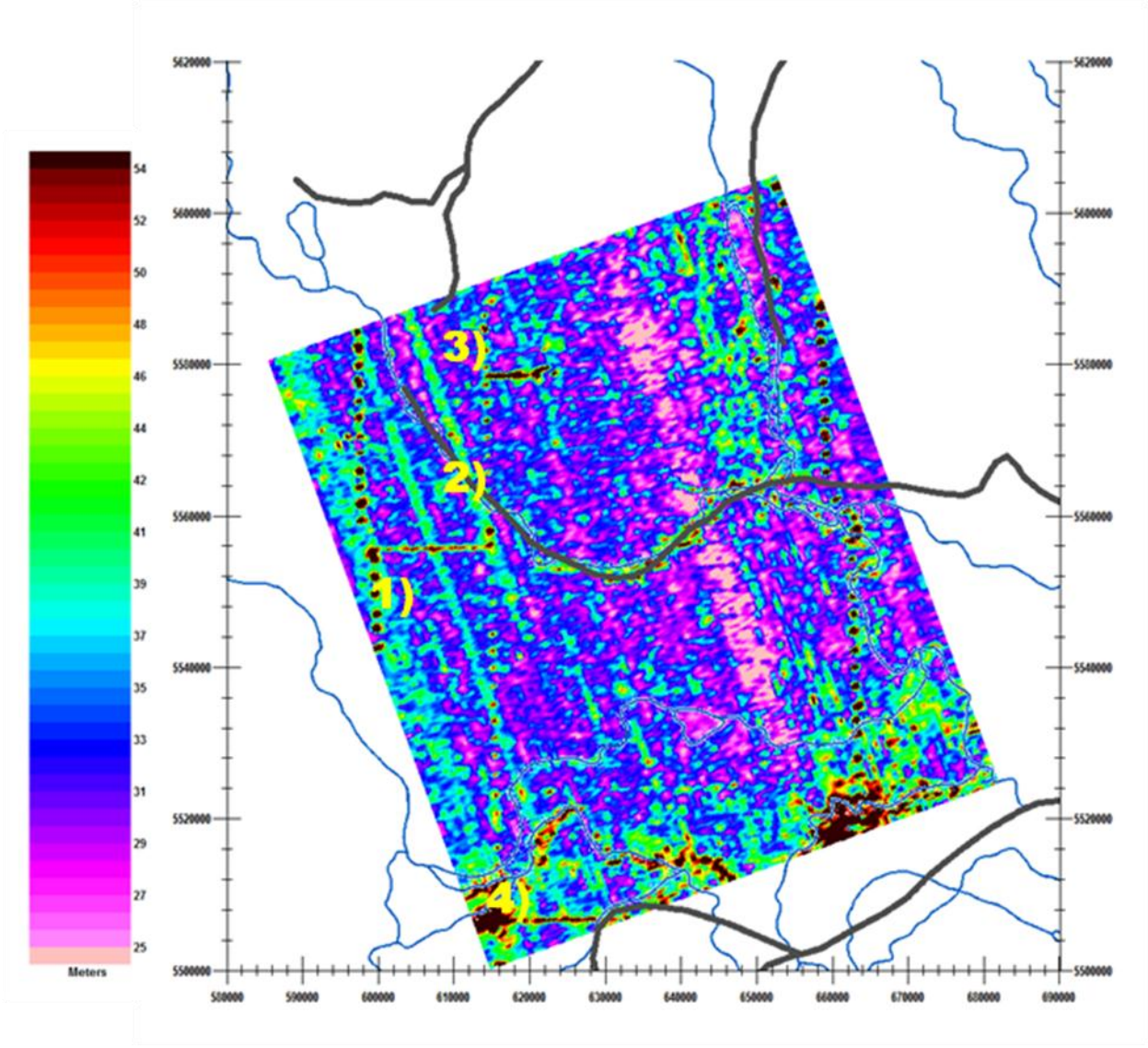

Figure 84: Altimeter for Area 4 with rivers, lakes, and power lines shown.

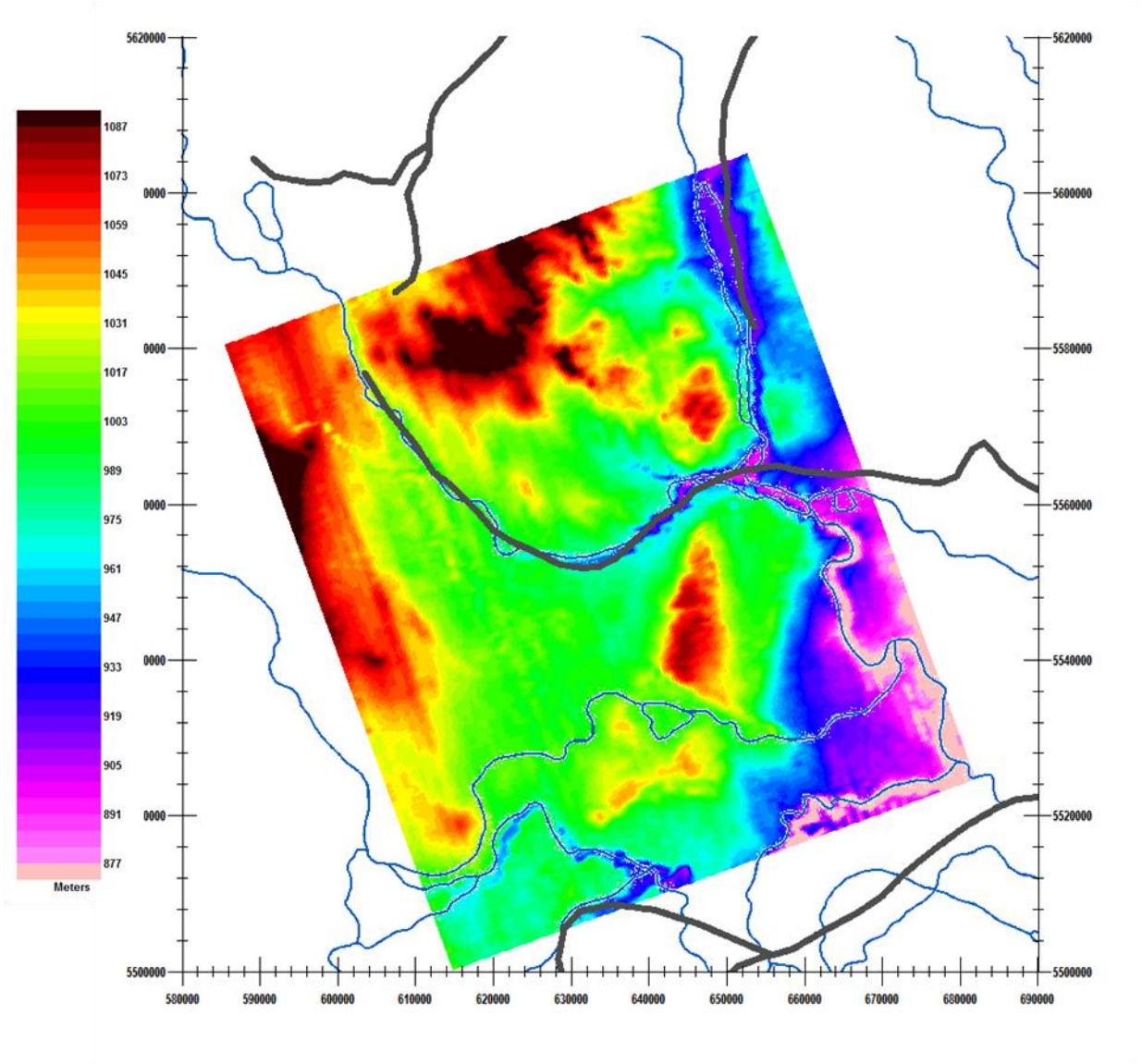

Figure 85: DTM with rivers, lakes and power lines overlaid.

Several features stand out in the data by early mid-times (**Figure** 86). The feature outlined in white as an amplitude low appears more defined into later times; the high along the lake/river in the NE is interesting as is the body (A) which is a resistivity low which stands out more and more into late times.

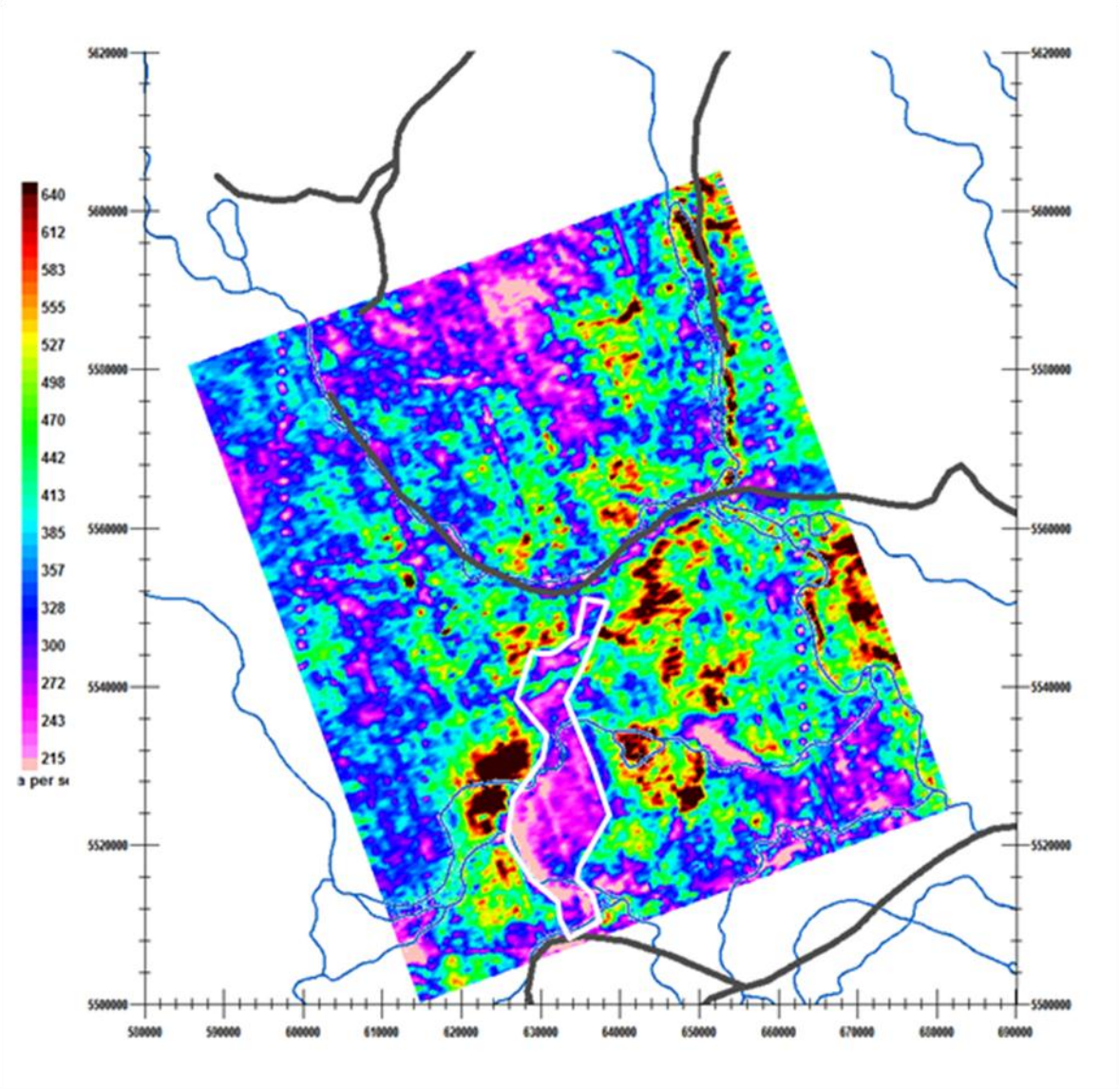

Figure 86: Channel 14 for Area 4 with rivers, lakes, and power lines overlaid.

By early late-time these features are all still evident although the large resistive feature indicated in the previous slide appears to continue northward to connect with another structure.

The central paleochannel now appears to follow the mapped trend to the east but in the north it appears to bend more northward as indicated by B-B' but there is still strong evidence that the paleochannel actually turns south rather than north at the centre of the area.

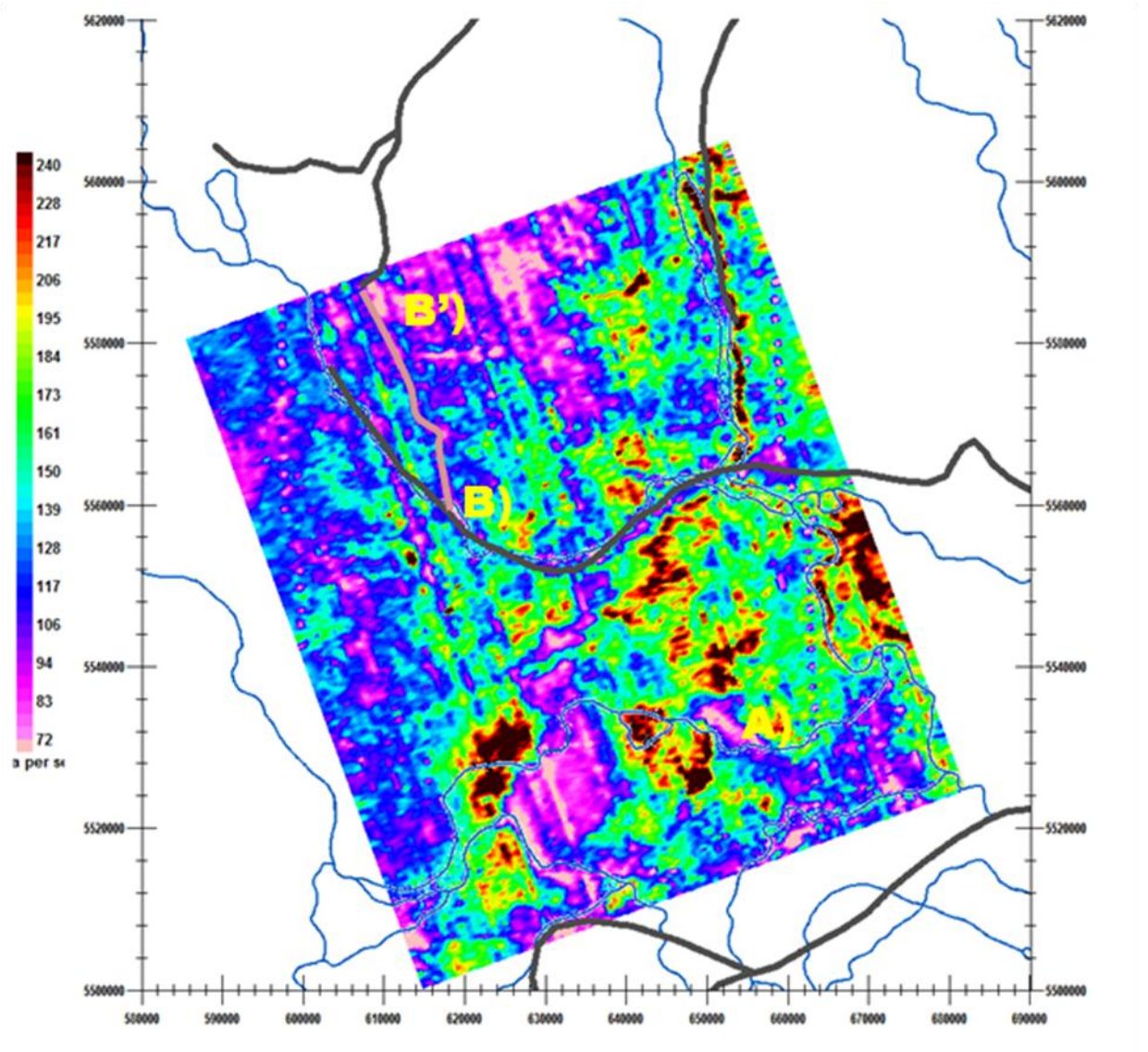

Figure 87: Channel 19 for Area 4 with rivers, lakes, and power lines overlaid

7.4.2 Interpretation of Original Inversions

We start with an inversion depth at 65m. Although the grid is somewhat streaky, two structures appear evident. The first is paleochannel (A) which rather than turning north in the center of the area appears to turn south (blue-grey) towards the large resistive basin-like structure (B) to the SW which appeared strongly in the data displays. Paleochannel (C) unusually follows a resistivity low along the lake and river which would indicate that that it is not gravel type structure but rather more sandy or clayey. The apparently resistive body (D) which appears in the data appears as a resistive low. There is no evidence that paleochannel (A) turns north as indicated by the paleochannel map.

While the structure (A)-(B) may appear somewhat vague is this figure, no matter how you look at the inversions whether in the raw profile form or as a grid as displays here or in the actual data, one cannot but see this structure. We will attempt to convince the reader with further figures.

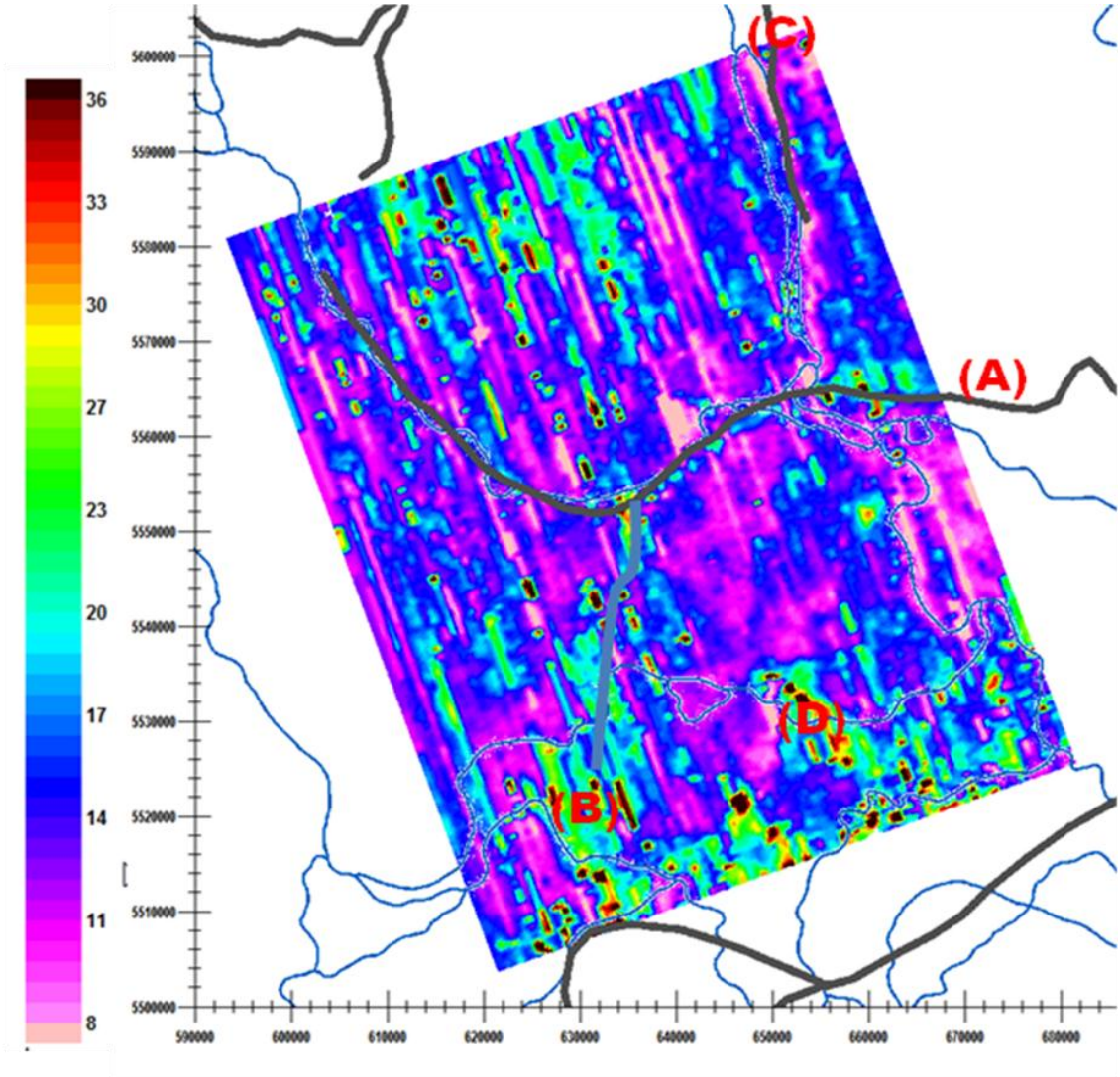

Figure 88: Area 4 depth slice at 65 m.

The inversion slice at 60m is shown in **Figure** 89. Features (A), (B) and (C) are indicated as before. Feature (D) indicates a finer resistive area within the overall resistive area.

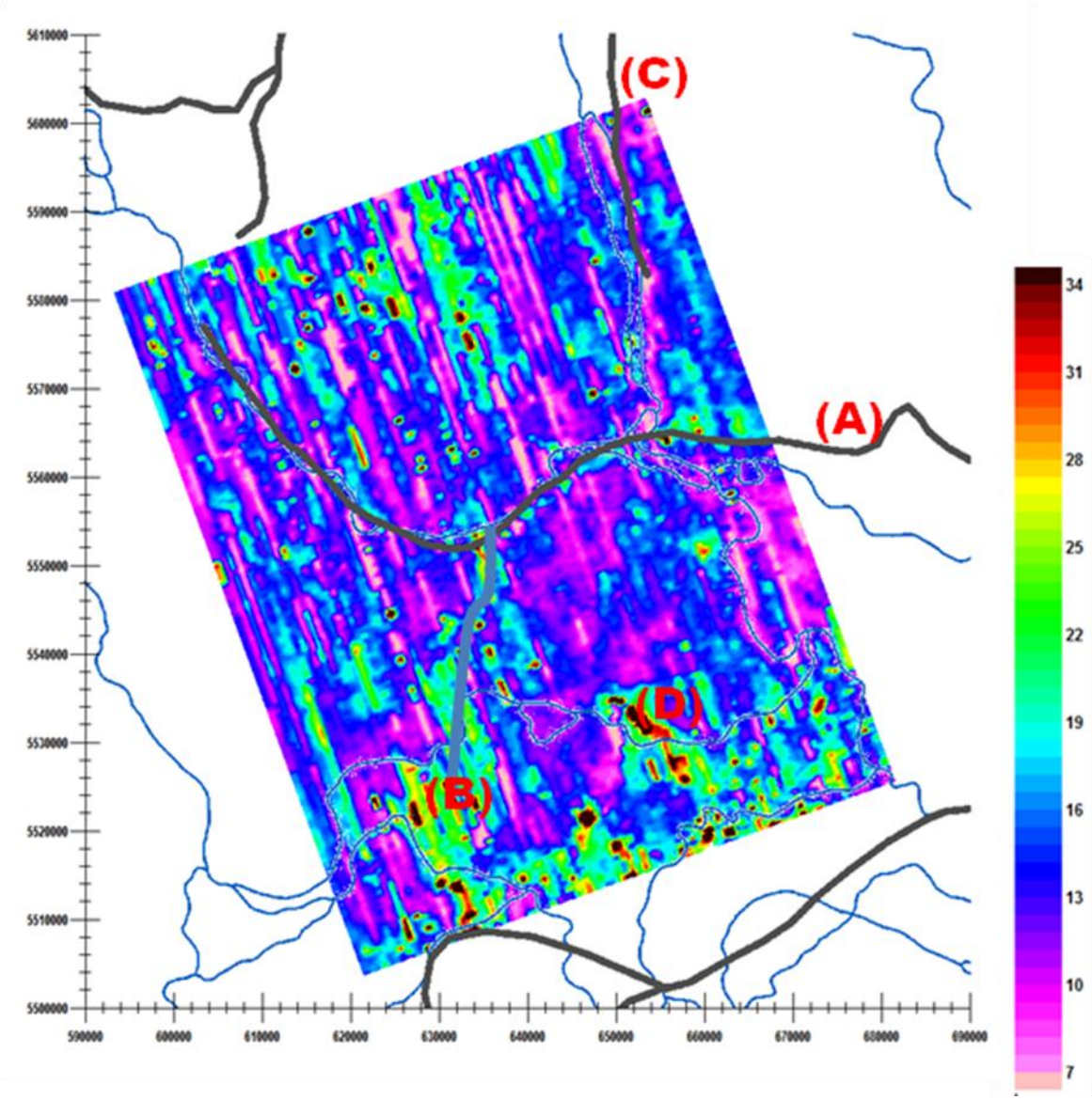

Figure 89: Area 4 depth slice at 60 m.

The inversion slice at 45m is shown in **Figure** 90. Features (A), (B) and (C) are somewhat less clear but the trend still appears. Feature (D) indicates a more focused high resistivity area within the structure. Again, there is no evidence that paleochannel (A) turns north in the central area although there is some indication that there is a small branch at (E). Structure (C) still appears as a resistivity low indicating a resistivity low.

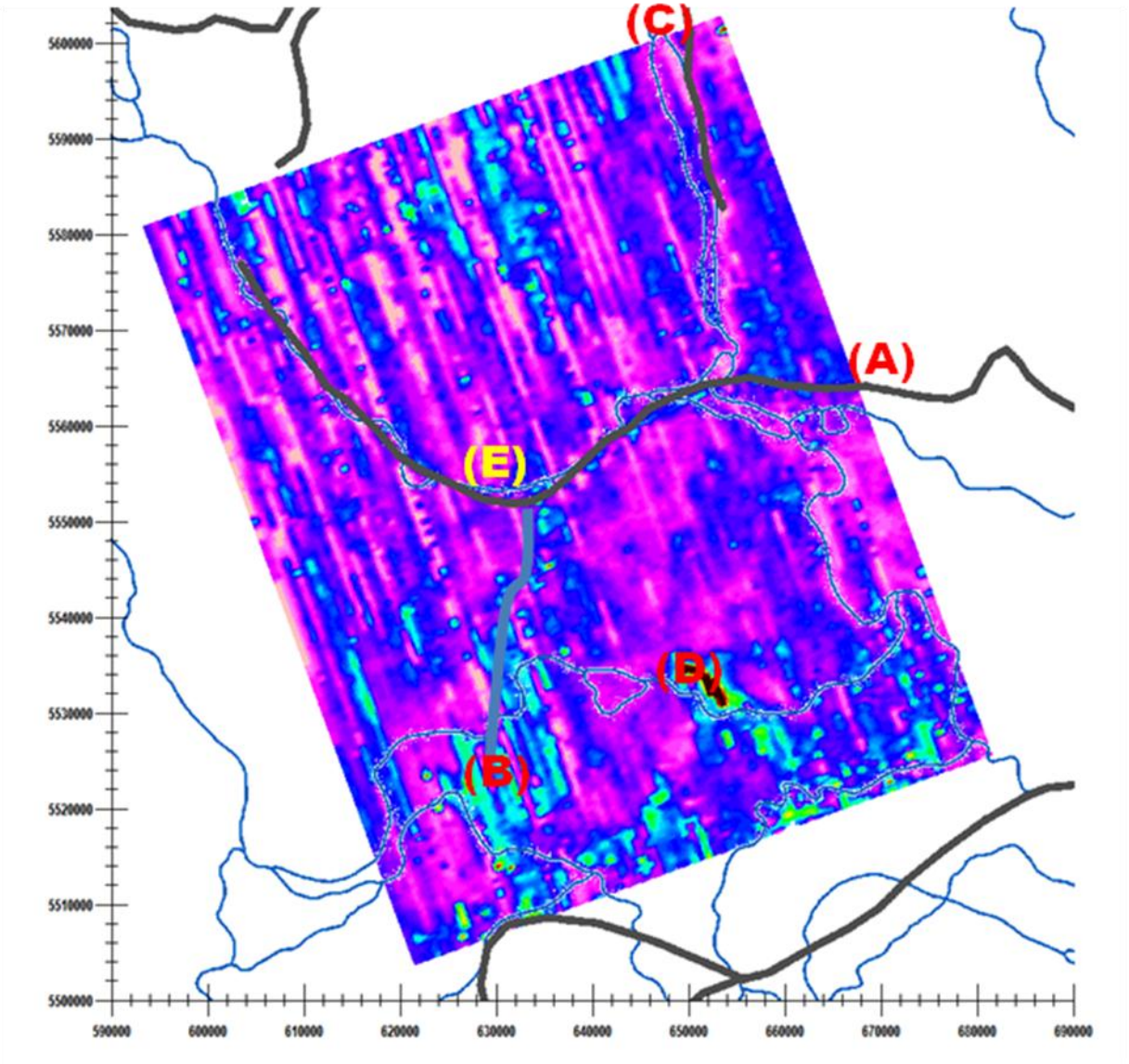

Figure 90: Area 4 depth slice at 45 m.

The inversion slice at 30m is shown. Features (A), (B) and (C) are as somewhat less clear but the trend still appears evident. Feature (D) indicates a more focused high resistivity area within the structure. Again, there is no evidence that paleochannel (A) turns north in the central area although there is some indication that there is a small branch at (E). Structure (C) still appears as a resistivity low indicating a resistivity low.

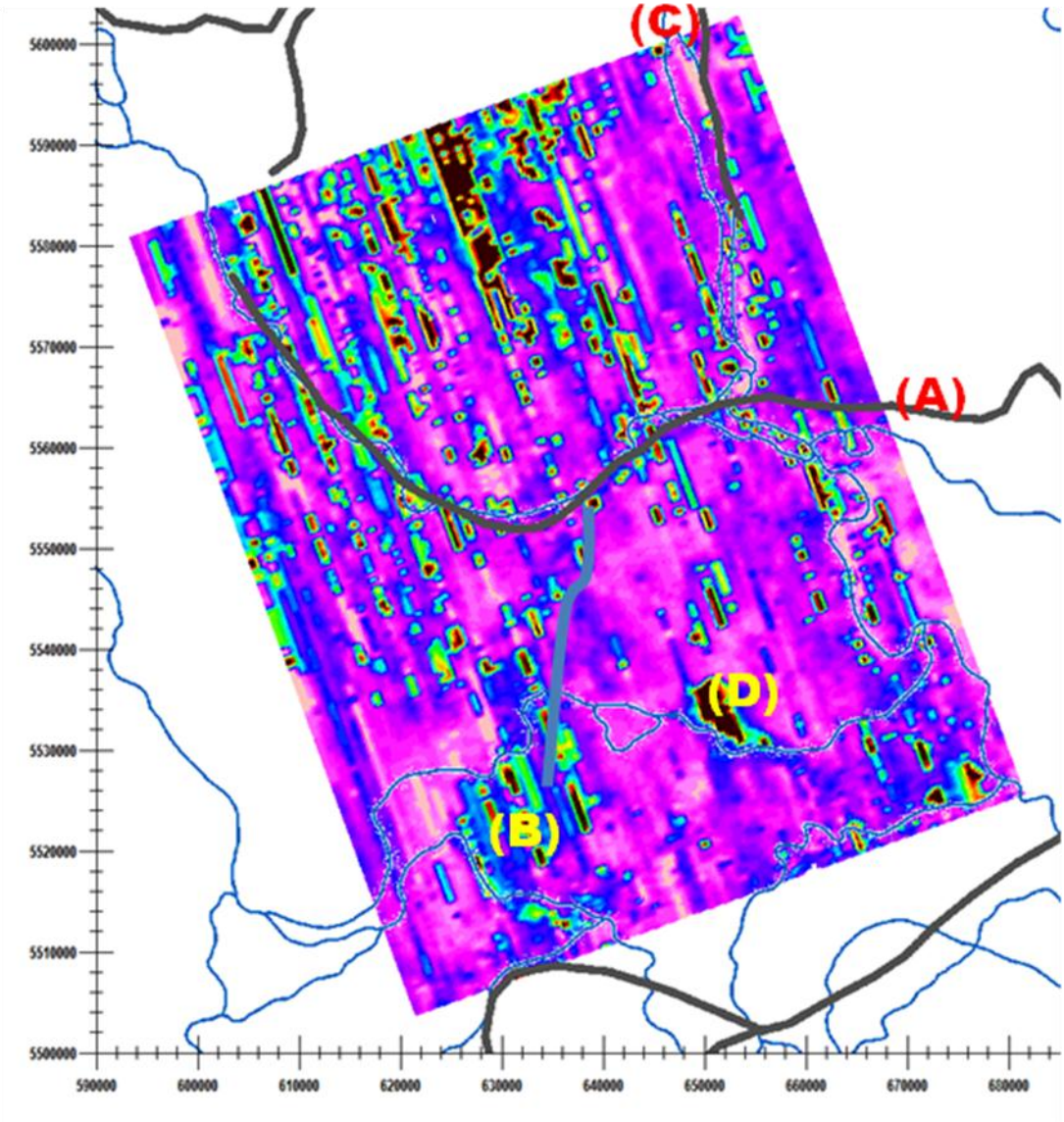

Figure 91: Area 4 30 m depth slice.

7.4.3 Interpretation of Smooth, Shallow Inversions

The inversion slice at 20m is shown for this approach. Although, the inversions are still somewhat "streaky" between some lines, shallow features are more evident than in the deeper inversion approach. Features (A) can be seen quite clearly and now continues west and north along the mapped river. Feature (C) is quite evident and continues south along the river system. Suggested paleochannel (B) and associated gravel beds is now evident at this shallow depth. Inversions to shallower depths are very similar to the 30m depth as is to be expected from this approach.

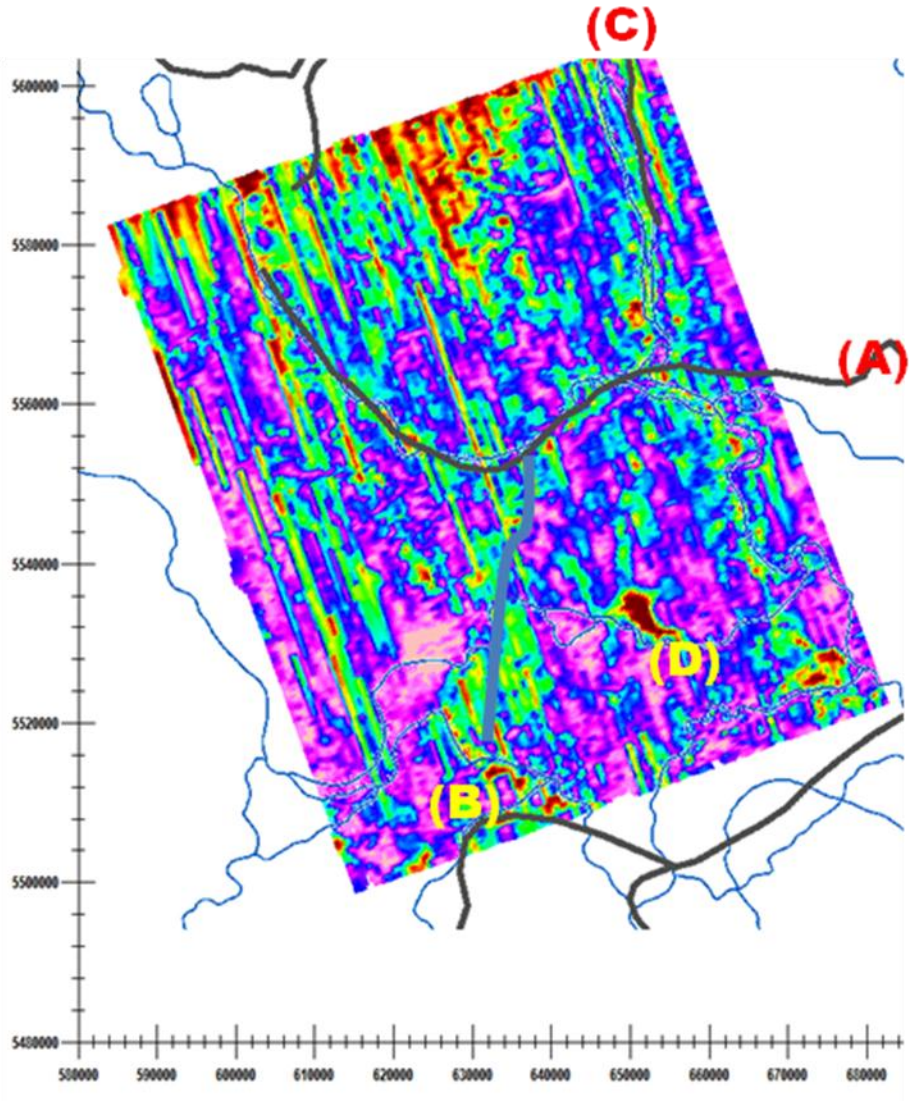

Figure 92: 20 m depth slice for Area 4 (shallow, smooth inversions). Rivers are marked as thin blue lines and paleochannels as thicker grey lines.

The inversion slice at 46m is shown for this approach in **Figure 93**. Some streaking still remains in the inversions are. Features (A) can be seen less clearly than at 30m but still apparently continues west and north along the mapped river. Feature (C) is but a thin conductor can now be seen between the more resistive areas on either side. Suggested paleochannel (B) and associated gravel beds less evident. Item (D) still stands out strongly.

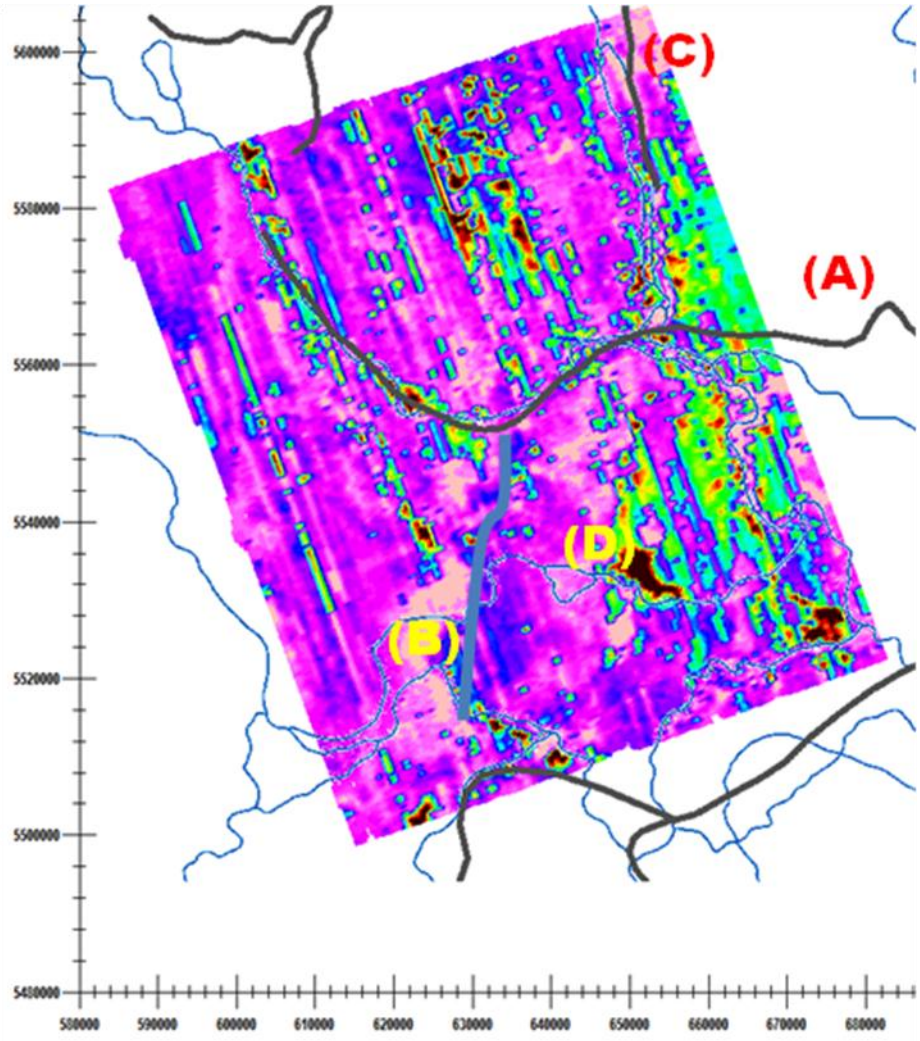

Figure 93: 46 m depth slice for Area 4 (shallow, smooth inversions). Rivers are marked as thin blue lines and paleochannels as thicker grey lines.

The inversion slice at 56m is shown for this approach in **Figure 94**. Feature (A) can be seen as a resistive structure as expected for deeper gravels but now apparently terminates at (A') before turning south along item (B). Item (C) appears now as a wider conductor implying more water content or more clay sediment content. Item (D) is still strongly evident but now appears to have a SE extension.

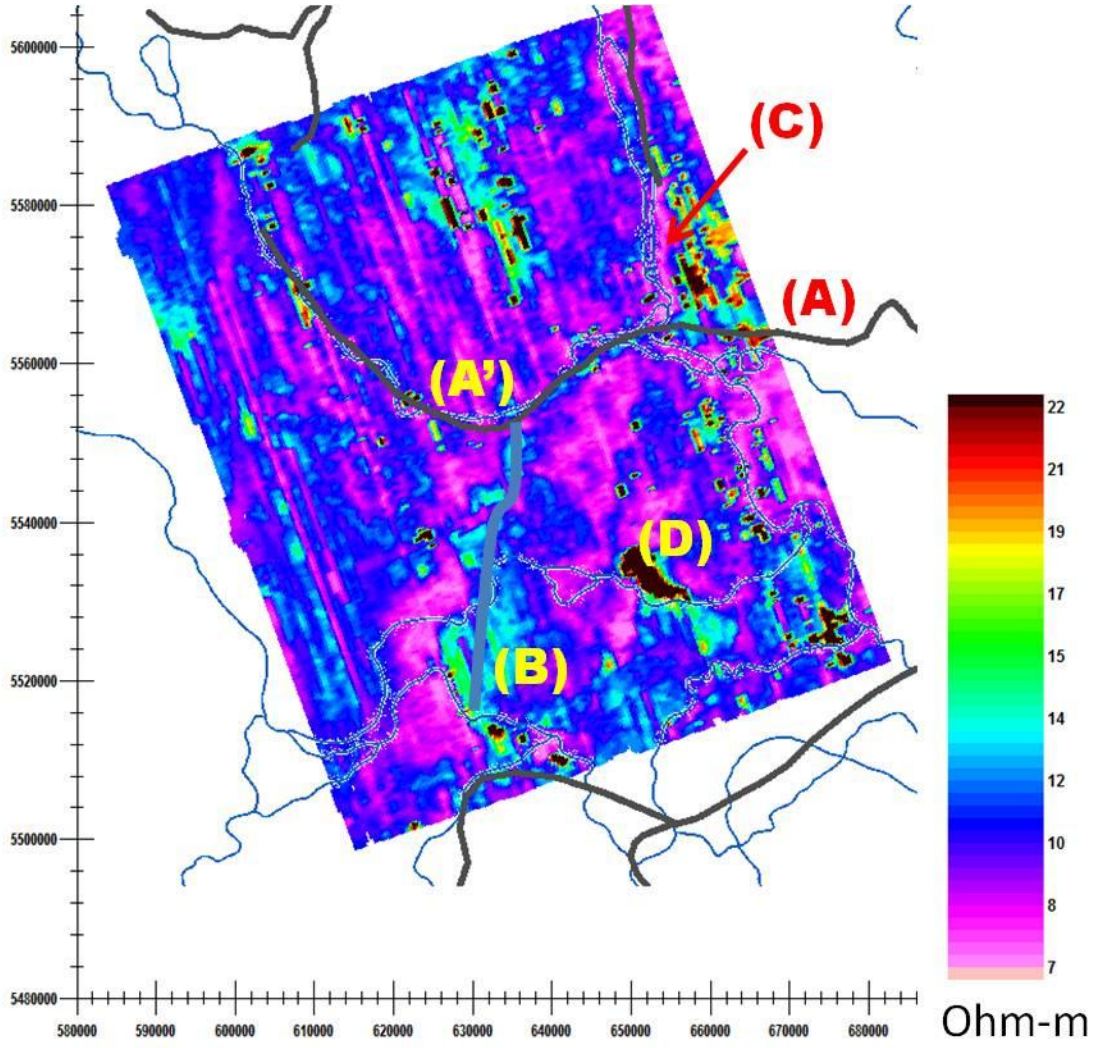

Figure 94: 56 m depth slice for Area 4 (shallow, smooth inversions). Rivers are marked as thin blue lines and paleochannels as thicker grey lines.

The inversion slice at 64m for the shallow inversion is shown in **Figure 95**. The connection between the eastern portion of (A) and the southern feature is now again very evident at this depth as it was at 60m in the deep inversion approach.

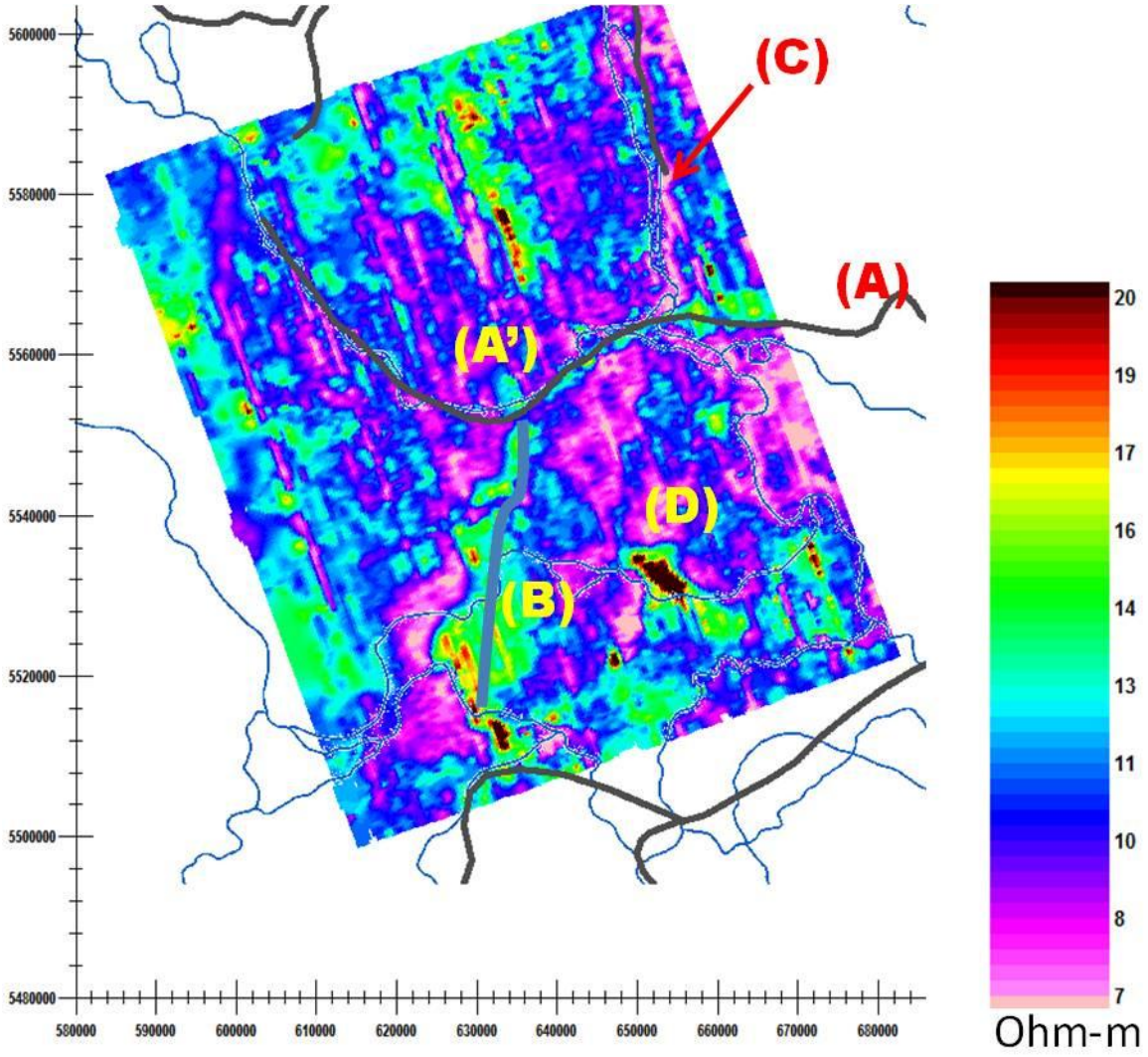

Figure 95: 64 m depth slice for Area 4 (shallow, smooth inversions). Rivers are marked as thin blue lines and paleochannels as thicker grey lines.

The inversion slice at 70m is shown for this approach. The connection of (A) into (B) is now even more evident. (C) is more distinct and the southern portion of the river flow can be seen quite sharply. The spatial extent of (D) continues to grow larger at depth.

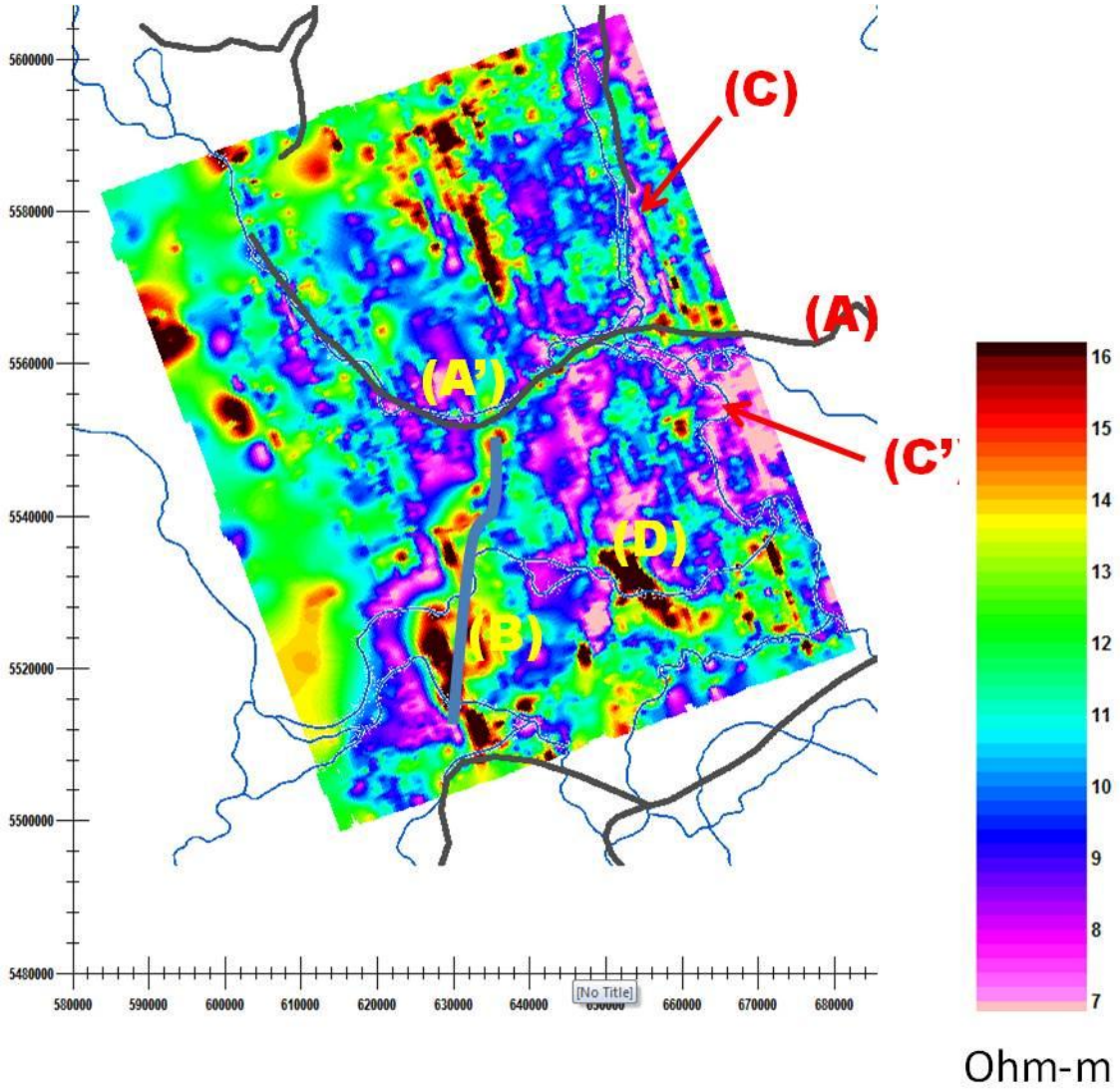

Figure 96: 70 m depth slice for Area 4 (shallow, smooth inversions). Rivers are marked as thin blue lines and paleochannels as thicker grey lines.

The inversion slice at 76m is presented in Figure 97. Item (B) now appears continuous north to south. At (B') it is consistent with the structure identified in Area 1 (NW). At (B''), it appears to connect to another mapped aquifer in the south. The interpreted gravels beds at (B) now appear to have a focused area which is more resistive.

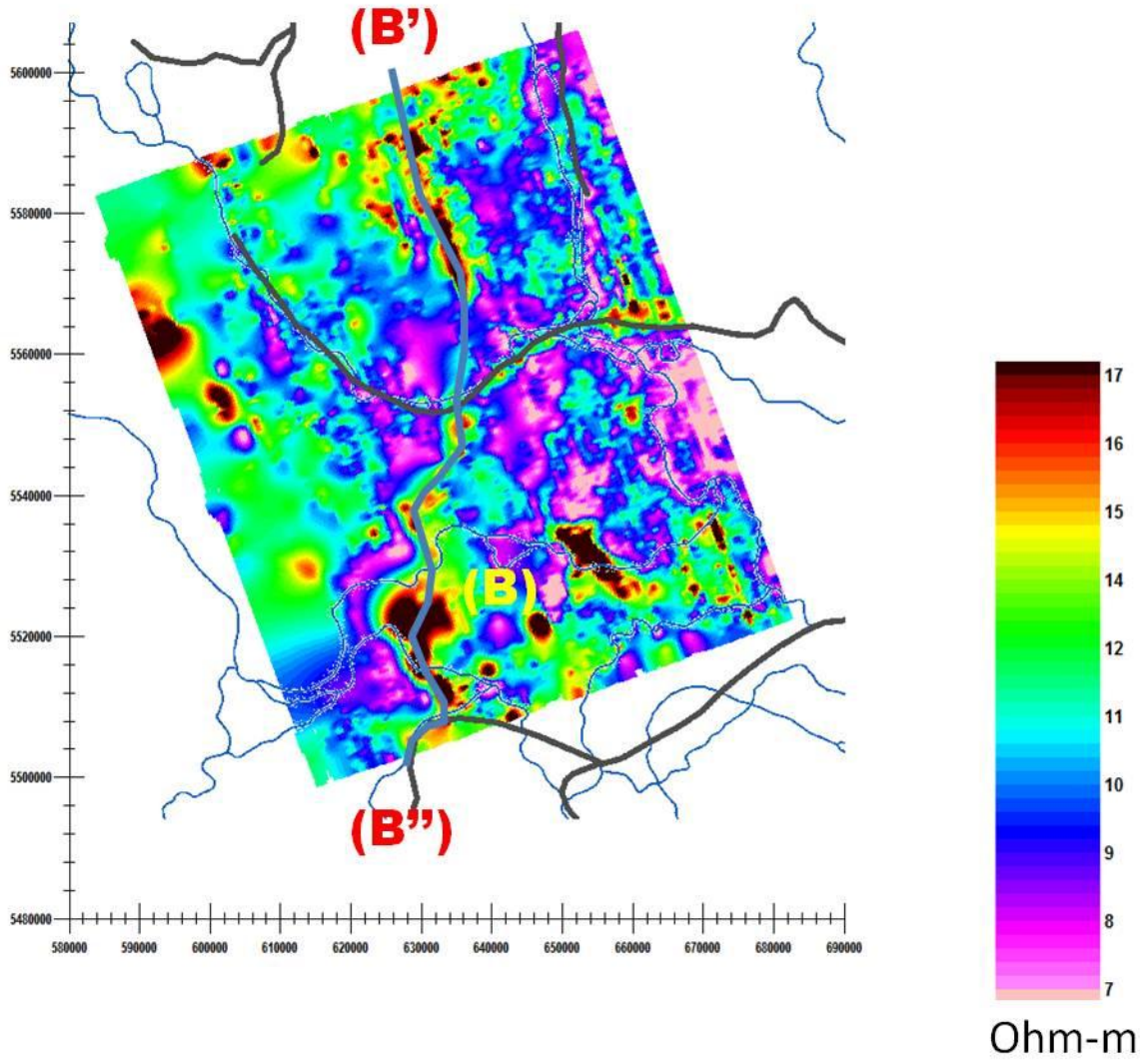

Figure 97: 76 m depth slice for Area 4 (shallow, smooth inversions). Rivers are marked as thin blue lines and paleochannels as thicker grey lines.

7.5 Summary

In this preliminary interpretation of the survey data, our main observations were:

1) There is some correlation of the data with known power lines and other linear features which are assumed to be additional power lines. Data around these features was removed at the initial quality control procedures.

2) There is correlation with some known rivers, primarily as a result of the increased flight altitude over rivers that are associated with significant topographic lows.

3) There is significant correlation of highly-resistive areas in the inversion slices with some known paleochannels and sand/gravel aquifers. Additional areas of interest have been noted.

4) In general, more features are visible near the surface in the shallow, smooth inversions than in the original, deeper inversions.

8.0 Limitations of Survey

Below is a general discussion of the limitations of the survey in terms of the design of the survey and data quality. Despite these limitations, we believe that the inversion results contain significant information on the subsurface. Further collection of ground TEM data at sites with known geology would assist in determining how to best interpret the data.

8.1 Limitations—Survey Design

8.1.1 Line Spacing

Traverse lines were spaced at 750 m. Thus, the resistivity structure between lines must be interpolated over a significant distance many times greater than the depth of penetration of the data. Any paleochannels parallel to and between survey lines may not be detected; similarly, small sand/gravel aquifers between lines may not be observed. However, in general the geology is smoothly varying and known channels are roughly perpendicular to survey lines. As such, the wide line spacing is not considered a major limitation.

Unfortunately, the data does exhibit some line-to-line effects (see previous sections), and if the anomalous lines are removed then the line spacing is well over a kilometer in some areas.

8.1.2 Reflies

A small number of repeats were flown, including some lines flown with both Mike and November (see Section 3.0). Additional reflies would have assisted in understanding the repeatability of the data and the issues with the late-time decays.

In particular, we typically recommend that a calibration line of about 2 km be flown each flight to monitor the repeatability of the data. Should the data along a survey line appear to be anomalous, the calibration line data for that flight could be examined to see if there was anything unusual, based on comparison with data collected along the calibration line in previous flights. Such a calibration line is thus useful for quality control.

8.1.3 Calibration Site

Although there are geophysical and lithological logs for comparison, the absence of any ground EM data is a significant limitation in understanding and interpreting the airborne EM results. The resistivity logs are insufficient for calibration purposes as the values of the resistivities given in the logs are not reliable (see Section 6.0).

For AEM surveys, it is our practice to recommend a ground calibration site where ground EM is collected such that the results may be compared with that of the AEM survey. If the same model fits the ground EM and AEM data, this would increase confidence in the AEM data. Any differences in the results would be carefully examined. The systems may differ in their resolution, but results should generally be

consistent. This has proven extremely useful in other studies (Dickinson, *et al*, 2010, David and Groom, 2009) and is now common practice for the USGS in their airborne EM studies for groundwater applications. It is advantageous to select a site in which detailed geological information is also available so that the resistivity structure can be correlated with lithology.

The persistent presence of a resistive layer taken to be 100 Ohm m at depth in the inversions was speculated to be caused by filtering of the data. If a ground EM survey with a penetration of 200 m or more had been performed somewhere under the AEM survey, we would have been able to conclude whether or not this boundary is geologic, or whether it is an artifact of the system and adjusted the inversion strategy accordingly.

In light of the data quality issues, the absence of a ground calibration site is particularly problematic, and limits our ability to fully assess how these quality issues affect the inversion results.

8.2 Limitations – Data Quality

In Section 7.0, some correlation of known paleochannels and sand/gravel aquifers with resistors in the depth slices was noted. Particularly strong correlation is noted in Area 2. It is not known whether this is due to different characteristics of the paleochannels and sand/gravel aquifers or if improved data quality may have allowed for their detection. There was a single paleochannel in Area 2 that was not observed in the initial inversions, but was imaged in the shallow, smooth inversions which, due to the inversion settings, were less affected by inconsistencies in the data. At least in this example, the data quality appears to have impacted resolution of the channel.

In Section 6.2, it was concluded that the inversion results did not resolve the lithology within the Horseshoe Canyon. Similarly, no clear difference was noted between the Paskapoo, Scollard, and Horseshoe Canyon formations. The Bearpaw was distinguished by a slightly lower resistivity than the other formations; however, this difference was subtle. This limited resolution of sedimentary layers may have been affected in part by the noise in the data at mid-late time. Cleaner data may have allowed further discrimination in the basement. However, it is believed that lack of resolution within the basement is at least in part due to lack of (or limited) resistivity contrast between lithologies, as supported by resistivity logs.

The noise in the late-time data limited the depth resolution of the system to about 150m and often much less depending on the area. Had the data been clean throughout all thirty channels, depth resolution would have been improved and it is possible that deeper aquifers could have been detected. However, even with superior data quality, depth resolution is significantly limited by the high conductivity of the ground.

8.3 Limitations—Inversion Procedures

Each of the four areas was inverted in one to four pieces and then these pieces were merged. It is possible that, to account for differences in data quality and to some extent geology, inverting the data in smaller pieces with different settings would have produced better results. Inverting the data in smaller batches would have allowed us to:

1) Decrease the misfit where the data quality was good.
2) Invert a smaller or greater number of channels depending on the quality of the late-time data.
3) Constrain the model differently in each section, and adjust the number of layers as needed.
4) Make adjustments to the early-time amplitude where needed (particularly in Area 4).

This may have improved the fit with the data in areas where the noise level was low, and potentially additional layers could have been discriminated. However, time limitations did not permit an inversion study of this detail.

9.0 Conclusions

Although the data is generally of good quality, it does show some significant inconsistencies at mid-late times. This is observed by examination of reflies and tie-line intersections. As well, there are some inconsistencies in the amplitude of the very early-time data. These aspects result is a streaky appearance when displaying the inversions as depth slices. However, the cross-sectional inversions are consistent along the lines and represent the data extremely well. A second set of inversions in which fewer channels were inverted and in which the top two layers were not discriminated was later performed. Removal of the late channels from the inversions, as well as inverting for fewer layers, improved the line-to-line consistency of the inversion depth slices. The improvement in the inversions with these settings confirms the weakness in certain aspects of the data. However, it should be noted that with an environment so conducting and with such slight variations in the resistivities of the various formations that data with even smaller noise levels may still not have been insufficient in order to allow procedures for inversion to be carried out with such haste and in such large blocks.

The smooth, shallow style inversions generally contain improved results at shallow depths. This result is principally because those channels that were most inconsistent between survey lines were not used in these inversions. The improved results in the second set of inversions supports our conclusion that these channels (the first channel and many of the late-time channels) are insufficiently accurate to allow discrimination within the top two strata across the entire areas.

As a result of our careful analyses of the data, we believe that there are limitations due to the data quality. These limitations on the AEM data are not unusual in our experience and the lack of any ground TDEM data is extremely limiting. However, the inversions do show correlation with many known paleochannels and also sand and gravel deposits, and we believe that in their present form, the inversions can be used to locate further paleochannels and sand/gravel aquifers. Additional calibration information should allow even more information to be extracted from the data in the future.

A preliminary interpretation has been provided for each of the four areas. Several extensions of paleochannels have been indicated, as well as other possible areas of interest.

Due to the desire to use the data for quantitative analysis and due to the nature of the resistivities in these areas, extremely high quality data is required to obtain good structural resolution to the depths of the paleochannels and sand/gravel beds. To our knowledge, such detailed analyses of the data quality were not performed in the previous surveys for AENV or at least not reported. We have had extensive experience with the GeoTEM system as used in previous AENV surveys and particularly in similar geological environments and for groundwater purposes. Despite the issues of data quality in this survey, it is our belief that the results with the AeroTEM III system provide more structural resolution than would be obtained from Fugro fixed-wing AEM systems (Davis and Groom, 2009, Dickinson *et al*, 2010)

10.0 Recommendations

One of our major recommendations for further surveys would be to allow more time for the inversion procedures. While older smooth inversion techniques are rather rapid, newer more calibrated inversion procedures require significantly more care to perform both from a quality control aspect and from a computation time aspect.

To obtain the best results from the data, it is recommended that ground TDEM surveys be conducted at several locations throughout the survey block, and that these results be used to assess the data and the inversions then be repeated with information obtained via the ground surveys. We consider the lack of ground calibration to be a significant barrier in obtaining quality inversion results, and without any ground calibration, we do not know if the data is correct. Although some geophysical logs are available, these are insufficient for calibration purposes and there is in fact limited consistency in the resistivities in the logs.

More specifically, it is recommended that the ground surveys have the following specifications:

a) CRONE TEM system: The only properly designed impulse TEM system with accurate and correct turn off ramps and channel positioning which would allow sufficiently accurate comparisons to the AeroTEM III data.
b) A fixed loop survey with a loop size of at least 200x200m with measurements made both inside and outside the loop
c) Borehole resistivity logs performed close to the ground TEM surveys.

We believe that more precise inversion results can be obtained if smaller sections of the data were inverted each with their own inversion settings. We have previously used ground TEM results to assist in constraining AEM inversions (Dickinson et al, 2010, Davis and Groom, 2009) with good success.

Furthermore, in addition to being used to inform the inversion settings, the calibration data would assist in determining how to relate the EM results to geology and interpret the inversion depth slices.

10.1 Suggested Locations for Calibration Sites

Figure 98 shows the recommended design for the CRONE TEM surveys for calibration. It is recommended that at least one in-loop and two out-of-loop readings should be taken north, south, east and west of the loop. With an additional measurement at the center of the loop, data should be collected at a total of thirteen stations for a given loop. The out-of-loop stations are recommended at half the loop size from the edge of the loop (100 m) and the second at least 250 m from the edge of the

loop. The purpose of measuring at the same separation from the loop in different directions is to examine the dimensionality at the ground. E.g. if the ground is well represented by a 1D model, the reading at a given separation will be the same in all directions from the center of the loop, whereas differences in the decays would indicate a more complex subsurface structure.

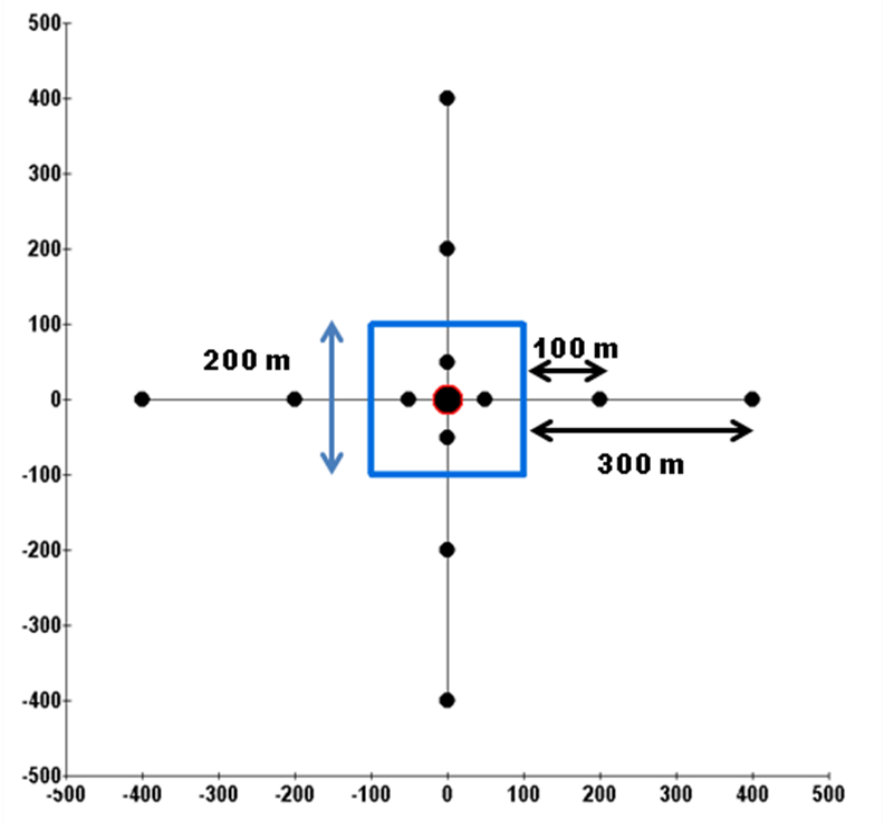

Figure 98: Recommended survey design for CRONE TEM survey.

Recommended locations for the calibration sites are given in the following four figures. We suggest that data be collected at multiple calibration sites for best results, and have made one recommendation per area. The recommended locations have fairly uniform resistivities laterally in the depth slices.

Approximate coordinates of suggested calibration sites:

Area 1 (NW): (607000, 5605000)
Area 2 (NE): (670000, 5635000)
Area 3 (SE): (694000, 5584000)
Area 4 (SW): (628000, 5522000)

A range of resistivity values is represented by these sites. E.g. The Area 3 site is within an area of low resistivity, and the Area 4 site is over a resistive structure at depth.

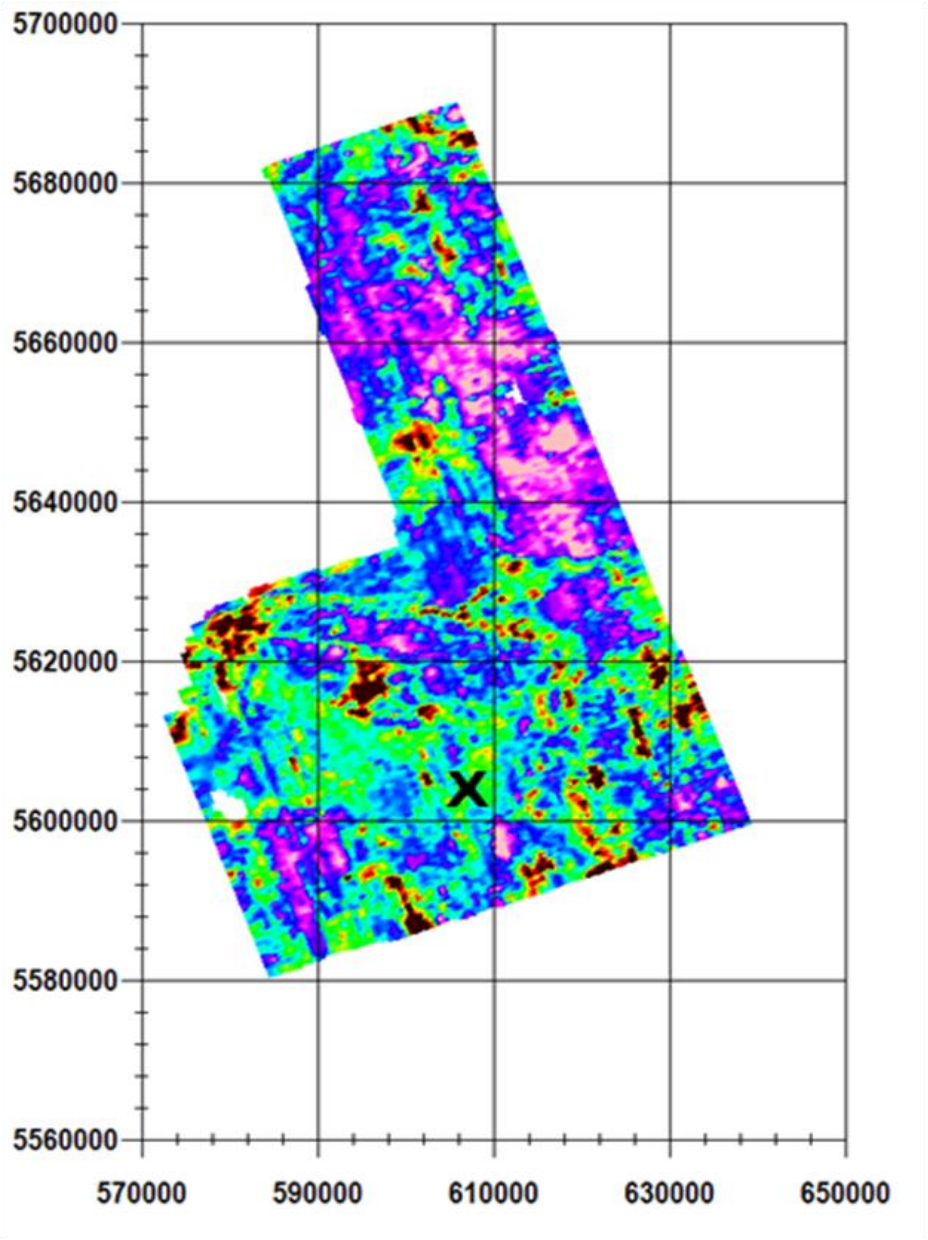

Figure 99: Recommended calibration site in Area 1 (X) near (607000, 5605000).

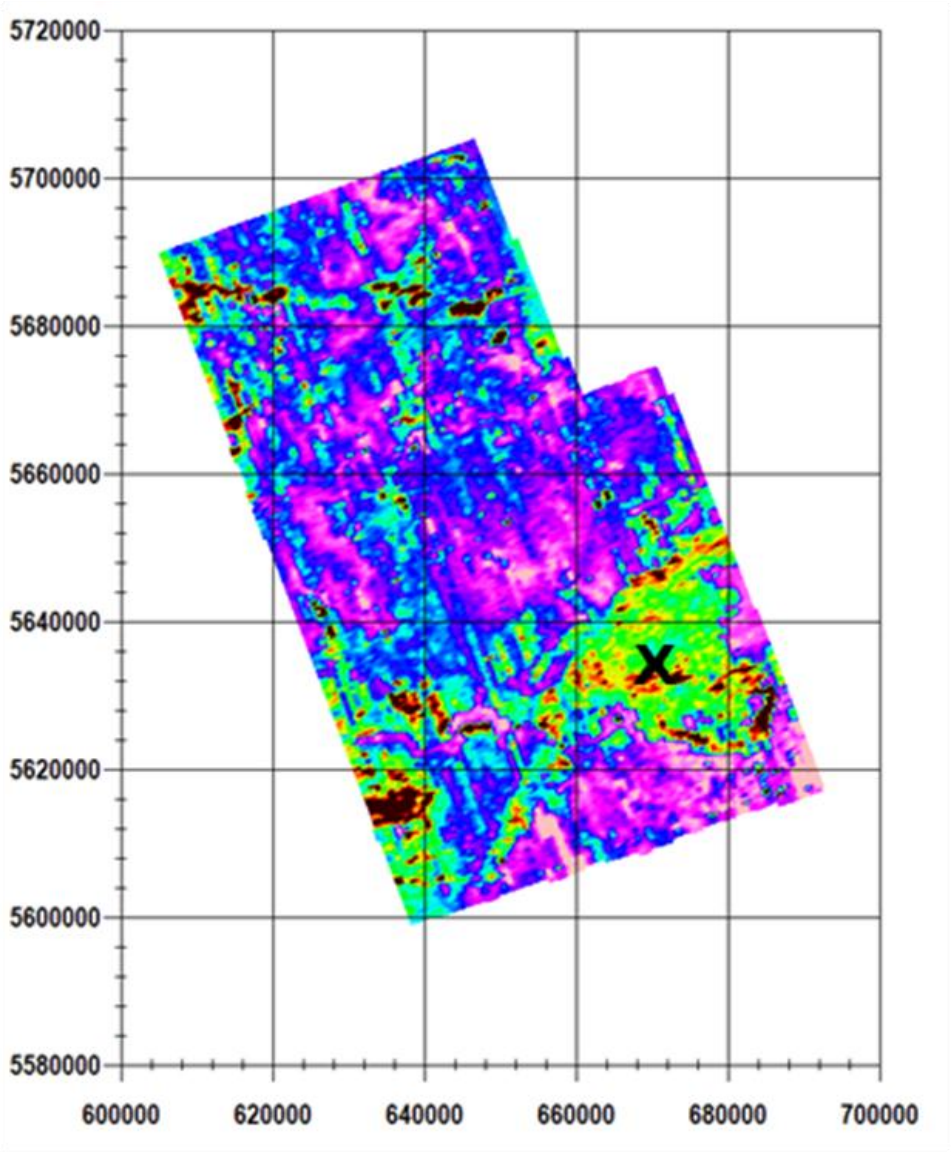

Figure 100: Recommended calibration site in Area 2 near (670000, 5635000).

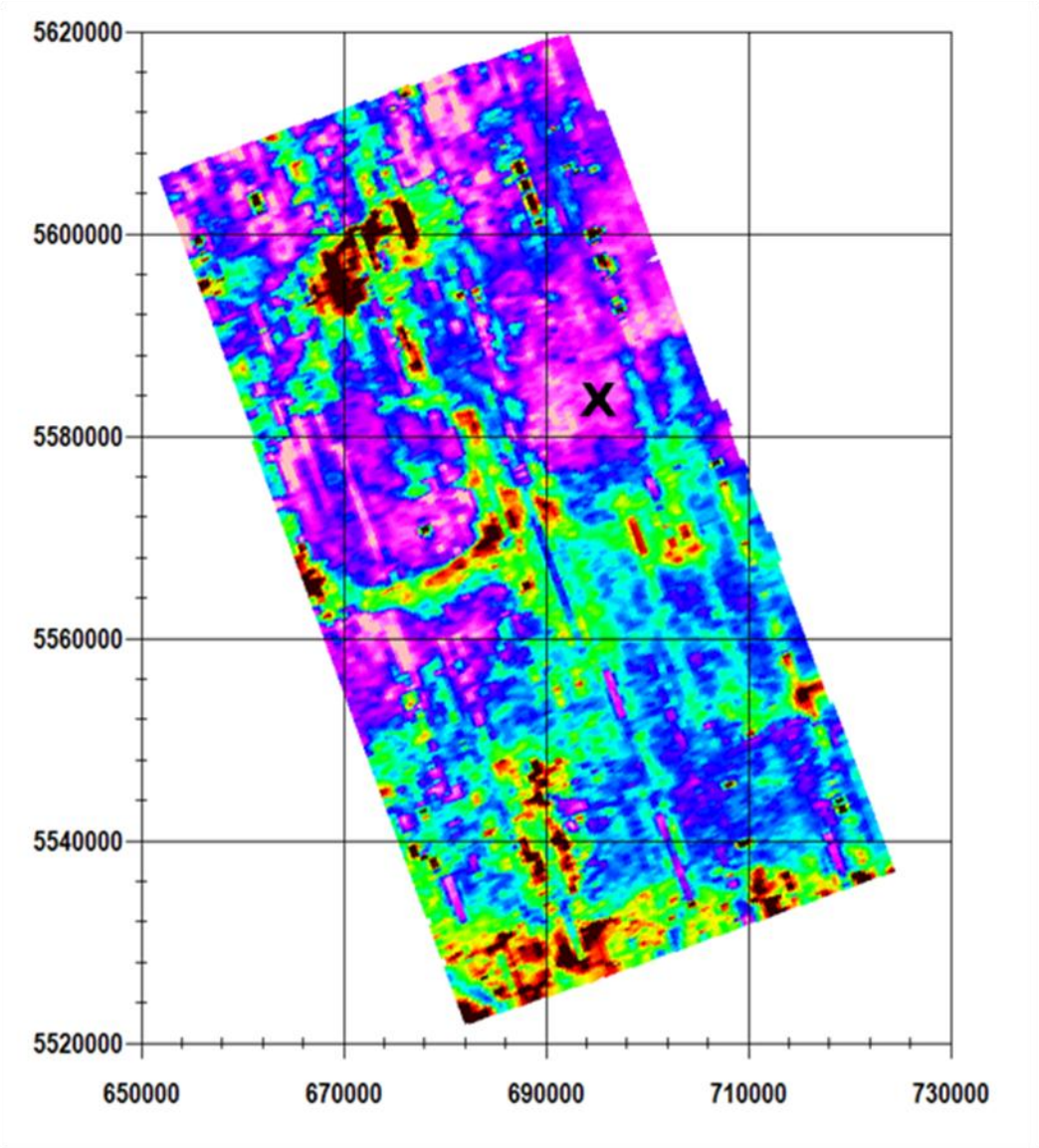

Figure 101: Recommended calibration site in Area 3 near (694000, 5584000).

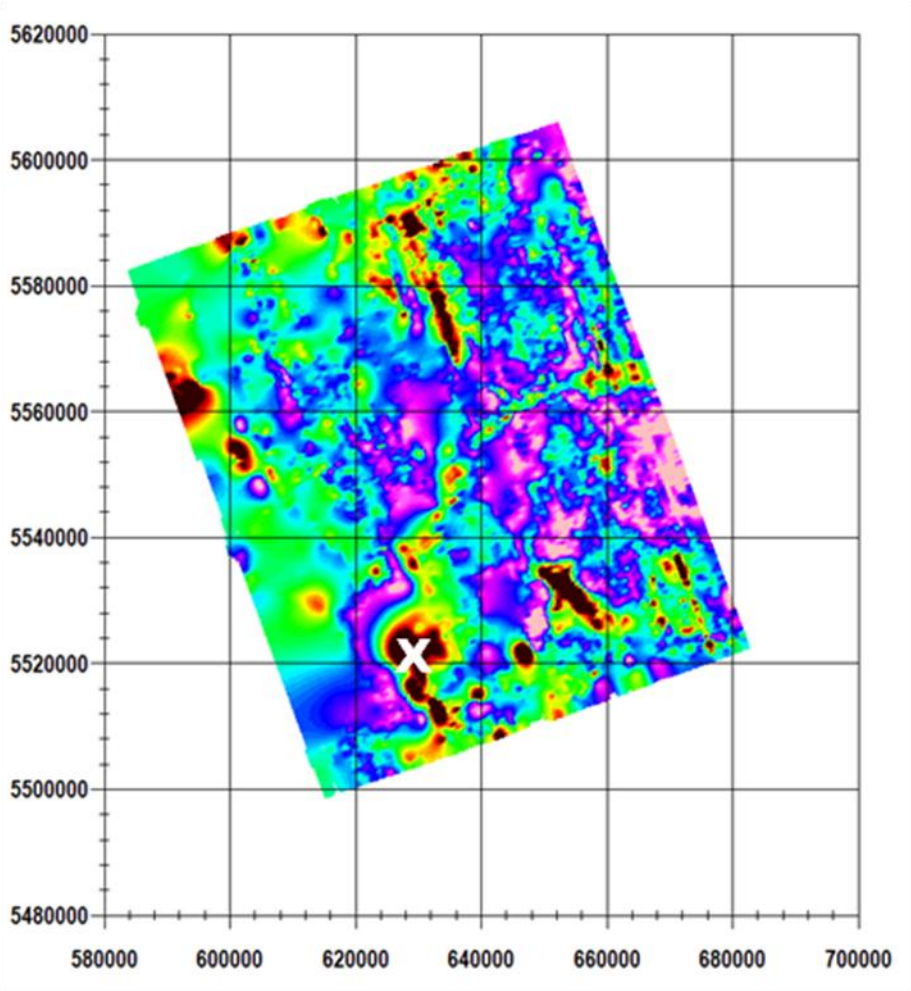

Figure 102: Recommended calibration site in Area 4 near (568000, 5523000).

References

Davis, L.J. and R.W.Groom, (2009). A comparison of airborne and ground electromagnetic data near the Grand Canyon. **SEG Extended Abstracts**, 79th Annual Meeting, p.764-768.

Dickinson, J.E., D.R. Pool, R.W. Groom, and L.J. Davis. (2010) Inference of lithological distribution in an alluvial aquifer using airborne transient electromagnetic surveys. **Geophysics**, 75 (4). pp. WA149-WA161.

Hamilton, W.N., C.W. Langenberg, M.C. Price, and D.K.Chao. (1998) Alberta Geological Survey. Geological map of Alberta (MAP 236).

Hydrogeological Consultants Ltd. (2003) Wheatland County, Part of the South Saskatchewan River Basin. Twp 021 to 028, R17 to 26, W4M. Regional Groundwater Assessment.

Hydrogeological Consultants Ltd. (2007) Vulcan County, Part of the South Saskatchewan River Basin. Twp 013 to 022, R16 to 26, W4M. Regional Groundwater Assessment.

Pawlowicz, J.G., M.M. Fenton and L.D. Andriashek. (2007) Alberta Geological Survey. Bedrock thalwegs, 1:2 000 000 scale (GIS data, line features).